

# **Monitoring and Modeling of Ultrafine Particles and Black Carbon at the Los Angeles International Airport**

**Elinor Fanning, Rong Chun Yu, Rong Lu, and John Froines (PI)  
University of California, Los Angeles**

**Final Report  
ARB Contract #04-325**

**June 20, 2007**

Prepared for the California Air Resources Board and the  
California Environmental Protection Agency

The statements and conclusions in this Report are those of the contractor and not necessarily those of the California Air Resources Board. The mention of commercial products, their source, or their use in connection with material reported herein is not to be construed as actual or implied endorsement of such products.

## ACKNOWLEDGEMENTS

About the authors: Rong Chun (RC) Yu directed and performed most of the field work. Rong Lu performed and reported on the modeling work. Elinor Fanning was the primary report author. Data analysis and interpretation was collaborative between all authors.

The study was funded by the California Air Resources Board, contract # 04-325, which was made possible by EPA Grant #XA-96918801-1 to ARB (Program: CAA Special Purpose Activities - LAX Study, October 31, 2005 to April 30, 2006). Additional support was provided by the Southern California Particle Center (EPA grant #RD-83241301).

Appreciation is due to Los Angeles World Airports (LAWA) for granting access to the airfield runway location and to the Proud Bird Field. ARB provided field study equipment, including a Scanning Mobility Particle Sizer, Condensation Particle Counter, Aethalometer, laptop computers, E-BAM, canisters with associated sampling trains, and cartridges with associated sampling devices. The South Coast Air Quality Management District provided access to their monitoring site near Hastings/Westchester Blvd, Los Angeles.

Dr. Constantinos Sioutas, at the University of Southern California, provided invaluable expert guidance and review for the project, from conception through preparation of the final report. Yi Fang Zhu and Bill Grant volunteered excellent technical consultation, field assistance. We thank Arantza Eiguren-Fernandez for analysis of the PAH data and helpful discussion. Alvin Wong contributed support for field studies.

This Report was submitted in fulfillment of ARB contract number 04-325, Monitoring and Modeling of Ultrafine Particles and Black Carbon at the Los Angeles International Airport by Dr. John Froines and the University of California under the sponsorship of the California Air Resources Board. Work was completed as of November 16, 2006, and a revised report finalized June 20, 2007.

# TABLE OF CONTENTS

Abstract.....	viii
Executive Summary.....	ix
1. Introduction	
Research Objectives.....	1
Background and Rationale.....	2
2. Near Source Study	
Overview.....	5
Methods.....	5
Results.....	12
Discussion .....	20
3. Downwind Study	
Overview.....	23
Methods.....	24
Results.....	25
Discussion .....	34
4. Community Study	
Overview.....	38
Methods.....	38
Results.....	40
Discussion .....	45
5. Modeling Study	
Overview.....	48
Model Configurations.....	48
Aircraft Emissions Factors.....	49
Estimate and Calibrate Black Carbon Emissions.....	53
Dispersion of Aircraft Emissions to Community Locations.....	57
Discussion.....	59
6. Overall Summary and Conclusions.....	61
7. Recommendations.....	64
8. References.....	66
9. Appendix.....	68

# FIGURES AND TABLES

## Figures

### **Chapter 2: Near Source Study**

- Figure 2-1 Locations of near source site at LAX blast fence (BF) and background reference sites (AQMD)
- Figure 2-2 Bird's eye view of runway 25R and the LAX blast fence near source sampling location
- Figure 2-3 Close up view of the LAX blast fence sampling site
- Figure 2-4 Particle number size distributions at near source and background sites
- Figure 2-5 Time profile of total CPC counts and identification of aircraft at runways 25R and 25L
- Figure 2-6 Temporal profile of 15 nm particles at the blast fence
- Figure 2-7 Temporal profile of 30 nm PM at blast fence during a take off event

### **Chapter 3: Downwind Study**

- Figure 3-1 Aerial map showing Proud Bird field and downwind study sites
- Figure 3-2 Box plot of 15 nm particle data, downwind of runway 25R
- Figure 3-3 Box plot of upper quartile of 15 nm particle data collected downwind of runway 25R
- Figure 3-4 Temporal profile of 15 nm particle concentrations at the LAX blast fence and a site 110 m downwind of the blast fence
- Figure 3-5 Temporal profile of 15 nm particle concentrations at the LAX blast fence and a site 170 m downwind of the blast fence
- Figure 3-6 Box plot of black carbon data collected downwind of runway 25R
- Figure 3-7 Box plot of upper quartile of black carbon data collected downwind of runway 25R
- Figure 3-8 Box plot of 15 nm particle data collected downwind of runway 25L
- Figure 3-9 Box plot of upper quartile of 15 nm particle data collected downwind of runway 25L
- Figure 3-10 Box plot of black carbon data collected downwind of runway 25L
- Figure 3-11 Box plot of upper quartile of black carbon data collected downwind of runway 25L

## **Chapter 4: Community Study**

- Figure 4-1 Location of the six community sites relative to LAX
- Figure 4-2 Distribution of wind direction during June 2006 monitoring
- Figure 4-3 Particle size distributions of the six community sites in related to the near source LAX blast fence and the background AQMD site
- Figure 4-4 Particle size distributions of local resident, synagogue, and Whelan School, located right beneath the landing path
- Figure 4-5 Particle size distribution of fire station and Lennox School District sites.

## **Chapter 5: Modeling**

- Figure 5-1 Model domains and locations used for the LAX simulation
- Figure 5-2 The ICAO landing and take-off cycle (LTO).
- Figure 5-3 A linear relationship between black carbon emission factor and aircraft engine thrust level.
- Figure 5-4 Model predicted aircraft signals at the blast fence location. The emission rates have been calibrated. The take-off and landing of aircraft near the blast fence location are shown as peaks in the figure.
- Figure 5-5a Model predicted concentrations at blast fence
- Figure 5-5b BC measurements at the blast fence location
- Figure 5-6 Averaged black carbon concentrations from 09/24/2006 8:00 to 9:00 PST near LAX.
- Figure 5-7 Averaged black carbon concentrations from 09/24/2006 13:00: to 14:00 PST from LAX. The see-breeze moves the black carbon to the east.
- Figure 5-8 Averaged black carbon concentrations from 09/24/2006 23:00 to 24:00 PST.

## **Tables**

### **Chapter 2: Near Source Study**

- Table 2-1 Instruments used in the Airport Study
- Table 2-2 PM<sub>2.5</sub> concentrations (in  $\mu\text{g}/\text{m}^3$ ) at the blast fence and background reference site (2005 summer study)
- Table 2-3 Vapor and particle phase PAH concentrations at AQMD background site and LAX blast fence
- Table 2-4 Concentrations (in ppb) of measured VOCs at the near source (LAX\_BF) and background (AQMD) sites during Sep05 and May06 sampling campaigns

Table 2-5 Comparisons of VOCs between sites and between two sampling campaigns

### **Chapter 3: Downwind Study**

Table 3-1 Aircraft departures on runway 25R associated with data profiled in Figure 3-4.

Table 3-2 Aircraft departures on runway 25R associated with data profiled in Figure 3-5.

Table 3-3 15nm Particle Concentrations (dN/dlogDp in #/cm<sup>3</sup>) at LAX blast fence, near Aviation Blvd, and study locations in the Proud Bird Field

### **Chapter 4: Community Study**

Table 4-1 Characteristics of six community sites.

Table 4-2 15 nm Particle Concentration (dN/dlogDp in #/cm<sup>3</sup>) Profile at six Community Sites

Table 4-3 PM<sub>2.5</sub> mass, black carbon mass, and PMN<sub>10-100</sub><sup>a</sup> concentration at six community sites LAX blast fence and background reference site

### **Chapter 5: Modeling**

Table 5-1 Domains used for the simulation

Table 5-2 Representative LTO cycle times for several aircraft categories (in minutes)

Table 5-3 Aircraft Activity Data Table from LAX

Table 5-4 Aircraft engine thrust level and estimated BC emission factor of the operating modes in the ICAO standard LTO cycle

### **Chapter 6: Summary and Conclusions**

Table 6-1 Summary statistic from three field studies of 15 nm ultrafine particles (UFP), total number concentration of UFP in sizes between 10 to 100 nm (PMN<sub>10-100</sub>), black carbon (BC), and particulate matters in particles less than 2.5 μm

## ABSTRACT

A study to monitor and model ultrafine particles (UFP) and black carbon was performed at and in the vicinity of Los Angeles International Airport. The study was designed to capture the highly time-varying nature of ultrafine particle emission from aircraft by using near real time instruments. Three field studies were performed in Los Angeles during 2005-2006. Field studies used near real time instruments to measure the number concentrations of UFP with high temporal resolution. Size distributions of ultrafine particles collected immediately downwind of aircraft take off showed very high number concentrations of UFP, with the highest numbers found at a particle size of approximately 14 nm ( $dN/d\log D_p = 1.4 \times 10^6$ ). The highest spikes in the time profile of UFP number concentrations were clearly correlated with aircraft take off events. Total UFP counts exceeded  $10^7/\text{cm}^3$  during some monitored take offs. Time averaged concentrations of  $\text{PM}_{2.5}$  mass and two carbonyl compounds, formaldehyde and acrolein, were elevated at the airport site relative to a background reference site. Other volatile organic compound concentrations were unremarkable. 15 nm particles can be detected 600 m east of LAX, and spikes of particle number were again associated temporally with aircraft activity. Farther downwind, number concentrations of UFP collected in a residential community approximately 2-3 km east of LAX were intermediate in concentration between the airport runway and the background reference site. The curve shape of the UFP size distribution at the community sites was similar to that of the runway site, with peak particle numbers occurring between 10 and 20 nm. While number concentrations of very small particles were high at the community locations studied, the mass-based measures of particulate matter exposure used in this study, black carbon and  $\text{PM}_{2.5}$  concentration, did not indicate elevated exposures in the community. The results of the project demonstrate that in-use commercial aircraft at LAX emit large quantities of UFP at the lower end of currently measurable particle size ranges. 10-20 nm particles emitted from aircraft are also present at relatively high number concentrations in an adjacent community but an expanded and more in-depth study is needed to determine whether aircraft are indeed the source. In addition, toxicological research on aircraft emitted particulate matter is needed to characterize the potential public health impacts, and a complete chemical characterization of aircraft emitted PM is important to enhance understanding of exposure and public health implications.

# EXECUTIVE SUMMARY

## **Background**

A study monitoring and modeling ultrafine particles and black carbon was performed at and in the vicinity of Los Angeles International Airport. Airports are important sources of particulate matter in urban airsheds yet regulators and public health agencies have little data available to them that address the characteristics of particles emitted from aircraft and the potential impact on exposure and health in adjacent communities. Previous efforts to study airport-related particulate matter have generally relied on time integrated measurements and instruments that do not capture ultrafine combustion particles emitted from aircraft. This study attempted to address this important data gap, on a scale that was exploratory in nature and thus somewhat limited in scope. The study results provide an initial characterization of ultrafine particulate matter associated with LAX aircraft operations that provides the basis for further in-depth studies including PM compositional characterization, toxicology and health effects studies.

## **Methods**

The project was comprised of three field studies, performed in Los Angeles in 2005-2006, and a modeling component. The field studies used near real time instruments to measure number concentrations of UFP with high temporal resolution. Overall size distributions of UFP and concentrations of particles at selected sizes were obtained 140m downwind of a major aircraft take-off location, a background reference site to the north of the airport that is minimally influenced by aircraft pollution, and six community sites located 1.8 – 3.5 km to the east of LAX in a primarily residential area. Sampling was not performed simultaneously at the different community locations. Number concentrations of 15 nm particles were studied at ten sites in a field immediately to the east of LAX, at distances ranging from 220-610m from the point on the runway at which take off is typically initiated. As with the community study, downwind locations were serially, rather than simultaneously sampled. Sampling for black carbon mass and PM<sub>2.5</sub> mass was performed concurrent with the UFP work at most of the sampling sites in the field studies. At the airport location, monitoring was performed for carbon monoxide, carbon dioxide, polycyclic aromatic hydrocarbons, and selected volatile organic compounds. Data on time varying factors such as aircraft arrivals and departures, wind speed and direction, temperature and traffic counts were collected from airport sources to assist with statistical analysis of temporal variability in particle concentrations.

## **Results**

Size distribution and total particle counts of ultrafine particles monitored immediately downwind of aircraft take off showed very high concentrations of UFP. At this sampling site, the greatest numbers of particles were observed at a particle size of approximately 15 nm. Average number concentration at 14nm was  $dN/d\log D_p = 1.4 \times 10^6$ . The peaks in the temporal profiles of UFP number concentrations occurred during aircraft take off events, with total UFP counts exceeding the capacity of the CPC during take offs. In the second field study, the downwind study, 15 nm particles were measured simultaneously at the take off runway and at five locations east (downwind) of the runway, to see whether take off associated spikes in particle levels could be detected at these distances (ranging from 210-660m). The results show clearly that the temporal pattern of particle number concentrations at downwind sites are driven by runway activity. UFP number concentrations at the background reference site were substantially lower than at the

runway and the size distribution was notably different. Average UFP levels monitored at six community sites were intermediate between the average concentrations observed at the airport runway and background location. The size distribution of UFP collected at all six community sites was similar in shape to that of the runway site, with peak particle numbers occurring between 10 and 20 nm. Neither black carbon mass nor  $PM_{2.5}$  mass was elevated in the community. The findings of the study have implications for the impact of aircraft emissions on air quality on both a local and regional scale, and for the estimation of PM exposure from major sources.

## **Conclusions**

Field work was carried out in three phases: at the airport, immediately downwind of the airport, and further downwind in a nearby community. The near-source study found that in-use commercial aircraft at LAX emit large quantities of UFP at the lower end of the currently measurable particle size range. Spikes of 15 nm particles can be detected and associated temporally with aircraft activity up to 600m east of LAX. 10-20 nm particles are also present at relatively high number concentrations in a residential community approximately 2-3 km downwind of LAX, but these UFP could not be definitively associated with aircraft. Temporal correlation of UFP with aircraft activity patterns was not feasible for the community data because of the long time gap between field observations and official aircraft activity log data collected at LAX. However, indirect evidence from the study suggests that approaching aircraft may be a key source of temporal spikes on UFP size-selected profiles, and responsible for the peak of particles in the 10-20 nm range observed in the overall size distribution of UFPs at these locations. Motor vehicle emissions from I-405 were considered as another potential source, but the patterns of particle numbers observed at community sites are not consistent with a freeway source. Further work is needed to define the contribution of aircraft to community UFP exposures. Potential differences in size distribution, chemical characteristics and community exposure between particles emitted during take off in comparison to particles emitted while aircraft are approaching is also an area for further study. While number concentrations of very small particles were high at the community locations studied, the mass-based measures of particulate matter exposure used in this study, black carbon and  $PM_{2.5}$  concentration, did not indicate elevated exposures in the community. Black carbon and  $PM_{2.5}$  do not appear to be adequate for describing exposure to aircraft derived particulate matter. Toxicological research on aircraft emitted particulate matter is needed in order to characterize the potential public health impacts, and a complete chemical characterization of aircraft emitted PM is needed to enhance understanding of exposure and toxicology findings.

# 1. Introduction

## 1.1 Objectives and Specific Aims

The objectives of this study “Monitoring and Modeling of Ultrafine Particles and Black Carbon at the Los Angeles International Airport (LAX) were:

- 1) To characterize number concentrations of ultrafine particles (UFP) and black carbon mass concentration associated with aircraft take-offs, using near real-time monitoring instruments.
- 2) To examine concentrations of UFP numbers and black carbon mass in ambient air at and near LAX as a function of temporal and spatial patterns of aircraft traffic, local meteorology and other time-varying factors that could potentially explain variability.
- 3) To investigate the contribution of aircraft emissions to local ambient PM in neighborhoods downwind of LAX.

The study was designed to investigate the following hypotheses:

- 1) Aircraft arrivals and departures at LAX emit UFP, PM<sub>2.5</sub> and black carbon resulting in levels at the airport that are detectable above ambient background.
- 2) A concentration gradient of aircraft emitted PM extends from LAX to community sites downwind of the airport.
- 3) The concentration gradient can be explained by air dispersion processes, mainly as a function of the distance from the airport sources, wind speed and direction, and by the time-varying source strength of airport operations.

Five specific aims were developed to address the hypotheses and pursue the research objectives.

Specific Aim 1: To measure UFP number concentration, PM<sub>2.5</sub> mass concentration and black carbon mass concentration at a near source site and an upwind background site, during two seasons. (pertains to Objective 1 and hypothesis 1)

Specific Aim 2: To characterize dispersion of aircraft emissions by assessing the UFP number concentration and black carbon mass concentration within 600 m downwind of take-off emissions. (This aim pertains to objective 1 and hypothesis 2 and was developed and approved as an additional aim by the contract officer during the period of the contract).

Specific Aim 3: To perform a statistical analysis of highly time-resolved data collected in the first two aims to explain the time-varying nature of pollutant concentrations by temporal patterns in aircraft activity, in the context of other time varying factors such as local meteorology. (addresses objective 2 and hypotheses 1, 2).

Specific Aim 4: To examine the potential contribution of dispersed aircraft PM to community exposure levels in the vicinity of LAX, using instruments installed at the near source site simultaneously with instruments installed at various sites in an adjacent community.

Specific Aim 5: To model the dispersion of aircraft emitted black carbon near LAX, using measurement data collected in Aims 1 and 2 to evaluate model predictions.

## *1.2 Background and Rationale*

The South Coast air basin is a non-attainment area for the California fine particulate matter (PM<sub>2.5</sub>) ambient air quality standard, and will be designated as a non-attainment area under the national PM<sub>2.5</sub> standard at the end of this year. No health-based standards are in place for ultrafine particulate matter (UFP), yet these particles possess properties that raise significant health concerns. Ambient UFP often contain high levels of redox-cycling organic compounds. These particles generate oxygen radicals, have greater potency to induce oxidative stress responses than larger particles, and are associated with inflammatory effects in lung tissue and cultured cells (Li et al, 2003; Donaldson et al, 2002). After inhalation, UFP can translocate to extrapulmonary tissues, such as brain and liver (Oberdorster, 2004), and are taken up by cells to lodge in mitochondria, producing toxic effects in these organelles (Xia et al, 2004). While effects in epidemiological studies have been more difficult to establish due largely to exposure assessment issues, UFP have been implicated in exacerbation of asthma (Peters et al, 1997) and with cardiovascular effects (Elder et al, 2004). Due to the likely role of UFP in the toxicity and health effects associated with combustion-related particulate air pollution, improved understanding of ambient exposure levels and the relative contributions of key airborne particulate matter (PM) sources to UFP exposure is needed. It is critical to characterize spatial variation in contribution of PM sources to ambient UFP, since some sources may be responsible for especially high impacts in nearby communities. The studies reported here have provided data that will help to clarify the role Los Angeles International Airport (LAX) as a source of ambient UFP at the airport and in adjacent communities, and provide the basis for further detailed studies of LAX associated PM.

The contribution of aircraft emissions to PM exposure levels, and to UFP in particular, could be significant. Recent PM studies carried out near freeways (Zhu et al. 2002a&b) have demonstrated a concentration gradient for UFP, black carbon, and CO; concentrations many times higher than ambient were measured immediately adjacent to freeways with exponential decrease in particle number observed over distances of 100-300 meters. Similarly, communities in close proximity to major airports could experience elevated levels of combustion-related PM that derive from aircraft and other airport activities. Fixed site routine monitoring sites provide little information about the spatial variability in PM levels that is needed to evaluate the impact of near-source exposures from sources such as motor vehicle and airport traffic. In addition, the complex temporal patterns of emissions from aircraft are difficult to resolve with routine time-integrated monitoring methods.

While the potential importance of airport-related sources has been recognized in recent years few studies have reported measurements of particulate air pollution at or near large airports. The South Coast Air Quality Management District (AQMD) conducted a series of monitoring campaigns during the years from 1998 – 2001 (AQMD 2000a, 2000b, 2001). Dustfall of large particles, volatile organic compounds (VOC), carbon monoxide (CO), PM10 mass, organic (OC) and elemental carbon (EC) were among the endpoints measured at several locations in the vicinity of LAX. The AQMD studies used time-integrated sampling methods, typically sampling over 8 – 24 hour periods.

The findings from these exploratory studies were limited in their ability to address airport PM emissions. AQMD concluded that the monitoring site chosen to capture airport emissions was also highly influenced by vehicle traffic along Aviation Boulevard. It was difficult to make conclusions regarding the sources of the PM measured at this site. EC levels at an Aviation Blvd. site nearest to the airport were higher than those measured at other points along Aviation, which suggested that LAX was a contributing source of EC, but the methods used were unable to differentiate sources. The data for PM10 mass did not show clearly that the site nearest the airport had the highest levels. It may be that PM10 is an insensitive measurement, since it is expected that airport operations have a greater impact on UFP and fine PM levels than on coarse PM downwind of the airport. AQMD concluded that "it is not possible to determine what portion of the measured PM10 values are due to operations at LAX, traffic associated with the movement of goods and passengers in and out of LAX, non-LAX related traffic on the major arterials (Aviation Blvd, and the 405 freeway), or some other source" (AQMD 2000a).

Comparison of pollutant levels across the selected monitoring locations indicated that in general, PM10 mass, EC, OC, and mobile source-related air toxics (benzene, 1,3 butadiene, and formaldehyde) were more concentrated east of the airport than at a comparison site north of the airport, consistent with airport sources and prevailing west to east winds playing a role. Benzene and 1,3 butadiene levels showed a decreasing concentration gradient with increasing distance from the airport (AQMD 2000a). Proximity to heavy traffic corridors (Aviation Blvd and the 405 Freeway) appeared to result in higher PM, EC, OC and mobile source air toxics measurements, regardless of the location with respect to the airport (AQMD 2001). The findings suggest that the time-integrated sampling methods used in these studies may have obscured the impact of airport sources on local community exposure levels.

Two AQMD studies reported on microscopic analysis of PM fallout collected on glass plates under the LAX landing path. In the first study (AQMD 2000a), combusted oil soot particles greater than 50 microns were observed, and the authors concluded that aircraft could be contributing to soot fallout. However, in a second study conducted in spring 2000 (AQMD 2000b), these large, pitted particles suggestive of high temperature oil combustion were not reported; fallout composition was not inconsistent with other areas of the LA basin. AQMD was unable to conclude whether LAX contributes to large particle fallout at the study sites.

Pilot studies designed by ARB investigators to compare variation in fine and UFP measured in communities to levels measured at fixed site monitors found that very high counts of small particles (<600nm) were present downwind of LAX (Westerdahl et al, 2003a & b). Distribution of particle numbers by size showed that maximum particle counts were in the 10-20nm range, indicating combustion as the likely source. A small-scale study by Bloch (2002) suggested that jet engines may emit high concentrations of ultrafine particles in or near airports.

Together, the available studies suggest that the airport or nearby major traffic arterials may contribute to greater PM levels in communities on the east side of LAX than on the north and south sides, consistent with the location of traffic arterials and the predominant west to east wind patterns near the coast. The studies are relatively limited. UFP monitoring was done only in the pilot work by ARB. Spatial distribution of UFP has not been studied in communities adjacent to

LAX. With the absence of effective source tracers for jet fuel and lack of studies that address the size-resolved composition of ambient particulate, it has not been possible to partition the impacts of aircraft emissions from those of motor vehicles on the ground. The time-integrated sampling approach used in the AQMD studies apparently lacks the sensitivity to detect potentially large quantities of emissions from aircraft operations over repeated short time periods.

Given this background, the current study was proposed to focus on UFP at and in the vicinity of LAX, using instruments with high time resolution to capture the high temporal variability in aircraft source emissions. Monitoring locations were selected to minimize the confounding impact of traffic arterials. The relative contribution of aircraft and other mobile source factors to the overall impact of the airport on ambient PM is an important question in the design of effective control strategies, but is difficult to address at this time due to inadequate availability of source tracers. This study applied statistical analysis of time resolved measurement data as an alternate approach to source tracer methods to assess the contribution of aircraft emissions to downwind PM levels. The work reported here will build the groundwork for in-depth studies of particle composition and relevant gaseous and vapor phase pollutants in the future.

## 2. Near Source Study

### 2.1 Overview

The general objective of the first project component was to measure target pollutant levels during aircraft take-off as near to a busy runway as practicable, and compare the results to measurements taken at an upwind background location. Semi-continuous instruments to monitor UFP number concentrations, particle size distribution and black carbon were assembled, installed, and operated at a near-source site at LAX immediately downwind (about 140 m) of a major departure runway. Time integrated instruments were used to monitor fine PM<sub>2.5</sub>, CO<sub>2</sub>, selected polycyclic aromatic hydrocarbons (PAH) and organic vapor phase compounds. The upwind site was installed with the same instruments, to provide background data for comparison. The main near-source study was carried out in September 2005; a limited second study was performed in Feb/March 2006 to enable evaluation of seasonal effects on the research findings.

The purposes of monitoring PM at the near source site were 1) to determine which measured pollutants displayed elevated concentrations at the runway in comparison to the background site, and 2) to determine how PM and associated pollutant measures varied with airport operations, especially exhaust from aircraft take-off thrust. To accomplish these purposes, data analysis included a comparison of summary statistics from the near-source and the background sites followed by a detailed analysis of the time profiles of ultrafine particle concentrations at the runway, in the context of aircraft departure times provided by LAX.

### 2.2 Methods

#### *LAX and Meteorology*

Los Angeles International Airport (LAX) is the world's fifth busiest passenger airport and ranks sixth in air cargo capacity. LAX is located at the western border of the South Coast Air Basin near the Pacific Ocean (N 33°56.55', W 118°24.48'). In 2003, LAX accommodated about 55 million passengers and 2 million tons of goods (LAX, 2004). Flights into and out of LAX typically proceed from east to west, with 96% of the departures to the west over the ocean and 94% of the arrivals landing from the east. Two runways are located to the north and two are to the south of the LAX central terminal complex. On average, 1,700 to 2,200 aircraft movements occur daily at LAX.

#### *Specific Sampling Sites*

The two sites used in this study were selected to contrast a near-source (blast fence) location at LAX with a background reference site that is upwind of LAX. Figure 2-1 shows the relative locations of the two sampling sites.

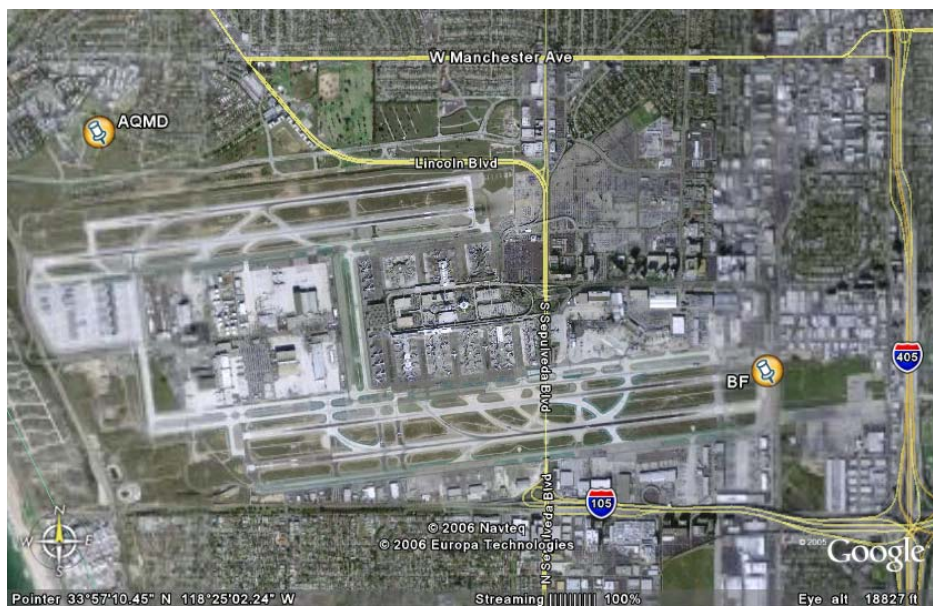


**Figure 2-1: Locations of near source site at LAX blast fence (BF) and background reference sites (AQMD).**

Downwind/Near-Source site: The near-source monitoring site was located at the east end of runway 25R at LAX. Runway 25R is primarily used for aircraft taking off to the west, directly against the prevailing wind, and accommodates 40% of the total departures at LAX. Some aircraft arrive on runway 25R but departures dominate runway activity. The runway sampling location is ideally positioned to capture emissions from aircraft take-off thrust: planes initiate take off close to the sampling site, then accelerate westward down the runway and away from the sampling site. Three fences, called “blast” fences, are positioned north to south across the end of runway 25R, and are designed to buffer the blast of jet exhaust associated with take off. Figure 2-2 illustrates the locations of the major and minor blast fences. The blast fence location is approximately 140m from the point on the runway at which departing aircraft initiate take-off. Two glass-fiber cabinets that accommodated the instruments used in this study sit underneath the major blast fence, and were made available to us by Los Angeles World Airports. The cabinets are equipped with power sources and provide protection for the equipment from the turbulent air and coarse dust clouds that regularly occur at this location. Figure 2-3 shows a close-up of the sampling site. An electrical panel connects power lines to the cabinets and distributed power outlets to which pumps and samplers were connected. An air-conditioning unit is available to provide cooling needed for the instruments placed inside the cabinet. The sampling probes for the SMPS/CPC and Aethalometer were initially inserted through slits in the fencing, to sample the air stream on the runway side of the blast fence, directly facing aircraft emission plume. However, in 2006 sampling campaigns the probes were placed behind the blast fence, with a cyclone to remove large particles, due to concerns that large particles blown by the blast clogged the orifice of the SMPS inlet and resulted in invalid data and potential damage to instruments.



**Figure 2-2: Bird's eye view of runway 25R and the LAX blast fence near source sampling location**



**Figure 2-3: Close up view of the LAX blast fence sampling site**

Upwind Background site: An upwind sampling site in a residential area north of LAX was chosen as a reference location. The site experiences a prevailing sea breeze, with no major PM sources upwind. There are two high schools nearby, which may introduce some bus emissions to the area, and there is light local traffic. This location is operated by the South Coast Air Quality Management District (AQMD), who generously provided access for the duration of the study.

#### *Sampling Dates*

Field sampling was performed during two time periods. The summer field study took place September 23-29, 2005. Sampling was performed over 24 hour intervals for time-integrated instruments and continuously for real-time instruments, starting at 12:00 pm on September 23

and ending at 14:00 pm on September 29, 2006. The winter field study was limited to the near source site (blast fence); data were not collected at the AQMD background site due to limited availability of instrumentation. At the blast fence, the winter sampling took place over several days in late February and early March, 2006, using a more limited set of instruments than the summer study.

*Instrumentation and Sampling Methods*

Descriptions of the instruments used in the study are provided below. The instrumentation is also relevant to the dispersion and community studies that are reported in Sections 3 and 4 of this report, below.

For the summer study, a set of instruments was installed at each of the two sampling sites: a SMPS/CPC along with a laptop computer for data integration, an Aethalometer, an E-BAM Particulate Monitor, a Tisch Sampler, a canister sampler for butadiene, benzene and acrolein, and a cartridge sampler for formaldehyde. In addition, meteorological data and CO concentrations collected at the AQMD site were supplemental to this study. Table 2-1 summarizes the instruments and the time intervals over which they were used in the monitoring protocol.

**Table 2-1-- Instruments used in the Airport Study**

<b>Site</b>	<b>Target Parameter(s)</b>	<b>Instrument (Supplier, Model)</b>	<b>Sampling Interval</b>
AQMD	Black Carbon	Aethalometers (Magee Scientific, AE-20)	5 minutes
AQMD	PM <sub>2.5</sub>	E-BAM (Met One Instruments)	30 minutes
AQMD	Particle Size Distribution	SMPS (DMA 3081)/ CPC (3785) (TSI)	2 minutes
AQMD	PAHs	Tisch Sampler (Tisch Environmental Inc. 1202)	~ 24 hrs
AQMD	Butadiene/Benzene/Acrolein	Canister sampler (ARB supplied)	~ 24 hrs
AQMD	Formaldehyde	Cartridge sampler (ARB supplied)	~ 24 hrs
LAX	Black Carbon	Aethalometers (Magee Scientific, AE-20)	5 or 10 minutes
LAX	PM <sub>2.5</sub>	E-BAM (Met One Instruments)	60 minutes
LAX	UFP Total or Size-specific Conc.	SMPS (DMA 3081)/ CPC (3025) (TSI)	1 second
LAX	Particle Size Distribution	SMPS (DMA 3081)/ CPC (3025) (TSI)	2 minutes
LAX	PAHs	Tisch Sampler (Tisch Environmental Inc. 1202)	~ 24 hrs
LAX	Butadiene/Benzene/Acrolein	Canister sampler (ARB supplied)	~ 24 hrs
LAX	Formaldehyde	Cartridge sampler (ARB supplied)	~ 24 hrs

A SMPS (TSI Classifier model: 3080, DMA model: 3081)/CPC (TSI model 3785) along with a laptop computer were used to measure particle concentrations and size distributions, ranging

from 7.64 to 289 nm in 102 size bins, at the AQMD background site. A second SMPS (TSI Classifier model: 3080, DMA model; 3081)/CPC (TSI model 3025), measuring particles in sizes from 6.15 to 225 nm in 101 size bins was used at the blast fence. In the two-minute scans performed for size distributions, particles are scanned for 100 seconds followed by a down scan that allows the voltage to be reset (down scan) for 20 seconds. Particle numbers in  $dN/d\log D_p$  were generated for each size bin during each two-minute scan. The instruments were frequently checked for proper functioning. Upon identifying abnormal responses, if any, they were examined and properly maintained in the field, such as cleaning of inlet impactor. All data were handled by TSI-provided software, Aerosol Instrument Manager (AIM) 5.3.1. ASCII coded data were exported from the AIM software and subsequently analyzed by Microsoft Excel or SAS software (SAS Institute, Cary, NC).

The SMPS/CPC was also used to conduct near continuous monitoring by performing particle counts over very short time intervals, to better capture take-off emissions. In these measurements, the DMA of the SMPS was adjusted to monitor a specific particle size and the CPC was used to count particle concentrations at the desired size every second, providing a real-time monitoring approach that could capture temporal variability in particle number concentrations. In the September study, monitoring was done for 7, 10, 20, 30, 50, 100, 150, and 200 nm on September 23 and at 8, 10, 15, 20, 30, 50, 75, 100, 150 and 200 nm particles on September 28. The monitoring time periods for one second scans lasted from 11 min to 77 minutes. In the winter study, similar one second scans were conducted for particles at 10, 15, 20, 30, 50, and 100 nm, on February 28, March 1 and 2.

Aethalometers (Magee Scientific, model AE-20) were used to measure black carbon (BC) at 880 nm. The instruments were set up to measure average BC concentrations over 5 minute intervals in the September study and over 10 minute intervals in the winter study. Data was retrieved from the instruments daily.

E-BAMs (Met One Instruments) were installed to measure  $PM_{2.5}$  at the LAX blast fence and the AQMD background site during the September study. The instrument operated continuously for 168 hrs. Hourly averaged concentrations were retrieved from the instruments after termination of monitoring efforts at the end of the sampling campaign periods, whether sampling duration was set up for 30 or 60 minutes.

$CO_2$  concentrations were measured at the LAX blast fence by a Q-Trak, which was set to integrate the concentration over one minute interval. As explained below, the instrument did not perform adequately under the field conditions, and the data were not pursued.

A Tisch Model 1202 sampler (Tisch, Cleves, OH) was deployed to obtain ambient samples of polycyclic aromatic hydrocarbon (PAH) species. The sampling train was the same as was reported in Eiguren-Fernandez et al. (2004). The unit contained a  $PM_{2.5}$  cyclone inlet, a fall column chamber, a filter holder, a PUF-XAD-4 resin holder, an electronic controller, a mass flow meter, and a vacuum pump. A sampling matrix that comprised XAD-4 resin and a Teflon coated glass fiber filter (TCGFF, 10.4cm) was used to collect vapor- and particle-phase PAHs, respectively. Collection of vapor-phase PAHs was carried out using 20g of XAD-4 (Acros Organics, NJ) resin held in a glass cylinder between two 400 mesh stainless steel screens, and a

2" PUF plug placed behind the screen to hold the ensemble together. The TCGFFs were cleaned by sonication using a solvent mix of dichloromethane:methanol and letting them dry in the oven till no odor was detected. In preparation for field use, PUFs were cleaned with distilled water and "compress-cleaned" using a mixture of hexane:methanol:methylene chloride (5:3:2 v/v) prior to matrix loading. After cleaning, PUFs were dried in an oven until no solvent odor could be readily detected. The XAD-4 resin was cleaned with triplicate rinses of water and methanol, using a Millipore filtering system. Cleaning was carried out in a Soxhlet system using methanol for 24 h, followed by methylene chloride for two 24 h periods. Once the XAD-4 was cleaned, it was placed in a vacuum oven at 40–50°C for 2–3 days until no odor was detected. Ten vapor- and particle-phase 24-hour samples were collected at the blast fence and the background site from September 23 to September 28, 2005. No Tisch sampling was performed during the winter campaign. Vapor- and particle-phase samples were analyzed separately to assess differences in the PAH profiles at each site. Sampled volume, measured by the sampler's mass flow meter, is corrected to 21.1°C and 1 atm. Prior to sampling, laboratory-prepared sampling matrices were stored in a conventional freezer and their transport to and from the field was accomplished using a cooler containing frozen blue ice. Once the samples were collected and returned to the laboratory, they were placed in a freezer until extraction and analysis. Previous work has shown that backup filters were not needed (PAH levels on backups were below LOD under the sampling and analysis methods used) (Eiguren-Fernandez et al, 2004).

SUMMA polished stainless steel canisters were used to collect ambient air for chemical analysis for 1,3-butadiene, benzene, and acrolein. In the field, a sampling train provided by ARB was connected to a canister. The train consists of metal tubing with an open-end for air entry, a critical orifice with a screw for flow control, a pressure gauge to measure canister vacuum pressure, metal tubing for connecting the train and the canister, and a concrete block stand to hold the sampling train. Canisters were initially depressed to –30 psi prior to use in the field. After connecting the sampling train and the canister, airflow at 0.003 liter per minute was calibrated at the beginning of each sampling. Sampling lasted for about 24 hrs. Air pressures at the beginning and at the end of sampling were recorded.

Cartridges containing silica gel (coated with acidified 2,4-dinitrophenylhydrazine, DNPH) as a solid absorbent were used to trap formaldehyde in ambient air. The cartridge was connected to a sampling train, consisting of a holding tripod and a pump drawing a flow rate at 0.7 liters per minute for a 24-hour period.

#### *Chemical Analytical Methods*

Details of the PAH quantification procedure have been described previously (Eiguren-Fernandez and Miguel 2003). Briefly, TCGFFs were extracted by ultrasonication with 15 mL of methylene chloride. The extraction procedure was performed in amber glass vials under yellowlight conditions. The extract was filtered and the volume reduced to ~5 mL; 1 mL was used for analysis; the remainder was frozen. The XAD-4 was also extracted by sonication. A 1mL aliquot was injected directly into the HPLC-FL system to measure naphthalene, acenaphthene, and fluorene. Another 1mL aliquot was concentrated to ~100uL for the analysis of higher molecular weight PAHs. One field matrix blank was extracted and analyzed for approximately every ten samples. PAH concentrations measured in blank filters and XAD-4 blanks were subtracted from the concentrations found in the samples. Eiguren-Fernandez et al. (2004) have

reported that the collection efficiency of the system ranges from 93–97% of the lower MW PAHs, including naphthalene, phenanthrene, fluoranthene, and pyrene. SRM 1649a was used to determine the analytical procedure precision (4.2%) and recovery efficiency (85%).

Canisters and cartridges were transferred to ARB for analysis following ARB protocols. Briefly, 1,3 butadiene and benzene were analyzed by capillary column gas chromatography with photo ionization detector (Method MLD057). In summary, an air sample is introduced into the analytical system from a pressurized canister through stainless steel or Teflon tubing with the aid of a mass flow controller (MFC) and a vacuum system. A digital readout attached to the MFC provides a visual indication of the proper sample flow during sampling. The sample passes through a Nafion dryer to remove moisture from the gas stream. It is trapped on a cryotrap at -150 °C. At this temperature, the desired components are solidified, while fixed gases, such as nitrogen (N<sub>2</sub>), oxygen (O<sub>2</sub>), and carbon dioxide (CO<sub>2</sub>), and methane (CH<sub>4</sub>) pass through the cryotrap to the vent. The system is then purged with ultra pure N<sub>2</sub> to flush sample remaining in the tubing or bypassing it on to the cryotrap, and to remove any excess light impurities. The cryotrap is isolated and rapidly heated to 125°C, followed by injection of the sample onto a DB-VRX capillary column. After a short hold at 125°C, the trap temperature is raised to a final temperature of 190°C. The sample mixture is separated into individual components by their interaction with the capillary column stationary phase in the temperature-programmed gas chromatography. A photo ionization detector detects the eluting components. 1,3-butadiene and benzene are subsequently identified and quantified, based upon the relative retention time.

High performance liquid chromatography (HPLC) (ARB Method MLD022) was used to determine level of formaldehyde collected into absorbent cartridges. During sampling, formaldehyde reacts with the DNPH to form hydrazone derivative. Acetonitrile is used to elute the derivative from the cartridges. The eluted derivative was quantified by reverse-phase HPLC with ultraviolet absorption detection at 360 nm.

#### *Data Analysis*

Outliers in the SMPS size distribution data were detected by identifying unusual increases in the value(s) of a particular size bin, in comparison to a typically smooth size distribution. These outliers are occasionally found in SMPS/CPC-generated data and were usually orders of magnitude higher than typical values found in the same size bin. Infrequent zero values were encountered in the SMPS/CPC data, and were removed from further analyses. Negative values from aethalometers were also removed from statistical analysis.

Meteorological data: Surface and upper air meteorological data collected at the AQMD reference site were used to analyze the meteorological conditions for the sampling campaign periods.

Summary statistics (mean and standard deviation) were computed for all measured pollutants. SMPS data collected over the duration of each study period were combined to generate an average size distribution for both the near source and background sites. Statistical computation and graph plotting were performed by SAS software (Version 9.1, SAS Institute, Cary, NC) or Excel 2000 (Microsoft Corporation).

Analysis of size-specific SMPS/CPC data from one second scans: A temporal profile of particle concentration was plotted from the one second CPC output for each particle size that was sampled. To analyze the highly resolved time vs. concentration data with respect to aircraft emissions, air traffic activity data were obtained from Los Angeles World Airports (LAWA). The data includes the logged departure time, arrival time, aircraft type and airline identification number for flight activity at each runway. “Arrival” and “departure” time is logged by the control tower when a plane passes detection radar, and these logs times are not necessarily coincident with the time at which a plane and its emissions are closest to the sampling instruments. In order to investigate the specific impact of aircraft take offs on ultrafine particles in each size range, the peaks in the particle concentration time profiles were matched with departure events from the airport logs, by manual inspection of the two related time series (concentration and aircraft activity). The range of peak concentrations, mean, standard deviation, geometric mean, and geometric standard deviation for each selected size were computed. In addition, the data from selected take-off events were used to model the aircraft emission during the complete cycle of an aircraft turning onto the runway, idling, and accelerating down the runway away from the blast fence sampling location, based on field notes collected during sampling.

SAS Proc GLM was used to test the differences in volatile organic compound concentrations between the near source and the background sites as well as between two sampling campaigns.

## 2.3 Results

### *Meteorology*

The local meteorological conditions during the study were mostly typical. In the summer study, conducted from September 21 to 27, 2005, a sea breeze developed in the morning leading to westerly and southwesterly winds over LAX from about 8 to 9 AM to early evening at a maximum speed of 8 - 11 mph. Lighter northeasterly winds from 1 to 3 mph associated with a land breeze appeared from midnight to early morning. The diurnal variations of temperature at LAX ranged from a daily minimum of about 57 °F in the early morning to daily maximums of 67 to 76 °F around noontime. High relative humidity persists at LAX due to the influence of marine air. In the winter study, the average temperature was 54 °F, with average daily minimum of 47.8 °F and average daily maximum of 60.3 °F during the study period. Winter wind speed averaged 4.6 mph, ranging from 0 to 16 mph, mostly typical sea breezes for this location.

### *Wildfire*

During the September study period there was a wildfire in Topanga Canyon, in the Thousand Oaks region north of the Santa Monica Mountains. The fire began in the late afternoon on September 28 and continued to the conclusion of the summer sampling campaign. The wildfire was located about 25 km northwest of LAX. During this period, there was also a weak Santa Ana event September 28-29 that resulted in a slight shift from the normal meteorological patterns. The typical southwesterly sea breeze over LAX reduced slightly to 4 – 6 mph during the daytime on September 29. The wind directions remained mostly normal. The maximum temperature reached 92° F with a relative humidity down to 27 %, lower than typical humidity. In spite of mostly southwesterly winds, a temporal analysis of aethalometer, SMPS/CPC and PAH data suggested that the wildfire plume resulted in increased black carbon, PM, and PAH

concentrations at the AQMD background site (data not shown). To better focus study results on the influence of the airport and reduce potential complications introduced by differential effects of the fire on our two monitoring locations, data collected during the wildfire was excluded from statistical analyses.

#### *Size Distributions of Ultrafine Particles*

Data from the two minute SMPS/CPC scans were averaged to yield an overall size distribution of particle number concentration at each location. In the September study, a total of 4,639 SMPS scans were recorded at the blast fence and 5,250 SMPS scans were recorded at the AQMD site. The size distribution for the winter campaign is based on 1,100 two minute scans conducted on February 22, 23, and 24. Aggregation of the data obtained from the SMPS yields a robust representative particle size distribution of each site, depicted in Figure 2-4 as the relationship between average mobility diameter,  $D_p$  (nm), and concentration  $dN/d\log D_p$ . Zero values were excluded. The distribution at the LAX blast fence in September '05 included particles ranging from 6.15 to 225 nm (mean particle diameter). The instrument used in the winter campaign and at the AQMD background site measures particles from 7.64 to 289 nm.

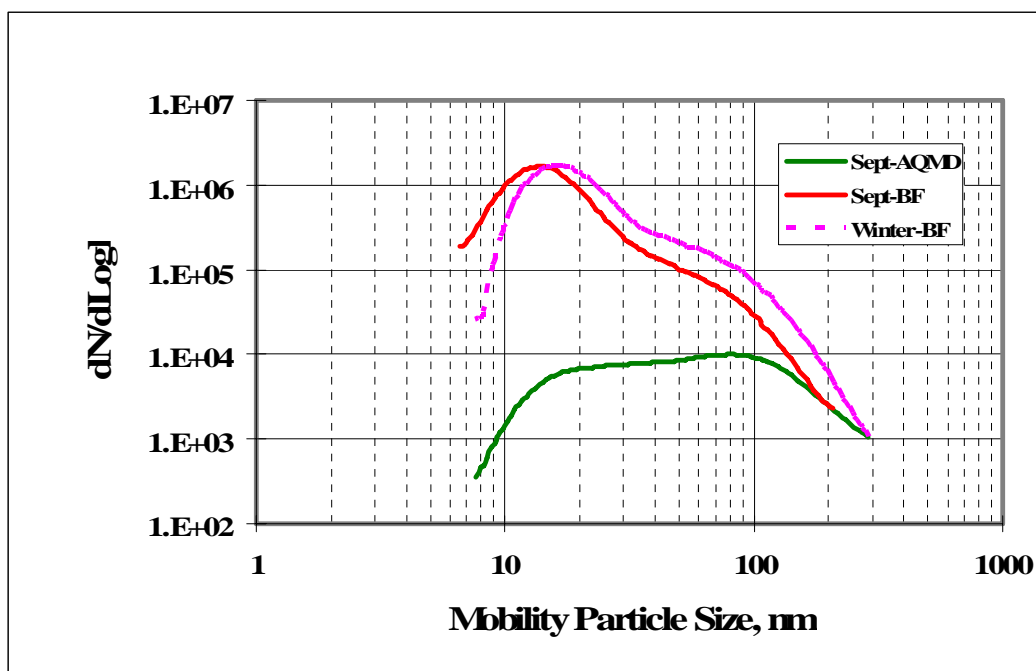


**Figure 2-4: SMPS 120 second scans from near source and background sites, aggregated for each location/sampling time. AQMD is the background site, BF is the blast fence near source site at the LAX runway**

Inspection of Figure 2-4 shows that the distribution of particle size measured at the blast fence is unimodal, with the peak number concentration occurring in the nucleation range at 14 nm ( $dN/d\log D_p = 1.4 \times 10^6$ ) in the summer study and 16.3 nm ( $dN/d\log D_p = 1.3 \times 10^6 \text{ #/cm}^3$ ) during the winter study. A shoulder in the distributions between 50 and 90 nm indicates a slight secondary mode in the accumulation range, for both summer and winter studies. The concentration of particles smaller than the peak mode averages between  $1.4 \times 10^5 \text{ #/cm}^3$  to  $1.4 \times 10^6 \text{ #/cm}^3$  at the blast fence. Concentrations of particles larger than the mode decrease gradually

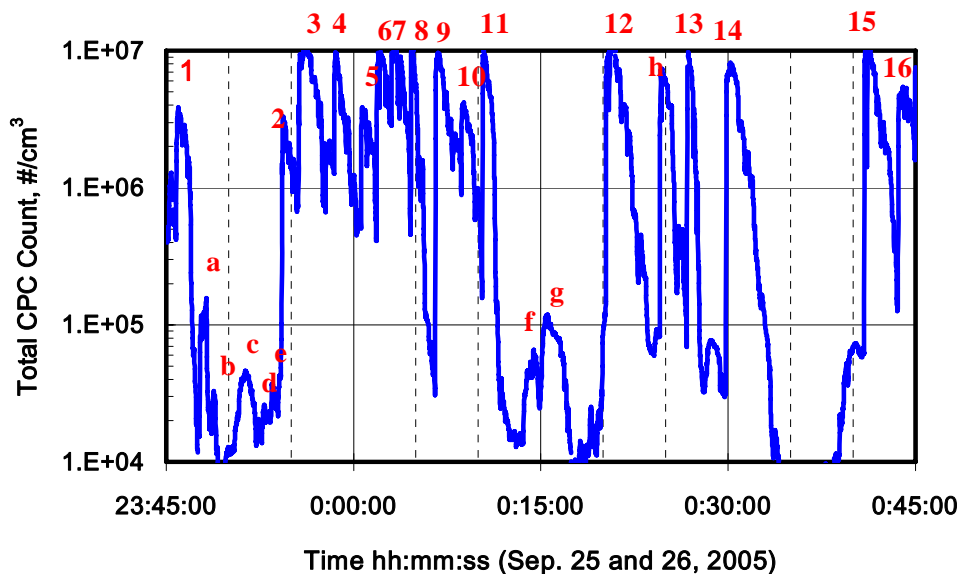
with size, down to about  $2 \times 10^3 \text{ \#/cm}^3$  for 255nm particles. Slight differences in the size distributions between September and the winter sampling campaigns might be contributed to different CPC models as well as the placements of sampling probes at the blast fence.

At the AQMD background site, the size distribution is substantially different. Particle number concentrations are lower throughout the size range and the distribution of particles by size is notably different from that at the blast fence. The defined peak in the 14 – 16 nm size range that characterizes the near source location is absent from the background reference site. At the background site, particles are more evenly distributed across the size range sampled by our instruments, with a weakly defined peak mode at about 80 nm. The concentration  $dN/d\log D_p$  at 80nm is approximately  $1 \times 10^4 \text{ \#/cm}^3$ .

### Total Particle Concentrations

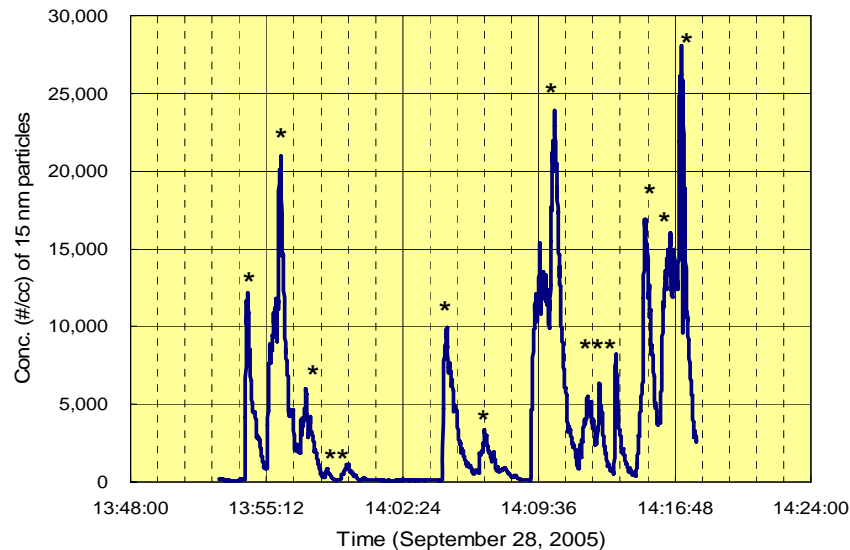
The CPC was used to determine the total concentration of particles within the size range 7 to <300 nm at the blast fence and background site, in one-second scans. At the blast fence, approximately 2% of the data points exceeded  $9.99 \times 10^6 \text{ \#/cm}^3$ , the upper limit of CPC reporting (TSI, 1999). Without the peak concentrations, averages drawn from this data are not informative to describe UFP numbers at the blast fence. A preliminary analysis has been performed of the total count data as a temporal profile. Figure 2-5 shows a selected time series of total counts, with LAX aircraft activity marked in numerals and letters. Numerals correspond to aircraft take-offs on runway 25R. Letters correspond to departures and arrivals on the parallel runway situated slightly to the south, runway 25L. Spikes in UFP concentration are clearly correlated with activity.

Figure 2-5: Time Profile of Total CPC Counts and Identification of Aircraft at Runways 25R and 25L



### Size Specific Particle Concentrations

Size specific particle counts over very short time intervals were performed to capture changes in particle concentration due to isolated aircraft take-off events. The one-second size specific data yielded a complex set of concentration vs. time data for several selected sizes of ultrafine particles. For each of the particle sizes monitored at the blast fence, the temporal profile of measured concentration was highly variable with many prominent peaks in the data. These peaks were associated with aircraft takeoffs, confirmed by inspection of LAX aircraft activity logs. Figure 2-6 depicts the concentration profile of 15 nm particles measured at the blast fence between 13:48 to 14:24 pm on September 28, with departing flights marked by asterisks. This time series clearly shows the variation in particle concentrations emitted from various aircraft taking off during the monitored time period. Specific airline identifiers are omitted, until a more complete analysis of aircraft makes and models can be undertaken. In the absence of a take off event, 15 nm particle concentrations ranged from 60 to 150 #/cm<sup>3</sup>, the baseline of the time profile in Figure 2-6. During take-off, aircraft generated large numbers of particles, ranging up to 28,000/cm<sup>3</sup>. The data from several of the particle sizes that were monitored showed a similar temporal pattern of peaks associated with aircraft activity to that in Figure 2-6 (data not shown).



**Figure 2-6: Temporal profile of 15 nm particles at the blast fence associated with aircraft activity. \*Aircraft take off events.**

The size specific data were also used to analyze the emissions of single cycles of all aircraft take-offs that occurred during a selected time period for the study, during which detailed field notes had been collected. A typical example of a take-off cycle is shown in Figure 2-7, which depicts the time profile of the concentration of 30 nm particles at the blast fence while an aircraft prepared for take-off from LAX. The aircraft traveled east on the 25R taxiway to the blast fence for departure. As shown in Figure 2-7, the concentrations of 30 nm particles gradually increased from a baseline level ~40 #/cc to ~2,800 #/cc. Upon arrival near the blast fence, the aircraft made a 180-degree turn from the taxiway (facing east) onto the 25R runway (facing west). The jet blast rotated in a clockwise direction from the west to the east, resulting in a slight decrease in

particle concentration. Following the 180-degree turn, the pilot initiated take-off, increasing the engine thrust level. The concentration of 30 nm particles dramatically elevated from 1,560 #/cm<sup>3</sup> to 17,200 #/cm<sup>3</sup>, a more than 10-fold increase. The aircraft accelerated along the runway, traveling toward the west away from the sampling location, continuously emitting particles that were blown by jet blast and later transported by prevailing wind toward the blast fence. The particles in this case were dispersed and the concentration (C, in #/cm<sup>3</sup>) exhibited decay characteristics that were described by exponential decay according to the following equation:  $C = C_0 \times e^{-kt} = 17,121 \times e^{-0.08575 \times T}$  ( $R^2=0.9927$ ), where  $T = 0$  is the second when the take-off was initiated and  $C_0$  (in#/cc) represents a characteristic constant for emissions of 30 nm particles for a specific take off event. It might be dependent upon the particle size and type of aircraft. The model constant  $k$  exhibits characteristics similar to particle dispersion in ambient or other physical processes, which might be dependent upon meteorological factors. Although the temporal profile in taxiing and idling prior to take off may vary substantially with specific events, the overall pattern of decay associated with take-offs was very similar. Note that Figure 2-6 is consistent with exponential decay following each peak.

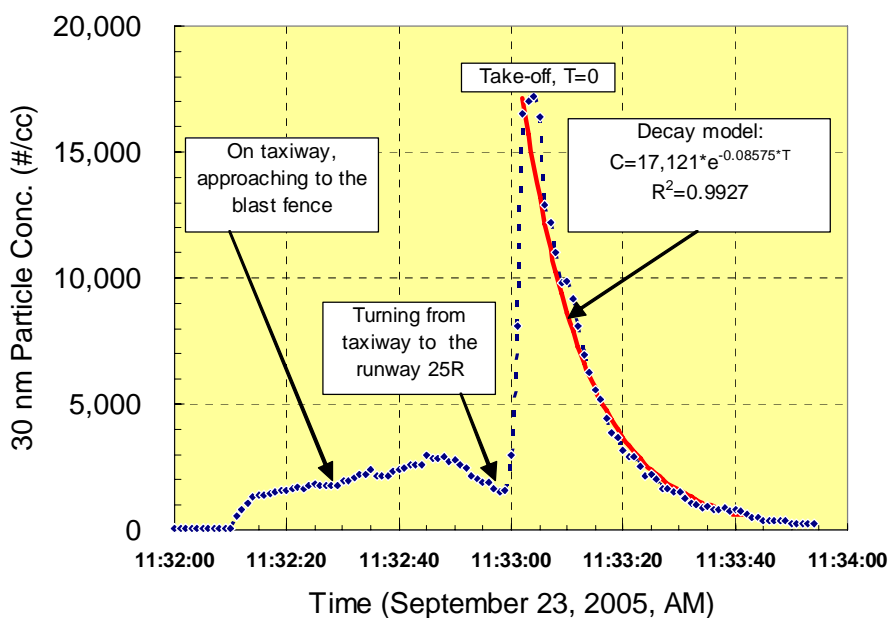


**Figure 2-7: Temporal Profile of 30 nm particles during a take off event**

### *Black Carbon*

The aethalometers was run at the blast fence for 131 continuous hours in September 2005, and 46 hours in May 2006. Sampling intervals were set to 5 min. in September and 10 min. in May. The September 2005 data provided 1,274 observations, with overall average black carbon concentrations at this location of  $13.9 \pm 14.3 \mu\text{g}/\text{m}^3$ . The May 2006 average was  $14.0 \pm 10.2 \mu\text{g}/\text{m}^3$  ( $n=142$ ). The averages for the two sampling periods were not significantly different from each other. At the background reference (AQMD) site, the instrument (5 min intervals) ran for 147 hours in September 2005. The average concentration of black carbon at AQMD site was

0.89 ± 1.2 µg/m<sup>3</sup> (n=1,713). The difference between the two sites was statistically significant (p < 0.001).

### *PM<sub>2.5</sub>*

Time averaged mass concentrations of PM<sub>2.5</sub> are shown in Table 2-2. The mean concentration at the LAX blast fence during the September study was 37.1 ± 15.4 µg/m<sup>3</sup>, which was significantly greater (p < 0.001) than concentrations measured at the background site (14.3 ± 9.9 µg/m<sup>3</sup>). Daily mean PM<sub>2.5</sub> concentrations of the LAX site varied between 32 to 42 µg/m<sup>3</sup> and were consistently significantly greater than the daily means (9 to 18 µg/m<sup>3</sup>) at the AQMD site (P < 0.001 for daily comparisons). Because each measurement is an hourly average, an analysis showing temporal association of PM<sub>2.5</sub> with aircraft activity is not possible at this time.

**Table 2-2: PM<sub>2.5</sub> concentrations (in µg/m<sup>3</sup>) at the blast fence and background reference site (2005 summer study).**

Date	AQMD Mean ± SD	LAX-BF Mean ± SD
9/23/2005	17.8 ± 11.6	42.1 ± 10.9
9/24/2005	16.8 ± 11.2	36.0 ± 17.7
9/25/2005	14.0 ± 7.2	39.9 ± 14.9
9/26/2005	13.8 ± 10.3	36.9 ± 17.8
9/27/2005	9.3 ± 10.2	32.7 ± 21.5
9/28/2005	14.8 ± 9.8	37.9 ± 12.1
9/29/2005	13.3 ± 8.4	33.9 ± 8.5
Overall	14.3 ± 10.4	37.1 ± 15.4*

\*T-test of the difference between the two sites was significant, p<0.001

### *PM<sub>2.5</sub> Polycyclic Aromatic Hydrocarbons*

The results of the 5-day September 2005 sampling campaign for PAHs are summarized in Table 2-3. PAH concentrations at the background site are available for the September period only as noted in the methods section, above. Data collected during the Topanga Canyon wildfire was excluded, since PAH concentrations increased notably at the background site during that time and could therefore obscure the PAH profile associated with the airport (data not shown). At both the near source and reference sites naphthalene comprised 80-85% of the total vapor-phase PAH mass. Higher naphthalene levels were found at the LAX blast fence than at the reference site. Overall, the levels of vapor-phase PAH were consistently higher at the LAX blast fence but the differences between locations for individual species were not statistically significant.

Particle-phase PAH also differed between the two sites. The semivolatile PAHs (from phenanthrene to chrysene) were consistently higher at the LAX blast fence than the background site. On the other hand, the high molecular weight PAHs (from benzo[*a*]pyrene to indeno[1,2,3-*cd*]pyrene) were lower at the blast fence than the background site. Benzo[*ghi*]perylene was the highest concentration particle phase PAH at the background site. The differences in concentrations of individual particle-phase PAHs between the two sites are not statistically significant.

**Table 2-3: Vapor and Particle phase PAH concentrations at AQMD background site and LAX blast fence**

Phase	PAH	AQMD		LAX BF	
		Mean	SD	Mean	SD
<u>Unit: pg/m<sup>3</sup></u>					
Particle	Naphthalene	-	-	14.1	-
"	Fluorene	13.7	-	-	-
"	Phenanthrene	111.1	88.1	175.6	54.6
"	Anthracene	4.7	3.4	10.5	7.4
"	Fluoranthene	91.0	117.3	161.7	48.8
"	Pyrene	106.1	113.4	134.7	63.1
"	Benz[a]anthracene	23.0	19.7	36.4	34.7
"	Chrysene	48.4	46.1	78.2	55.7
"	Benzo[b]fluoranthene	55.6	38.3	56.0	42.8
"	Benzo[k]fluoranthene	22.9	17.9	18.7	15.5
"	Benzo[a]pyrene	46.7	43.0	28.1	33.2
"	Dibenz[a,h]anthracene	7.5	6.1	2.7	0.6
"	Benzo[ghi]perylene	121.2	101.0	49.0	57.1
"	Indeno[1,2,3-cd]pyrene	48.5	36.0	18.3	15.7
<u>Unit: ng/m<sup>3</sup></u>					
Vapor	Naphthalene	55.8	55.9	82.5	64.5
"	Acenaphthene	1.4	1.9	2.8	1.7
"	Fluorene	2.1	2.4	4.7	1.9
"	Phenanthrene	2.0	1.7	4.8	1.8
"	Anthracene	0.1	0.1	0.4	0.2
"	Fluoranthene	0.4	0.1	0.8	0.2
"	Pyrene	0.5	0.2	1.1	0.5
"	Benz[a]anthracene	0.2	0.1	0.2	0.1

### *Volatile Organic Compounds*

Concentration data for four VOCs of interest are summarized in Table 2-4. Comparisons between the two locations, and the two sampling times, are presented in Table 2-5. The mean concentration of formaldehyde at the blast fence was significantly (3-fold) higher than that at the AQMD background site ( $p = 0.006$ ), when data from both periods were combined. Acrolein was also higher at LAX blast fence than at the background site ( $p=0.034$ ), after adjusting for the difference between two sampling campaigns ( $p=0.006$ ). Note that two of three acrolein measurements in May 2005 were below the limit of detection (LOD). These values were estimated by  $LOD/2$ . There were no statistically significant differences in concentrations of benzene or butadiene between the two monitoring sites nor between the two sampling periods,

although butadiene was elevated at the blast fence in September. Concentrations of other VOCs measured during the May 2006 field study are shown in Appendix A; no significant differences were seen between the two sites in VOCs other than those presented in Table 2-4, and most compounds could not be detected.

**Table 2-4: Concentrations (in ppb) of measured VOCs at the near source (LAX\_BF) and background (AQMD) sites during Sep05 and May06 sampling campaigns**

<b>Compound</b>	<b>Period</b>	<b>AQMD</b>		<b>LAX_BF</b>	
		<b>Mean (N)</b>	<b>Std</b>	<b>Mean (N)</b>	<b>Std</b>
<b>Acrolein</b>	<b>May06</b>	0.52 (3) <sup>a</sup>	0.30 <sup>a</sup>	0.90 (3)	0.10
	<b>Sep05</b>	1.03 (3)	0.35	1.26 (4)	0.08
<b>Benzene</b>	<b>May06</b>	0.09 (3) <sup>a</sup>	0.03 <sup>a</sup>	0.27 (3)	0.04
	<b>Sep05</b>	0.42 (3)	0.29	0.52 (4)	0.57
<b>1,3-Butadiene</b>	<b>May06</b>	— <sup>b</sup>	— <sup>b</sup>	0.16 (3) <sup>a</sup>	0.11 <sup>a</sup>
	<b>Sep05</b>	0.15 (3)	0.08	0.36 (4)	0.23
<b>Formaldehyde</b>	<b>Sep05</b>	0.53 (5)	0.22	1.70 (5)	0.66

<sup>a</sup>1 or 2 values were below the limit of detection (LOD) and were estimated by LOD/2

<sup>b</sup>All 3 values were less than LOD

**Table 2-5: Comparisons of VOCs between sites and between two sampling campaigns**

<b>Compound</b>	<b>Comparison</b>	<b>p-value</b>
<b>Acrolein</b>	AQMD vs LAX_BF	0.034*
	Sep05 vs May06	0.006*
<b>Benzene</b>	AQMD vs LAX_BF	0.472
	Sep05 vs May06	0.163
<b>1,3-Butadiene</b>	AQMD vs LAX_BF	0.148
	Sep05 vs May06	0.170
<b>Formaldehyde</b>	AQMD vs LAX_BF	0.006*

\*Statistically significant difference

#### *Problems Encountered during the study*

Overall, the study at the blast fence was successful. The research objectives were mostly accomplished. The near source field site poses challenges associated with the high levels of dust and noise, which pose problems for successful operation of instrumentation and create discomfort for field staff.

Initially, inlet tubing for the SMPS and Aethalometer were placed upstream of the blast fence, through slits in the fencing. But the high PM concentrations including coarse dusts clogged the orifice upstream of the impactor, reduced flow to the instruments, and produced invalid readings. Based on this experience, later sampling was performed with the tubing outside of the white protective cabinets but behind the blast fence. A cyclone was added to filter out large particles that could damage the instruments. As the results show, very high particle counts are still obtained after relocating probes to reduce the impact of coarse dusts.

The probe of the Q-Trak became heavily contaminated with what appeared to be oily residuals from aircraft exhaust mixed with dust. This eventually damaged the sensors. Although we attempted to re-calibrate the sensors, the resulting data were judged questionable or invalid. The Q-trak is typically used in relatively clean ambient environments. If used again in a setting like the blast fence, we recommend that the Q-Trak sensor be better protected from dust.

Technical problems with canister sampling: Although instructions were followed for canister operation there was an unexpected pressure drop in some canisters, resulting in invalid canister samples for two days at the AQMD site and one day at the LAX blast fence.

Permit to access the LAX airfield: Since LAWA has stringent security procedures, we encountered a long delay (about 3 months) to obtain security clearances, badges, and driving permits to the airfield. Security badges and permits were not obtained until September 19, 2005, delaying the onset of field work.

## *2.4 Discussion*

Despite difficulties associated with the LAX field environment, the near source study successfully measured size distribution and size specific concentrations of ultrafine particles immediately downwind of a busy airport runway. Other pollutant concentrations were measured at both the near source and background locations for comparison, and have laid the groundwork for further work to characterize aircraft emissions and the impact of LAX on local air quality. Manuscripts are in preparation reporting results of the near source study, and will be submitted for publication in the upcoming months.

A central finding from the study is that the size distribution of ultrafine particles is notably different at the airport blast fence location (near source) in comparison to the background reference site (Figure 2-4). Note that the size distributions presented in Figure 2-4 represent averages of thousands of SMPS scans. At the blast fence, these aggregate distributions thus reflect samples that occurred during aircraft take off events as well as intermittent background particle levels. Significant differences between the near source site and background were found in the shape of the distribution as well as the average number concentrations across the distribution. The near source site was associated with much higher concentrations of UFP below 100 nm than was the reference site. The maximum concentration difference of 300 fold between the two sampling sites occurred for particles at the concentration mode of the near source distribution (14-16 nm): the average blast fence concentration of 14 nm particles in the summer study was  $1.38 \times 10^6$  compared to  $4.65 \times 10^3$  at the background reference site. The size distribution at the near source site has a pronounced mode at 14-16 nm, and particle number concentrations fall off gradually with particle size beyond the mode, reaching background levels at 200nm. In contrast, UFP concentrations at the background site did not vary substantially with size during the time periods sampled. At the reference site, the distribution of number concentrations increases gradually between about 15 and 80 nm; concentrations fall off at either end of that size range. There was a weak mode at 80 nm.

The size distribution of UFP particle numbers at the blast fence distribution reflects aircraft take off emissions at this location. The aggregate size distribution of the background site, in contrast,

may result from a combination of multiple sources. Examination of hourly-average size distributions at the background site indicates that the shape of the distribution varied at different times of day (data not shown). The aggregate distribution can be described as a combination of two mono-modal distributions and a third distribution without a clearly defined mode.

There was little seasonal effect on the distribution of particle number concentrations at the near source site. The distribution was shifted slightly to larger particle sizes, so that the mode was close to 16 than 14 nm during the winter campaign. This finding may reflect the cooler temperatures, increasing condensation of vapors. It may also be due to a slight systematic difference between the instruments used during the two sampling campaigns.

The very high variability in time vs. concentration profiles such as Figure 2-5 and 2-6 were explained in part by correlating peak particle number concentrations with aircraft take off event obtained from LAWA activity data. The largest spikes of both total particle counts and 15 nm particle counts recorded at the blast fence could be matched in time with aircraft take offs. The finding that spikes were associated with aircraft activity held for each of the UFP sizes that were monitored at the blast fence; the 15 nm temporal profile was selected for illustration in the results section, above. The UFP concentration peaks occur against a background concentration that is orders of magnitude lower in concentration and with substantially less temporal variability. For a future publication, we hope to analyze the data by aircraft type to determine what aircraft features are associated with the greatest emission of UFP. In addition, we are performing analysis of the mathematical properties of concentration decay curves in the 1 sec size specific datasets that describe dispersion of particles emitted at take off, as in Figure 2-7. The peaks and decays examined to date indicate that plume behavior generally follows an exponential decay process.

Average black carbon and PM<sub>2.5</sub> levels at the blast fence were significantly higher than average levels at the background site. This difference is presumably attributable largely to aircraft take off emissions with some additional contribution from ground activity at LAX. There are not other major PM sources in the immediate vicinity of the sampling site. The instruments used for BC and PM<sub>2.5</sub> measurements produced data that was time integrated over 5 minutes for black carbon and 60 minutes for PM<sub>2.5</sub> so that we were not able to match specific peaks of these pollutants with individual aircraft activity, as was possible for the UFP data.

In general, the results of the PAH sampling suggest that aircraft emissions are not unusually high in PAH. PAH at LAX were compared to the reference site which, like the airport, experiences fresh sea breezes during the day and the absence of significant upwind sources. The results show that there were no statistically significant differences in the levels of individual PAH species between the near source and background reference site. However, the pattern of concentrations observed was different at the blast fence vs. the background site. The blast fence was enriched for semi-volatile PAH relative to the background location. LAX had lower concentrations of heavy PAH however, especially notable for benzo[ghi]perylene, often considered a marker for light duty vehicle traffic (Table 2-3). The latter finding suggests that the background site was influenced by vehicular traffic to a greater extent than we had predicted, perhaps due to easterly flows during nighttime hours.

It is potentially informative to compare the results to PAH data for other locations in the Los Angeles Basin that were studied previously, using similar methodology (Eiguren-Fernandez et al, 2004). The blast fence concentrations of the lightest vapor phase PAH (naphthalene through anthracene) were within the range of values seen at other LAB sites. Fluoranthene, pyrene and benz[a]anthracene were somewhat elevated at the blast fence relative to both the AQMD background site and other sampled LAB locations. In contrast we observed that the heaviest particle phase PAH that were studied (dibenz[a,h]anthracene, benzo[ghi]perylene and indeno[1,2,3-cd]pyrene) were found at concentrations that fall in the lower end of the range observed in other community samples, and were lower than the levels measured at the background reference site. It should be noted that ambient concentrations of high molecular weight particle phase PAH are highly temperature dependent with increased concentrations in cold relative to warm weather. This renders comparisons of our findings to the annual average concentrations measured in Eiguren-Fernandez somewhat tenuous. As a general finding, it can be concluded that the data suggest a discernable difference in the pattern of concentrations of individual PAH species observed at the blast fence when compared to average patterns in the community.

Because naphthalene is a carcinogen and present at relatively high levels in the LAB, it was of interest to determine if aircraft could be an important source. Naphthalene levels were higher at the blast fence relative to background, and while the difference did not reach statistical significance the finding suggests that aircraft may be a relevant source of naphthalene. It should be noted, however, that the average naphthalene concentration measured at the LAX blast fence was within the range of annual average naphthalene concentrations measured at twelve LAB locations. Most of the communities studied likely experience a greater influence of roadway vehicles and other upwind sources than does the LAX blast fence location. The blast fence PAH concentrations were clearly greater than those measured in Lompoc, a rural community. The finding that much of the mass of vapor phase PAH at both the LAX and background locations was attributable to naphthalene is consistent with observations reported for several locations in the Los Angeles basin (Eiguren-Fernandez et al, 2004).

Concentrations of some VOC compounds were elevated at the blast fence relative to the background site. However, the marked differences between the two locations that were found in PM were not reflected in the VOC data. Formaldehyde levels were significantly higher than background at the near source site, which suggests LAX operations might be an important source of ambient formaldehyde. The concentrations were perhaps not remarkable in comparison to ambient levels in urban locations, but the blast fence location reflects aircraft and other airport sources alone, against a relatively pristine background of sea air, during typical meteorological conditions. Acrolein levels at the blast fence were also elevated relative to the background site. The acrolein findings are less conclusive due to technical difficulties in measuring this reactive carbonyl compound. Several measurements were below detection limits. Acrolein levels in Sep 05 sampling campaign were significantly higher than those in May 06 sampling campaign. Since acrolein is an atmospheric breakdown product as well as a primary emission, the seasonal difference may be attributable to higher ambient temperatures during September. The daily high temperature during Sep 05 sampling campaign was between 19 to 30°C; while during May 06 sampling campaign it ranges between 17.2 to 17.8°C.

## 3. Downwind Study

### 3.1 Overview

The study was designed to examine number concentrations of UFP and black carbon mass concentrations within a 600 m downwind of the near source blast fence site. In studies of ultrafine particles near busy freeways, it has been reported that the high levels of UFP measured at the freeway approach background levels within 300 m downwind (Zhu et al, 2002a, 2002b). It was therefore of interest to conduct a parallel study for the airport to enable comparison of particle dispersion between these two sources of combustion UFP. A study precisely parallel to the freeway studies is not possible for aircraft runways. Freeway emissions may be considered a line source of pollutant due to relatively continuous traffic flow. An airport runway carries relatively few aircraft. The large plume of exhaust emitted at departure and the minutes that elapse between aircraft departures create very high temporal variability over narrow time intervals, in contrast to a freeway. Another key difference from the freeway scenario is that jet exhaust travels at high velocity from the engine thrust toward sampling locations so that the plumes might be carried farther from the site of emission.

Taking these factors into consideration, a limited experiment was designed to examine UFP particle number concentrations and black carbon mass concentration at locations intermediate between the blast fence and the community sites, which are further to the east and would be studied subsequently. One second CPC scans at 15 nm were performed at five locations, at increasing distance downwind of the take-off runway, 25R. Aethalometers collected black carbon mass concentrations simultaneously, and a weather station was included in the van used for mobile sampling. Sampling was conducted in a field east of LAX that contains landing lights to guide arriving aircraft to runways 25R and 25L. To assess downwind concentrations from departing aircraft, five locations at increasing distance from runway 25R were selected, using the landing light structures as a guide to the downwind trajectory from the runway. A more limited number of samples were taken at similar downwind distances underneath the landing path to runway 25L, which is primarily used for arriving aircraft and was thus expected to have a different spatial distribution of pollutant levels.

The study addressed the following hypotheses:

1. Concentrations of UFP numbers and black carbon mass downwind of the departure runway are intermediate between concentrations measured at the blast fence and those further downwind, in residential communities
2. A concentration gradient, with decreasing concentration over distance from the source of take-off plumes will be observed.
3. In the absence of source tracer analysis, highly time-resolved data can be used to infer the source of particles downwind from the airport, by matching the pattern of particle concentrations observed with the pattern at the blast fence.

The hypotheses assume predominance of southwesterly sea breezes parallel to the runways, the most typical pattern at LAX.

## 3.2 Methods

### *Instrumentation and Sampling Locations*

Two SMPS/CPCs and two aethalometers (one of each provided by ARB and one of each by the Southern California Particle Center), and a Wizard III weather station were assembled for this study. One set of equipment, including the weather station, was installed at the blast fence to provide near source reference data. The other set of instruments was installed in a minivan and driven into a field located downwind of LAX immediately across Aviation Boulevard from the near source location at the 25R blast fence. This field is referred to as the Proud Bird field and houses the LAX landing lights. Battery packs served as the power source for the instruments in the minivan. The van was parked at 5 different locations along the downwind trajectories from runways 25R and 25L in the Proud Bird field (see map in Figure 3-1). Sample sites 1-5 were located from 10m to 400m downwind of the east side of Aviation Blvd, in line with runway 25R. Sites BF, 1, 2, 3, 4, and 5 were 140, 220, 250, 310, 410 and 610 meters downwind of the source (the point along the runway at which take off is typically initiated, marked 'T' on Figure 3-1). Sampling sites A-E beneath the aircraft approach route to runway 25L were spaced at similar distances: 13, 44, 88, 165, and 348 meters from the east margin of Aviation, equivalent to approximately 620, 660, 700, 780 and 960 meters downwind of the point along the runway where landing is primarily located (indicated by 'L' on Figure 3-1).

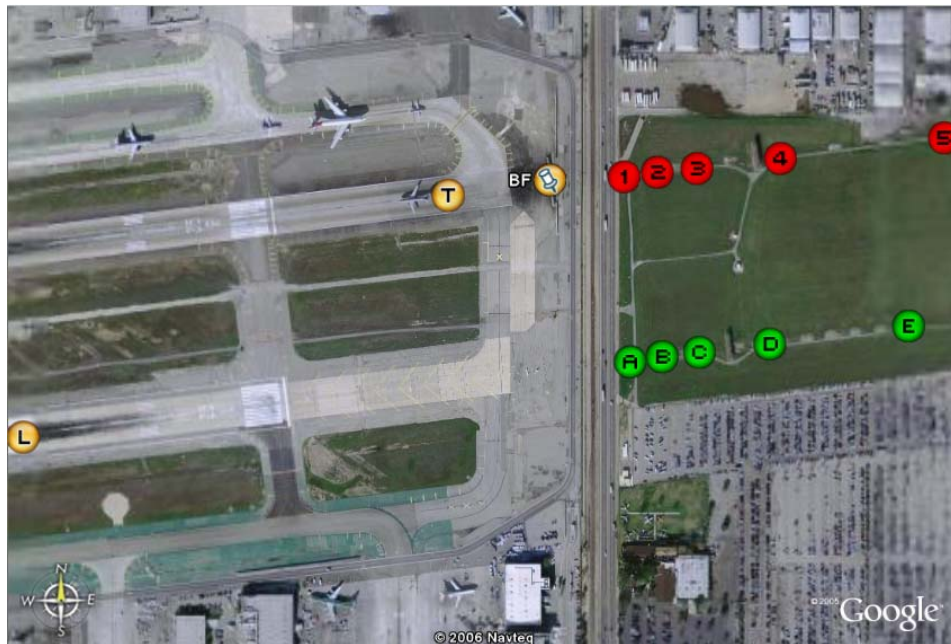


**Figure 3-1: Aerial map showing Proud Bird field and dispersion study sites. L: 25L Landing Point; T: 25R Take-off Point; BF: Blast Fence, 140 m distance from Point T; Red Marked sampling sites: 1-220m, 2-250m, 3-310m, 4-410m, and 5-610m from Point T; Green Marked sampling sites: A-620m, B-660m, C-700m, D-780m, E-960m from Point L.**

### *Sampling Times*

Sampling in the Proud Bird field occurred during two weeks in May 2006. Data was collected downwind from 25R over four days. Monitoring was performed at each location for approximately 2 hours on each of four different days. The data from the four days was combined for each site to enable analysis of summary statistics for black carbon and 15 nm PM.

Monitoring was performed under the landing path to 25L on one day, during which each of the five downwind sites was sampled for about 2 hours.

#### *Traffic Data*

Aviation Blvd. runs north/south, immediately upwind of the field in which the dispersion study was conducted. An automatic traffic counter installed by City of Los Angeles was used to monitor traffic during the study period. In addition, a single 44-minute sampling of 15 nm particle counts was performed at about midday on May 30, 2006 at a parking lot on the west side of Aviation Blvd. The location is not marked in Figure 3-1, but is at the bottom margin of the photo, due south of site 1 and A. This location is not influenced by aircraft on LAX runways and was selected to evaluate the potential impact of street traffic on the downwind study sites.

#### *Data Analysis*

Meteorological data were obtained from SCAQMD. Each measurement of 15 nm particles or black carbon was assigned a wind direction, derived from hourly wind data. Wind data are expressed as compass degrees, with 0 being due north. If the wind was from 200 to 290 degrees (corresponding to west and southwesterly winds) during a sampling period, the resulting data were considered to represent prevailing wind conditions, bringing aircraft emissions to the downwind sites. Analysis presented below was limited to the data collected under prevailing wind conditions.

Runway 25L is occasionally used for aircraft departures in addition to the more common arrivals, and this occurred several times during the sampling. In order to create a clearer basis for comparing plumes from arriving aircraft to departing aircraft, the 15 nm particle data collected downwind of 25L was sorted to exclude data associated with aircraft take offs on 25L.

Box-whisker plots were generated in SAS to compare the distributions of particle number concentration (in units of  $\log\#/cm^3$ ) obtained by the CPC, or black carbon (in units of  $\log\mu g/m^3$ ) at different sampling locations. The lines at the top of, within, and at the bottom of the box of a box-whisker plot represent the 3<sup>rd</sup> quartile, median, and 1<sup>st</sup> quartile of the data, respectively. The whiskers extend up to the highest extreme and down to the lowest extreme of the data, thus defining the range of the data. The upper quartiles of the wind-adjusted data sets were examined separately. From the near-source study, it was apparent that the blast fence experiences sharp spikes of short time duration when aircraft take off and these peaks in the data are clearly distinguished from a general background level that displayed a much lower temporal variability. Taking the upper quartile of measurements is an approximation for manual selection of peaks in the data that are attributable to aircraft plumes. Temporal profiles of particle concentrations were plotted for selected sampling runs. As in the near source study, the time profiles were matched to aircraft activity, to assess whether the spikes in concentration can be attributed to aircraft sources.

### **3.3 Results**

#### *15 nm Particles from 25R*

Figure 3-2 presents the distributions of number concentrations of 15 nm particles measured at increasing distances downwind of the departure runway, 25R. The box plots summarize all the particle number concentration data collected during prevailing wind conditions over the duration

of monitoring at the blast fence and locations 1 through 5 (see Figure 3-1 for locations). The observed concentrations are highly variable. The range of observed concentrations decreases slightly with distance, but remains highly variable. Average number concentrations of 15 nm particles did not change substantially with distance. The graphical analysis was repeated, using only the top quartile of concentrations, to illustrate how the highest concentrations varied with distance (Figure 3-3). Plotting only the top quartile of concentrations is a surrogate for manually inspecting the time series profiles of the data and selecting those concentration peaks that are associated with aircraft departures. The peak concentrations, as represented by the top quartile of data, show a pronounced decrease with increasing distance from the runway.

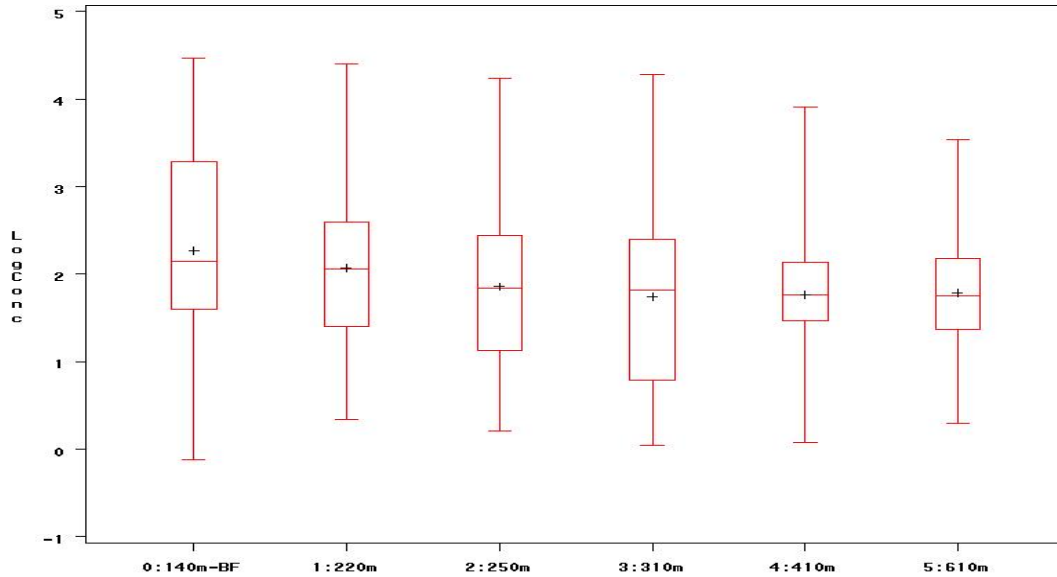


Figure 3-2: 15nm particle concentrations downwind of runway 25R. Locations are described in meters from aircraft take off position. BF: blast fence. Logconc =  $\log\#/cm^3$ .

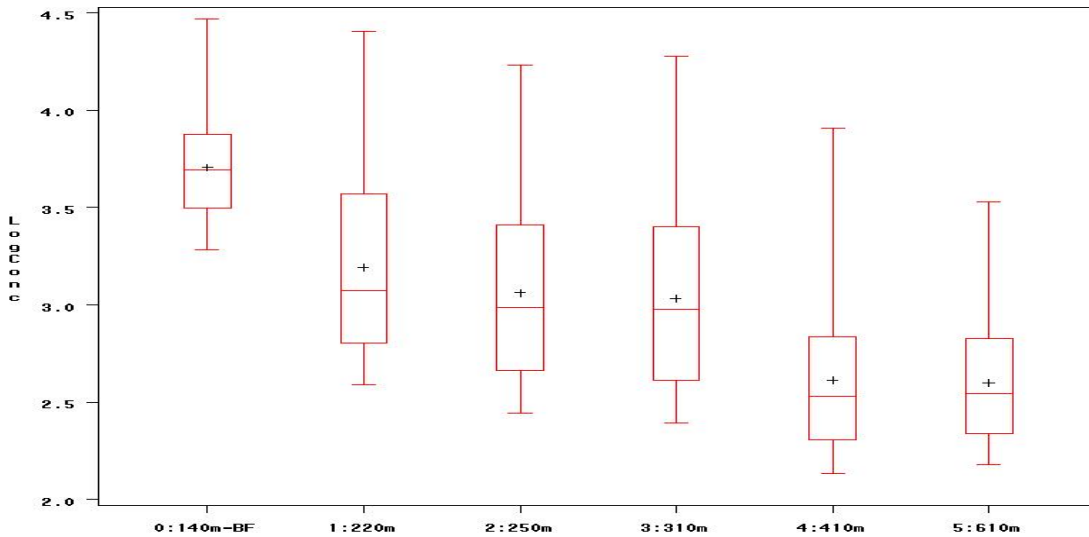


Figure 3-3: 15nm particle concentrations downwind of runway 25R, upper quartile data only. Locations are described in meters from aircraft take off position. BF: blast fence. Logconc =  $\log\#/cm^3$

Temporal profiles of 15 nm PM as measured at downwind locations were compared to profiles of simultaneous measurements at the blast fence near source site. Data from downwind locations 2 and 3 were plotted to illustrate the results. Figure 3-4 depicts the temporal variation in 15 nm particle number concentrations at the blast fence (red profile) and downwind site 2 (blue profile). Site 2 is approximately 110 m from the blast fence, and 250m from the source (the point on runway 25R at which take off is typically initiated). The data at the two locations was collected simultaneously during a period of approximately 30 minutes. The time profiles of particle concentration are very similar. The largest spikes of particle concentration are those associated with take off events, noted in the figure by numerals. Table 3-1 lists the aircraft activity noted by LAX during this period, for comparison with the figure. Take-off spikes of UFP were clearly detected at the downwind site, with a time lag of approximately 15-20 seconds. Figure 3-5 compares 15 nm number concentrations at the blast fence to Site 3, which is 170 m downwind of the blast fence and 310 m from the point of take-off. Again, UFP spikes observed at the blast fence are clearly detected downwind, with a time lag of approximately 20 seconds. Note that during the time period when there were no take-offs, there were no concentration spikes at either the blast fence or downwind location.

**Table 3-1: Aircraft departures on runway 25R associated with data profiled in Figure 3-4.**

Label	Time	ID	Type
1	16:02:08	UAL326	B752
2	16:03:59	AAL2454	MD82
3	16:06:08	SQC7987	B744
4	16:08:03	XAARQ	LJ31
5	16:09:27	COA1503	B738
6	16:11:55	AAL1744	MD83
7	16:16:36	AAL22	B762
8	16:18:08	SKW6526	CRJ2
9	16:19:08	UAL116	B763
10	16:22:22	EGF087	SF34
11	16:26:41	SKW6508	CRJ2
12	16:28:55	UAL28	B752
13	16:30:37	DLH453	A343
14	16:37:55	AAL180	B762
15	16:40:00	AAL1546	MD83
16	16:42:32	SKW6507	CRJ2

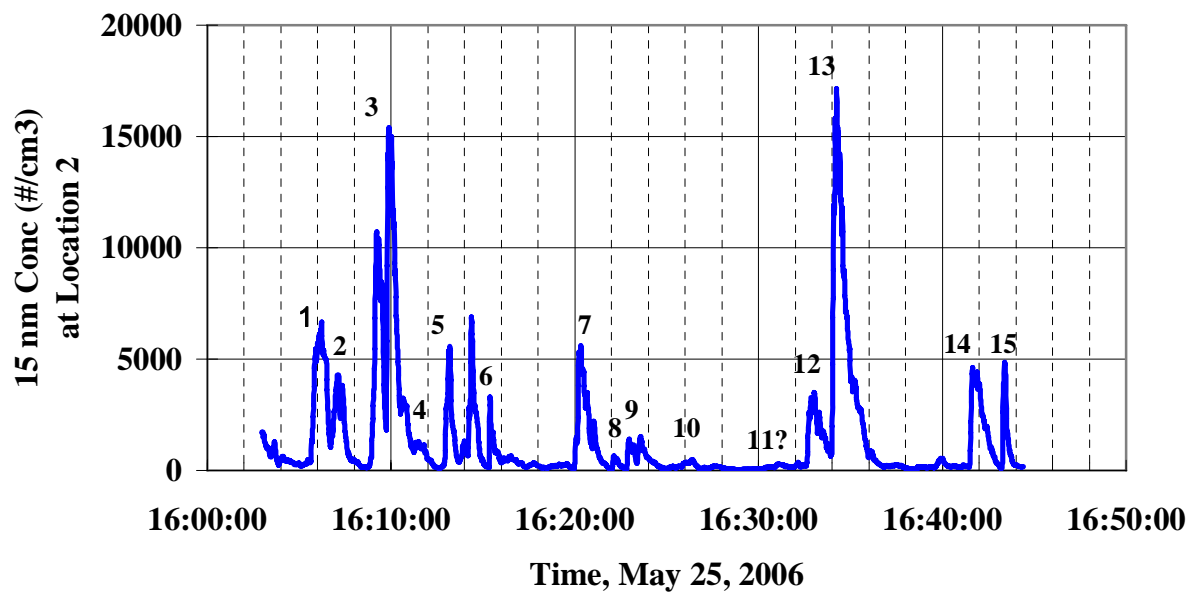
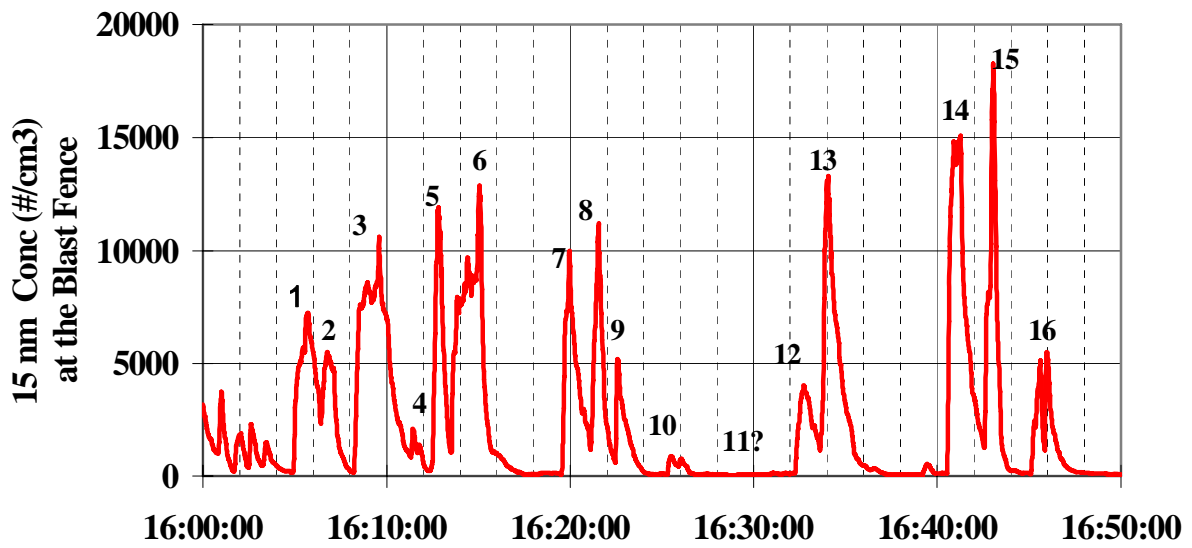
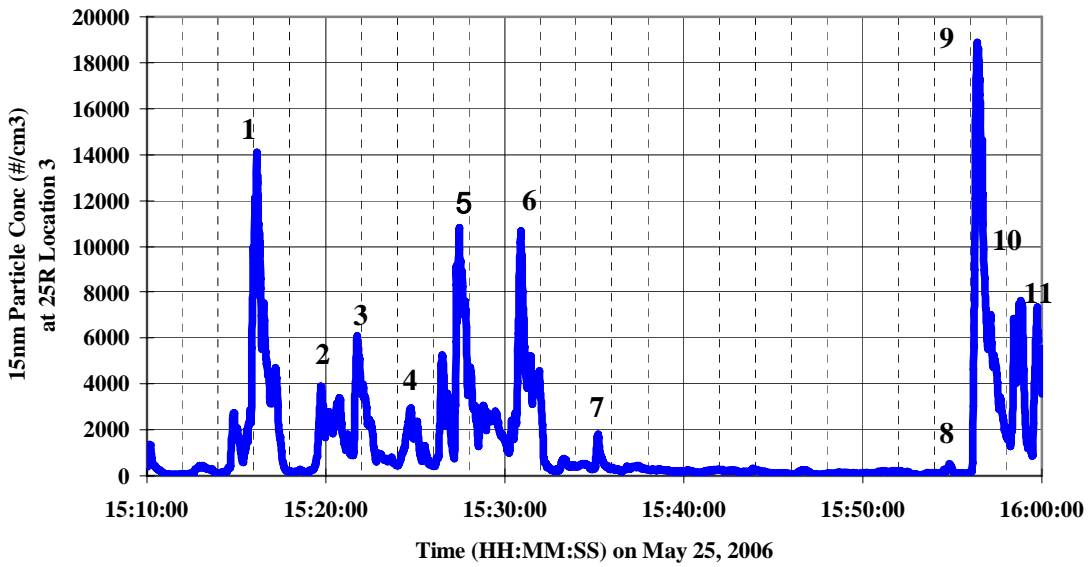
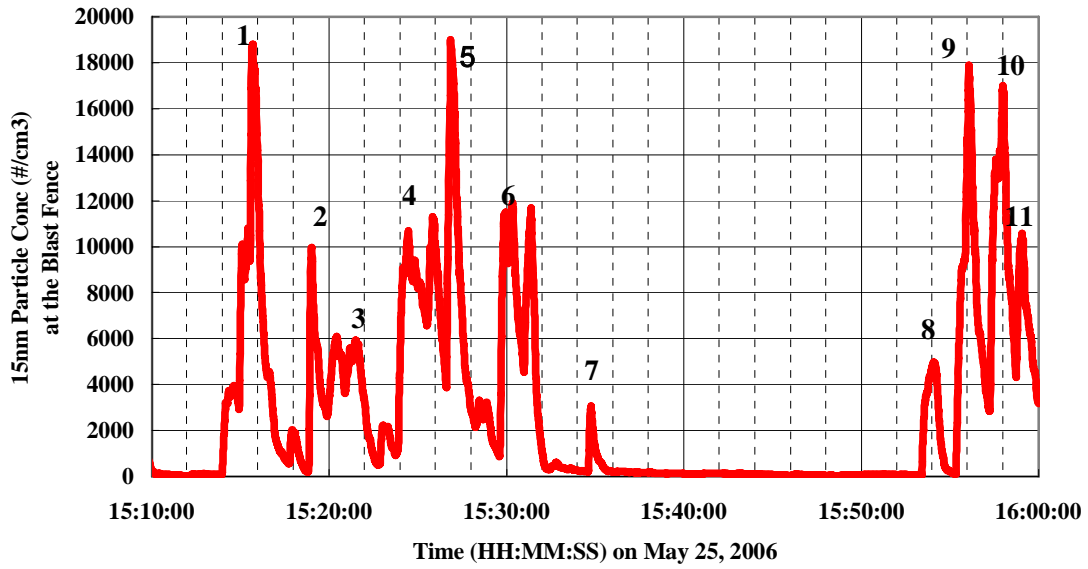


Figure 3-4: Temporal profile of 15 nm particle concentrations at the LAX blast fence (red, upper), and a site 110 m downwind of the blast fence (blue, lower) during the same time period. Aircraft departures logged by LAX are noted with numerals, see Table 3-1 for details.



**Figure 3-5: Temporal profile of 15 nm particle concentrations at the LAX blast fence (red, upper), and a site 170 m downwind of the blast fence (blue, lower), during the same time period. Aircraft departures logged by LAX are noted with numerals, see Table 3-2 for details.**

**Table 3-2: Aircraft departures on runway 25R associated with data profiled in Figure 3-5**

Label	1	2	3	4	5	6	7	8	9	10	11
Time	15:15	15:17	15:19	15:22	15:23	15:26	15:31	15:50	15:52	15:54	15:55
ID	SIA011	UAL164	N86TW	ACA744	DLH457	COA1597	AAL768	EGF085	CAL005	AAL2452	UAL114
Type	B744	B752	F2TH	A320	B744	B737	MD83	SF34	B744	B738	B763

*Black Carbon from 25R*

Figures 3-6 and 3-7 summarize black carbon concentrations at the blast fence and downwind sites 1-5, using all or just the upper quartile of data, respectively. The peak concentrations of black carbon (as estimated by the top quartile of the data in figure 3-6) fall off with distance. A concentration gradient is less evident when the complete data set is plotted, as seen in figure 3-6.

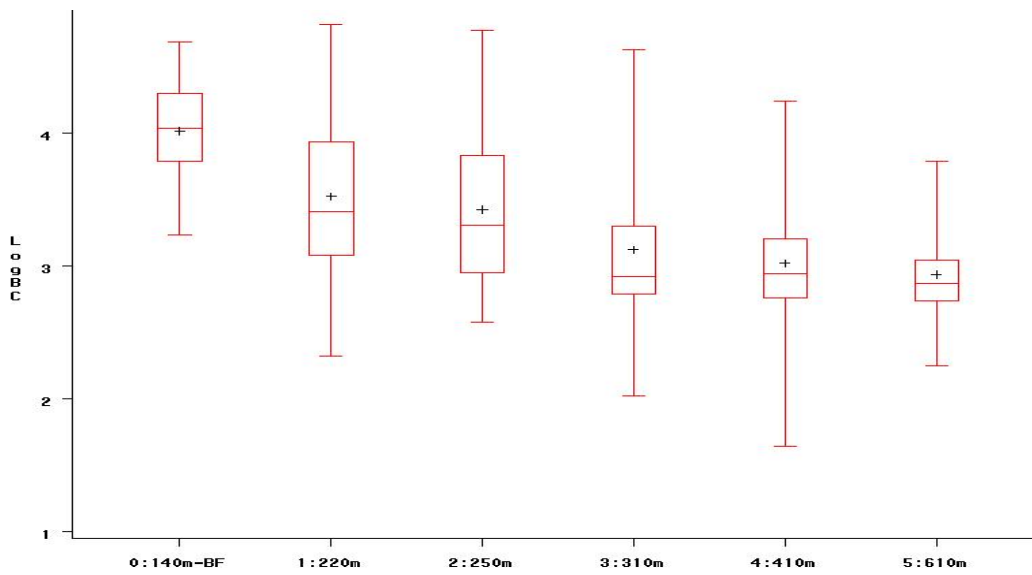


**Figure 3-6: Black carbon concentrations downwind of runway 25R. Locations are described in meters from aircraft take off position. BF: blast fence. LogBC =  $\log \mu\text{g}/\text{m}^3$**

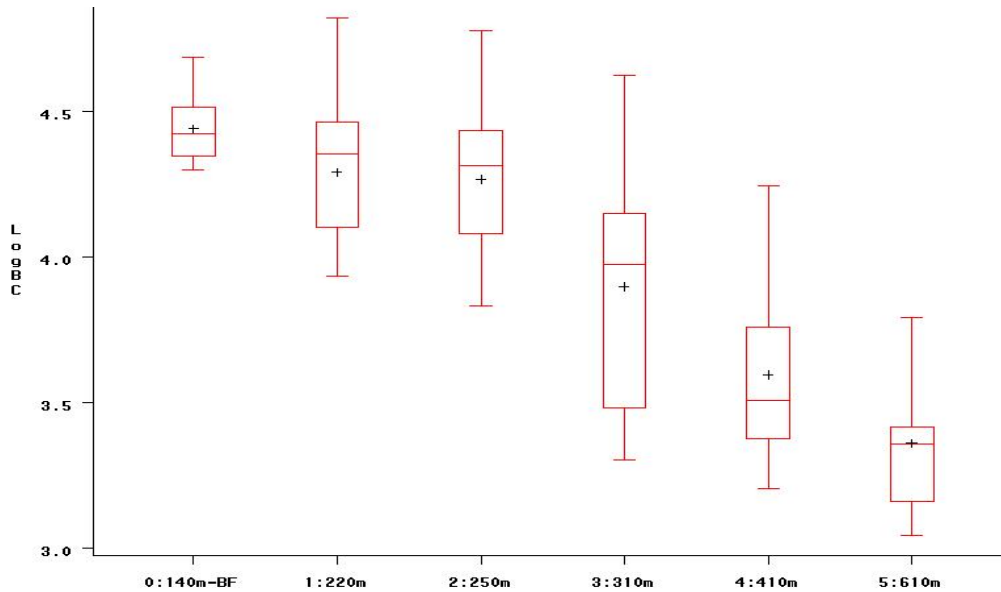


**Figure 3-7: Black carbon concentrations downwind of runway 25R, upper quartile data only. Locations are described in meters from aircraft take off position. BF: blast fence. LogBC =  $\log \mu\text{g}/\text{m}^3$**

#### *15 nm Particles and Black Carbon from Runway 25L*

A similar analysis to that described above for data collected downwind of runway 25R was performed for a set of locations under the landing approach to runway 25L. As noted in methods, we excluded the data associated with occasional aircraft departures on this runway, to enhance comparison of arriving and departing aircraft emissions. Box plots of 15 nm particle concentrations using the complete data set or the top quartile only are shown in Figures 3-8 and 3-9, respectively. Data on 15 nm particles from both runways are also summarized in Table 3-3. The average concentrations of particles (all data) were not significantly different than average concentrations observed downwind of runway 25R. Concentrations of 15 nm PM averaged roughly  $100/\text{cm}^3$  at all locations; the average concentration did not show a pattern with distance. Looking just at the top quartile of concentrations, the pronounced decrease over distance that was observed for the departure runway 25R does not appear downwind of 25L. Black carbon concentrations downwind of 25L did decrease with distance, and this was apparent when looking at either the complete data set (Figure 3-10) or the top quartile only (Figure 3-11).

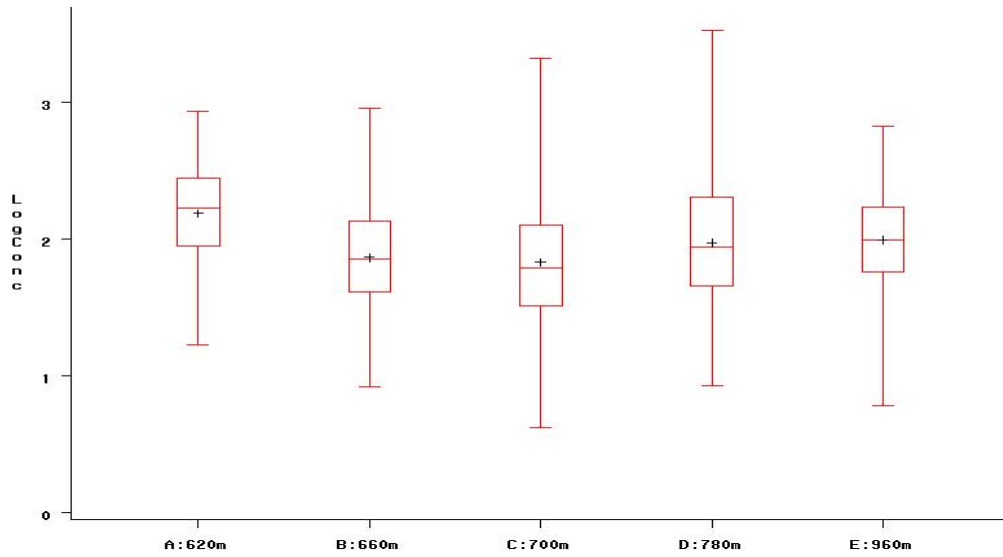


Figure 3-8: 15nm particle concentrations downwind of runway 25L. Locations are described in meters from aircraft landing point. Logconc =  $\log\#/cm^3$

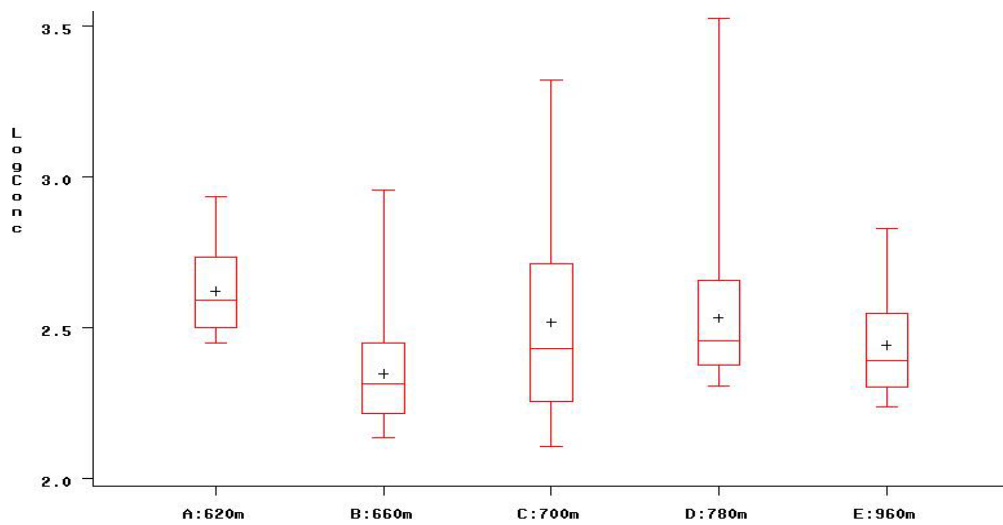
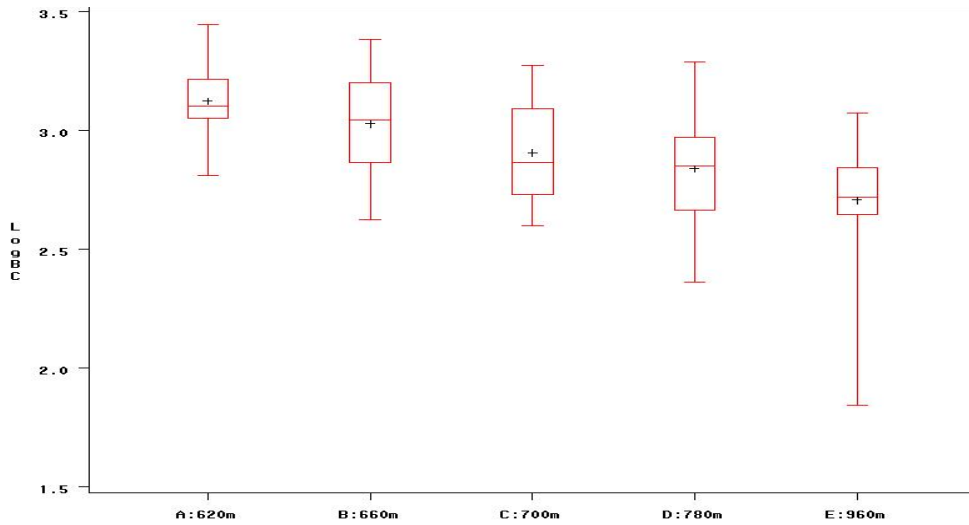
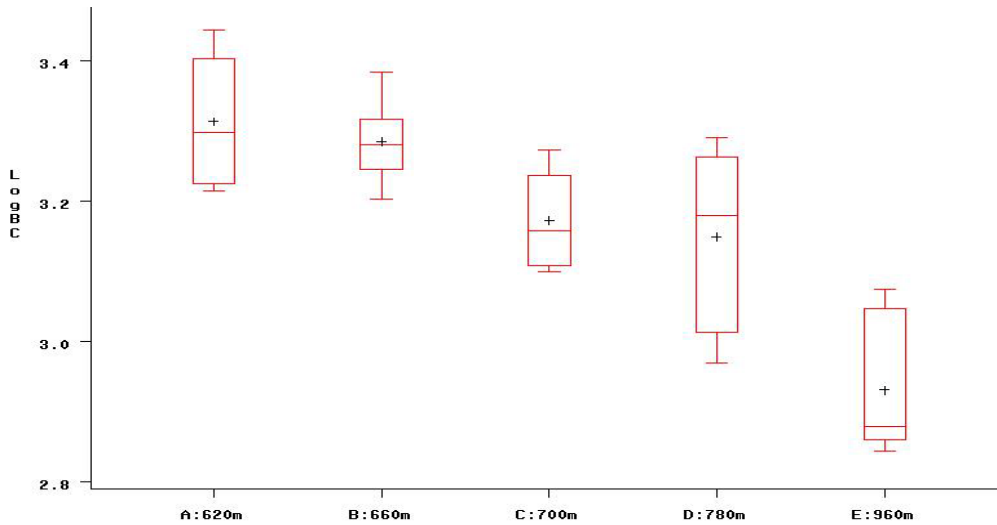


Figure 3-9: 15 nm particle data collected downwind of runway 25L, upper quartile only. Locations are described in meters from aircraft landing point. Logconc =  $\log\#/cm^3$



**Figure 3-10: Black carbon concentrations downwind of runway 25L. Locations are described in meters from aircraft landing point.  $\text{LogBC} = \log \mu\text{g}/\text{m}^3$**



**Figure 3-11: Upper quartile of black carbon concentrations downwind of runway 25L. Locations are described in meters from aircraft landing point.  $\text{LogBC} = \log \mu\text{g}/\text{m}^3$**

Table 3-3 presents summary data for 15 nm PM number concentrations, presented in the figures above. The data collected at the blast fence and in the 40-minute sampling performed adjacent to Aviation Blvd, but upwind of the runways is included for comparison. The 90<sup>th</sup> percentile particle concentrations were significantly higher downwind of 25R in comparison to 25L and this held for all five distances from the runways. Recall that data collected during occasional departures on runway 25L were excluded to better characterize any differences between arriving and departing aircraft effects. The difference between runways is less notable at the median particle number concentrations, which reflect background concentrations in the area.

**Table 3-3: 15nm Particle Concentrations (dN/dlogDp in #/cm<sup>3</sup>) at LAX blast fence (BF), near Aviation Blvd, and study locations in the Proud Bird Field (PBF)**

Location	1st Quartile	Median	3rd Quartile	90% Percentile
LAX BF-140 m <sup>a</sup>	55	247	2655	6936
PBF - 25R:				
1 – 220 m <sup>a</sup>	25	115	390	1640
2 – 250 m <sup>a</sup>	14	70	277	1380
3 – 310 m <sup>a</sup>	6	66	248	1460
4 – 410 m <sup>a</sup>	29	58	136	430
5 – 610 m <sup>a</sup>	23	56	152	442
PBF - 25L:				
A – 620 m <sup>b</sup>	89	169	281	419
B – 660 m <sup>b</sup>	41	72	137	229
C – 700 m <sup>b</sup>	33	61	128	344
D – 780 m <sup>b</sup>	45	88	204	320
E – 960 m <sup>b</sup>	57	99	173	281
Aviation Blvd traffic	32	39	57	82

<sup>a</sup>Distances from the take-off point of runway 25R.

<sup>b</sup>Distances from the landing point of runway 25L.

#### *Problems Encountered during the study*

No significant technical problems were encountered during the downwind study.

### **3.4 Discussion**

Near-continuous sampling of 15 nm particles at locations 220-610m downwind of runway 25R at LAX was the major focus of the downwind study. Simultaneous sampling was carried out at the near source site (the 25R blast fence), and some exploratory sampling beneath the approach to runway 25L was also performed. Black carbon mass concentrations were collected at all field locations in the downwind study. Data were analyzed by summary statistics and analysis of temporal profiles of 15 nm particle number concentrations, after reducing the data set to those observations collected during prevailing wind conditions. Size distribution data were not collected in this study due to the exploratory scope. Rather, the purpose was to carry out near real time sampling to capture temporal variability in 15 nm PM associated with aircraft activity.

As a general finding, number concentrations of 15 nm particles and concentrations of black carbon measured at downwind locations were lower than at the blast fence, indicating that aerosol associated with aircraft take-off disperses over the study distances (220-610 m from aircraft and 80-470 m from the blast fence). This finding supports the first hypothesis. The size distribution of UFP number was not assessed, so it is not currently known whether the size distribution undergoes shape changes as the plume moves away from the source and this is a significant limitation of the current study.

With regard to the second and third hypotheses, that a concentration gradient downwind from take-offs would be observed and that simultaneous sampling at the blast fence would allow source identification, the findings are somewhat more complicated although the data do support both hypotheses. An important finding is illustrated in figures 3-4 and 3-5. The temporal

profiles of 15 nm particles collected 110 and 170 m downwind of the blast fence were very similar to the profiles of particles collected simultaneously at the blast fence. The times of particle concentration peaks in the two downwind site profiles could be matched to the times of aircraft departures, with a somewhat variable time lags between the official recorded take off time, the observed spike of UFP at the blast fence, and the spikes observed farther downwind. Before the study was initiated, there was concern that obstruction of take off exhaust by the blast fence may complicate dispersion of aircraft exhaust plumes. However, the data demonstrate that exhaust plumes resulting from aircraft take-offs are easily detectable 300m downwind, within seconds after aircraft take-offs. Exhaust plumes from aircraft are emitted forcefully, and the results in Figures 3-4 and 3-5 indicate that aircraft exhaust plumes can travel considerable distances. While the impact of such 'forced' dispersion would be the subject of further research, take-off blasts could be felt by field staff at downwind sampling sites, providing some empirical evidence that the blast fence only impedes some part of the force and UFP are carried farther from the source than, for example, has been observed with passive dispersion from freeway traffic. Studies of UFP dispersion at busy freeways have reported that UFP concentrations diminish to background levels over distances of 100-300 m. An additional feature of interest is apparent in figure 3-5: during a time period when no take-offs occurred on runway 25R, 15 nm PM concentrations were low and steady at both the blast fence and downwind locations. This observation demonstrates again that downwind peak concentrations are dependent on aircraft activity.

Figures 3-3 and 3-7 show a consistent downwind decay for the upper quartile measurements of 15 nm particles and black carbon, respectively. Again, the results demonstrate that the blast fence does not entirely disperse aircraft take-off plumes and a spatial concentration gradient is formed from take-off derived particles, in agreement with the second study hypothesis. One explanation is that the vertical air redirection by the blast fence occurs only for the first few seconds along the approximately 90- second take-offs. As aircraft travel westward toward the Pacific Ocean, the exhaust plume may gradually mix with ambient air and become part of air parcels carried by prevailing wind along the trajectory over the downwind study sites.

It should be noted that the five downwind locations could not be sampled simultaneously so that the data cannot describe the dispersion behavior any single plume moving across the field. Some of the inter-location variation in the downwind field site may therefore arise from time-varying factors such as different aircraft, slight changes in meteorology, and local road traffic flux all of which may complicate comparisons between sampling locations. Wind direction has been accounted for to some extent by excluding data collected during times when the wind direction was from other than 200-290 degrees. The potential complications of the serial sampling are also offset somewhat by the fact that each location downwind of 25R on four different days.

Despite the clear association of peak particle concentrations at the downwind locations with peaks at the blast fence, the average concentration of 15 nm particles did not vary substantially with increasing distance from the blast fence (figure 3-2). The finding that average concentrations were not location dependent suggests that there is a background level of 15 nm particles at the downwind locations that is not directly influenced by take-off events. When data primarily associated with take off peaks was analyzed separately (by selecting the upper quartile of concentrations) a dispersion pattern across locations became apparent (figure 3-3). There is a

clear spatial gradient in the highest concentration spikes, decreasing over distance. Comparing 15 nm PM concentrations downwind of the take-off vs. landing runways, the average concentration under the landing path was somewhat lower than downwind of take offs but aerosol appears to distribute across the study field resulting in relatively homogenous time-averaged concentrations at all locations. Peak concentrations were clearly not spatially homogeneous though, and showed a clear trend to decrease with distance from take-offs, as discussed above.

A second concern during study planning was the potential inference of particles emitted by vehicles traveling on Aviation Blvd. A test SMPS/CPC monitoring was performed at a location immediately to the east of Aviation Blvd., but south of the downwind study sites and the airport runways. Particle concentrations were low, as shown in Table 3-3. A temporal analysis of that data (not shown) did not identify peaks with the characteristic shape and duration associated with aircraft takeoffs, but did display a pattern typical of passing vehicles. Aviation traffic appears to contribute at low levels to the background particle concentrations observed at the downwind locations, but does not produce peak concentrations of 15 nm particles comparable to those associated with aircraft takeoffs, and so the two sources are easily distinguished by carrying out temporal analyses and by limiting analysis at the downwind sites to the upper quartile of data. The findings show that traffic along Aviation Blvd has a negligible impact on the interpretation of the peak concentrations observed in this study.

Analysis of the concentrations of black carbon downwind of runway 25R yielded a similar pattern of findings to that observed for 15 nm particles at the same locations. Average concentrations of black carbon did not show a trend to decrease with distance. The top quartile of concentrations, which presumably reflects carbon contained in take-off plumes, did show a decreasing trend with increasing distance from the runway, as was observed with 15 nm PM. An analysis of temporal profiles of black carbon, in parallel to the figures describing 15 nm particles over time, could not be performed for black carbon because the aethalometer data is integrated over 5 minute intervals while aircraft take-off plumes show decay over periods of about one minute.

Under the landing path, concentrations of 15nm particles did not show a spatial gradient over the distances measured, regardless of whether the entire data set or top quartile was plotted. Note that particle concentrations collected during take-offs were not included, to emphasize particle concentrations that occur during landings. The lack of a spatial gradient can be attributed to the fact that aircraft-derived PM at these locations is emitted overhead from landing aircraft in contrast to the directional source (take-off exhaust) that creates the spatial gradient at locations downwind of 25R. Temporal analysis of particles at landing path locations did identify peaks of particle number concentration when aircraft passed overhead (data not shown). The peaks were substantial compared to background levels that occurred between landing aircraft, but were lower in concentration than peaks associated with aircraft take offs. The temporal patterns of particles under the landing path should be further analyzed as only a preliminary analysis has been done to date. The findings suggest that both departing and arriving aircraft emit 15 nm PM, but to assess whether the size distribution of emissions from landing aircraft differs from that observed for aircraft take-offs requires performing complete size distribution scans, and could not be done in this study.

In contrast to the findings on 15nm PM, black carbon concentrations clearly increased closer to the airport, under the landing path. It is not clear why black carbon would show the expected increase as planes draw closer overhead, yet a related pattern was not observed for 15 nm UFP. It is possible that increasing black carbon is not so much a function of the overhead distance of the plane, but of engine conditions for decelerating aircraft that result in higher black carbon emissions in the final moments of deceleration, while having a limited effect on the number concentrations of the very smallest particles.

## 4. Community Study

### 4.1 Overview

The objective of the community study was to conduct an initial characterization of UFP in neighborhoods downwind of LAX, and to investigate the potential contribution of aircraft emissions to local ambient PM levels. A minivan installed with monitoring equipment was deployed to monitor 15 nm particle number concentration, size distribution of particles ranging <10 - 200 nm and black carbon. An E-BAM mass monitor was installed beside the minivan to monitor hourly levels of PM<sub>2.5</sub>. This equipment was deployed over a four week period for three days at six community sites downwind of LAX runways and east of I-405. The sites were studied sequentially. Three of the six sites selected were located directly beneath the aircraft landing path. The other three were 1) slightly north of the landing path and close to I-405, 2) north of the landing path at a greater distance from I-405, and 3) south of the landing path and distant from the I-405.

The study was planned to explore the following hypotheses:

1. Ambient black carbon and UFP levels are elevated in communities downwind of LAX relative to an upwind reference site.
2. Elevated black carbon and UFP levels at downwind community sites are attributable to westward dispersion of plumes emitted at LAX and emissions from landing aircraft that pass directly overhead.
3. Community sites directly beneath the landing path experience greater UFP and black carbon levels than those to either side of the approach.

### 4.2 Methods

#### *Instrumentation and Sampling Locations*

A SMPS (TSI, model 3080, DMA model 381) along with a CPC (TSI, model 3025) were connected to a laptop computer to measure particle size distribution from 6.15 to 225 nm. Concentration of 15 nm particles was monitored over one second intervals by fixing the size in the SMPS. An Aethalometer (Magee Scientific, AE-20) was used to monitor black carbon over 3-5 minute time intervals. Instruments were set up in a minivan, with power supplied by 4 marine batteries installed in the vehicle. An E-BAM mass monitor (Met One) was installed near the minivan to monitor hourly PM<sub>2.5</sub>.

Sampling locations were selected in the Lennox and Inglewood areas, downwind of LAX, east of I-405, and north of I-105. Figure 4-1 shows the location of six community sites, with reference to the blast fence (BF) near source site, aircraft take-off point (T) on runway 25R, and aircraft landing point (L) on 25L. Detailed characteristics of the sites are shown in Table 4-1.

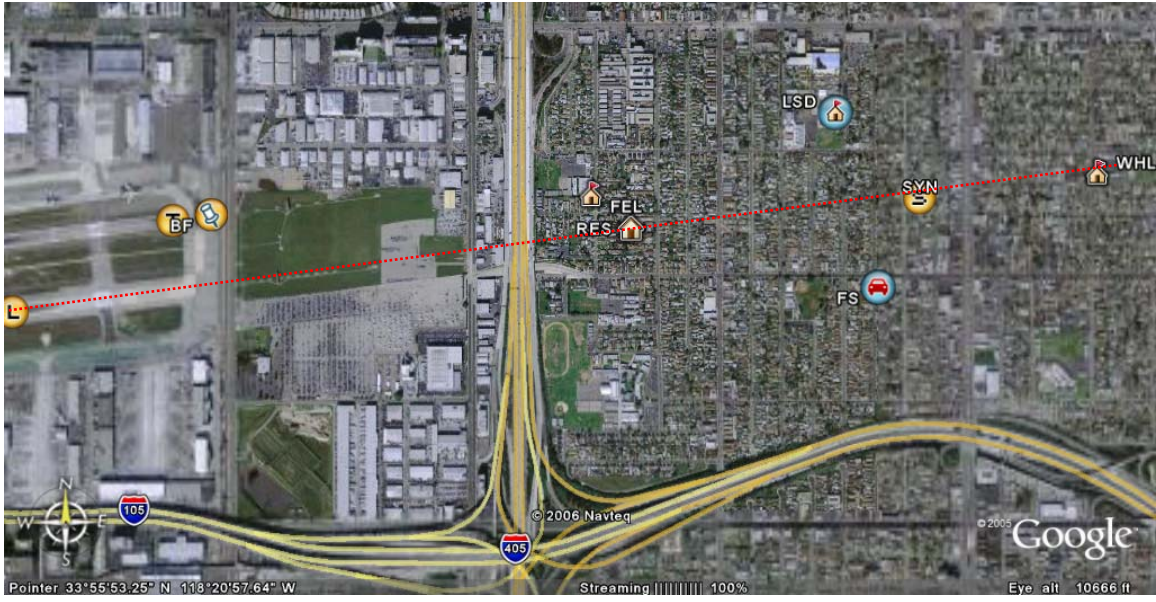


Figure 4-1: Location of six community sites. Red dotted line: aircraft landing path with a gliding angle = 3°. L: 25L Landing Point; T: 25R Take-off Point; BF: Blast Fence; FEL: Felton School; RES: a Buford local resident; SYN: a synagogue; WHL: Whelan School; FS: Fire Station; LSD: Lennox School District.

**Table 4-1: Characteristics of six community sites**

Site	Distance from I-405 (m)	Position relative to the landing path	Estimated aircraft altitude (m)
Felton School	200	120 m north	97
Local Resident	337	Directly beneath	104
Synagogue	1325	Directly beneath	156
Whelan School	1810	Directly beneath	182
Fire Station	1170	300 m south	150
Lennox School District	1030	300 m north	140

#### *Monitoring Campaign*

The field study took place in June 2006. At the beginning of each monitoring effort at a community site, a relatively safe and convenient location was chosen to park the minivan, to minimize effects of local traffic. The above mentioned instruments were installed at the synagogue from June 6 to 10, at the backyard of the local resident in the sampling area from June 12 to 15, at the fire station from June 15 to 19, at Whelan School from June 20 to 23, at Felton School from June 23 to 26, and at Lennox School District from June 26 to 30, 2006. Sampling intervals for each instrument were as stated above.

### *Data Analysis*

Meteorological data were obtained from SCAQMD. Each measurement was assigned a wind direction, based on hourly wind direction. Data were included under prevailing wind conditions if the wind direction was between 200 and 290 degrees (0 degree = wind blowing from the north). Otherwise, the data were excluded from the analyses presented below.

### *Method for Calculating $PMN_{10-100}$ :*

A metric referred to as  $PMN_{10-100}$  was developed for analysis.  $PMN_{10-100}$  is the total PM number concentration for particles with mobility size between 10 to 100 nm. In this study, SMPS and CPC were coupled together to collect PM size distribution from 6.15 to 225 nm by CPC model 3025 and 3022 and from 7.64 to 289 nm in the sizes by CPC model 3785. Thus, the sum of particle numbers originating from different instrument models couldn't be directly compared.  $PMN_{10-100}$  provides a convenient parameter to measure total counts of an important subset of UFP. 2-minute size scans were performed and are the basis of the computed metrics. Zero values occasionally occur in the SMPS/CPC scan data. Zero values were substituted by the average number concentration of non-missing and non-zero values from three sizes less than and three sizes greater than the desired size within the same size distribution for a time period. Number concentrations of particle sizes between 10 to 100 nm were summed first to obtain a raw  $PMN_{10-100}$ . Hourly concentrations were then estimated by averaging the raw  $PMN_{10-100}$  for each hour of interest. Site specific statistics of hourly  $PMN_{10-100}$ , as shown in Table 4-3, were estimated from hourly  $PMN_{10-100}$  collected for a sampling site. Mean, standard deviation, and number of wind adjusted hourly  $PMN_{10-100}$  were reported.

## **4.3 Results**

### *Wind Pattern*

Figure 4-2 is a frequency distribution of wind directions that occurred during the study period. Wind directions are described by compass reading, 0° being due north. Wind direction data was grouped into 10° intervals, from 180° to 300°. The LAX runway is situated at 260° relative to the community. During the community study period, winds arose most frequently from 230° to 250° (nearly 40%), somewhat more southerly than the direction of the runway and the expected prevailing winds. The wind direction may have resulted in a decrease in LAX-associated plumes at the study sites compared to what was expected during planning of the study.

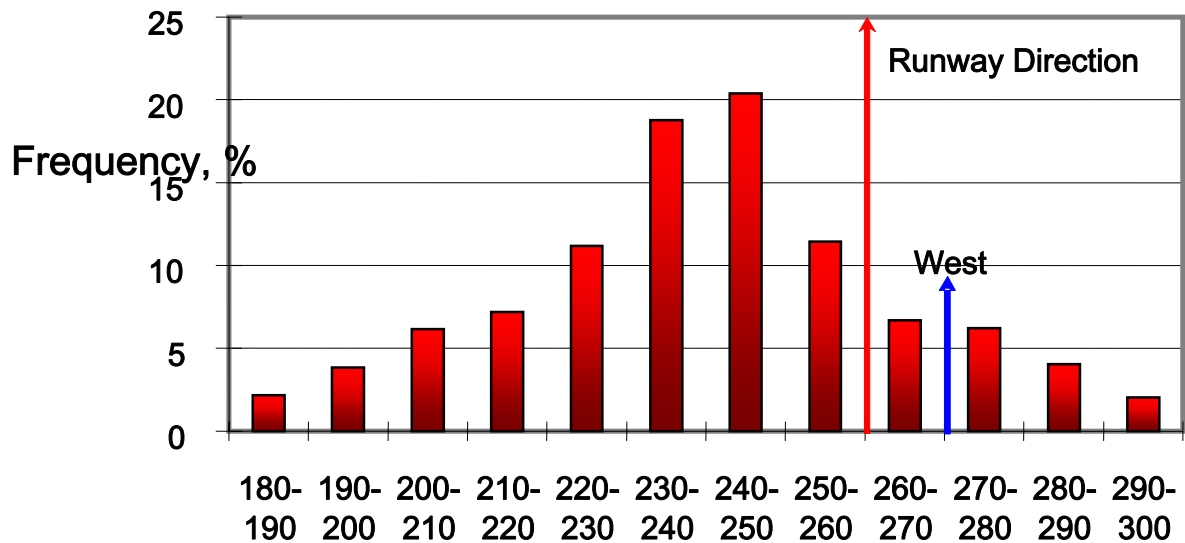


Figure 4-2: Distribution of wind direction in June 2006

#### *Particle Size Distributions*

Figure 4-3 depicts the particle size distributions obtained at community sites. Each distribution is the average of many SMPS 2 min. scans. Size distributions from the near source blast fence site (LAX-BF) and background reference site (AQMD) are included for comparison. For particles less than 40 nm, average concentrations at the six community locations greater than those observed at the background site, but less than at the near source site. Average concentrations of particles greater than 80 nm are slightly lower than those of the near source as well as the background sites.

Figure 4-4 depicts the size distributions obtained from SMPS scans at three selected community sites: resident, synagogue, and Whelan sites. These sites are located directly beneath the typical approach path to runway 25L at LAX (see figure 4-1). Comparing across the three sites, from east to west, smaller particles (< 15 nm) increase in concentration and the mode of the distribution shifts to a smaller particle size. In contrast, larger particles (15-50 nm) tend to increase slightly in number over the same distances. While the distributions are drawn from a large number of samples, and so are relatively robust, comparisons are limited by the fact that the sites were not observed simultaneously.

Figure 4-5 depicts UFP size distributions for the community sites not beneath the landing path, the fire station (300 m south of the landing path) and Lennox School District (300 m north of the landing path). For particles sizes less than 160 nm, number concentrations in Lennox School District are significantly higher than those measured at the fire station.

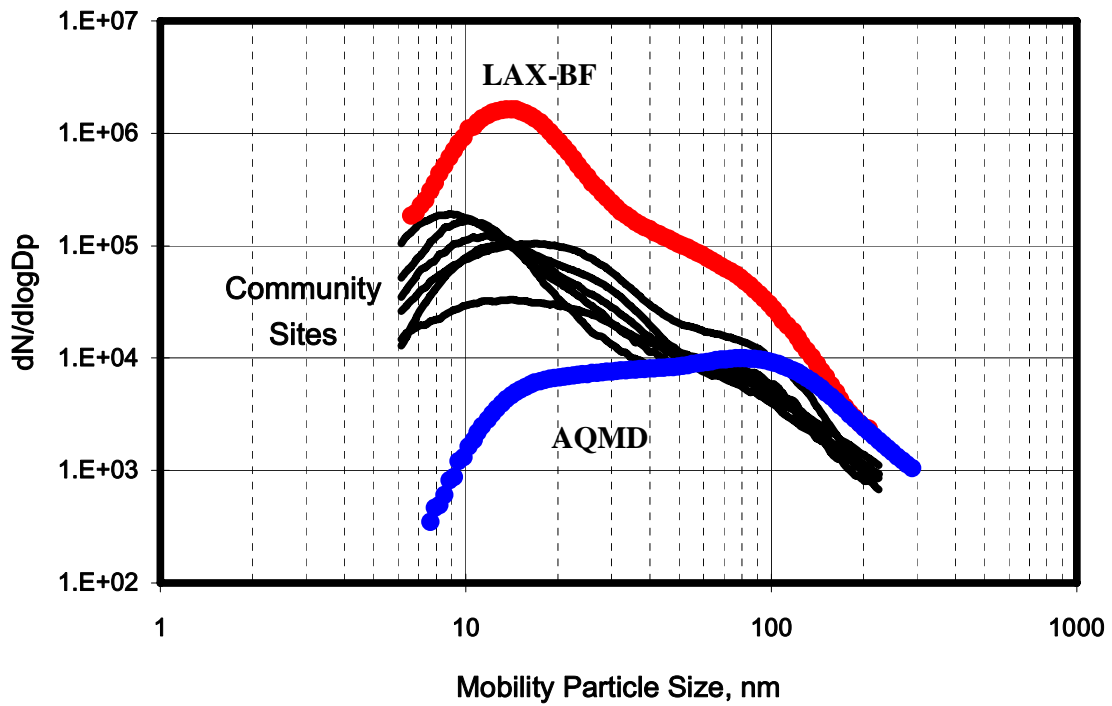


Figure 4-3: Particle size distributions of the six community sites in relation to the near source LAX blast fence (LAX-BF) and the background AQMD site. Sites were not sampled simultaneously.

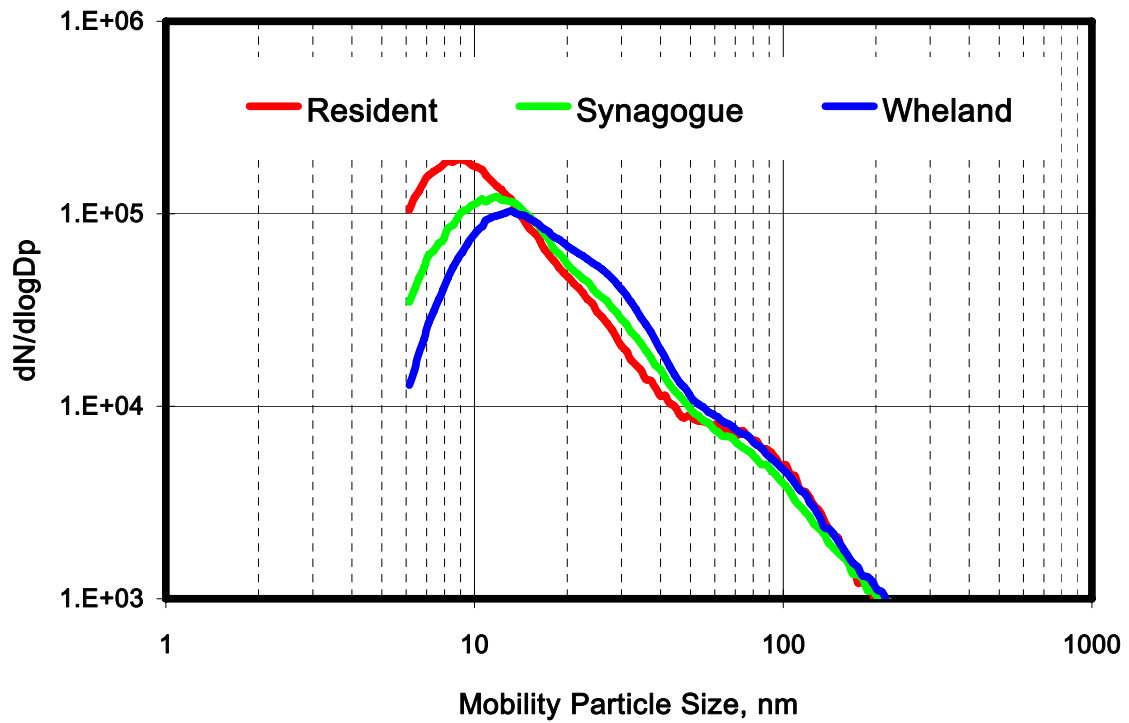


Figure 4-4: Particle size distributions of three community sites located directly beneath the landing path, arrayed west to east from "resident" to "Whelan". The three sites were not sampled simultaneously

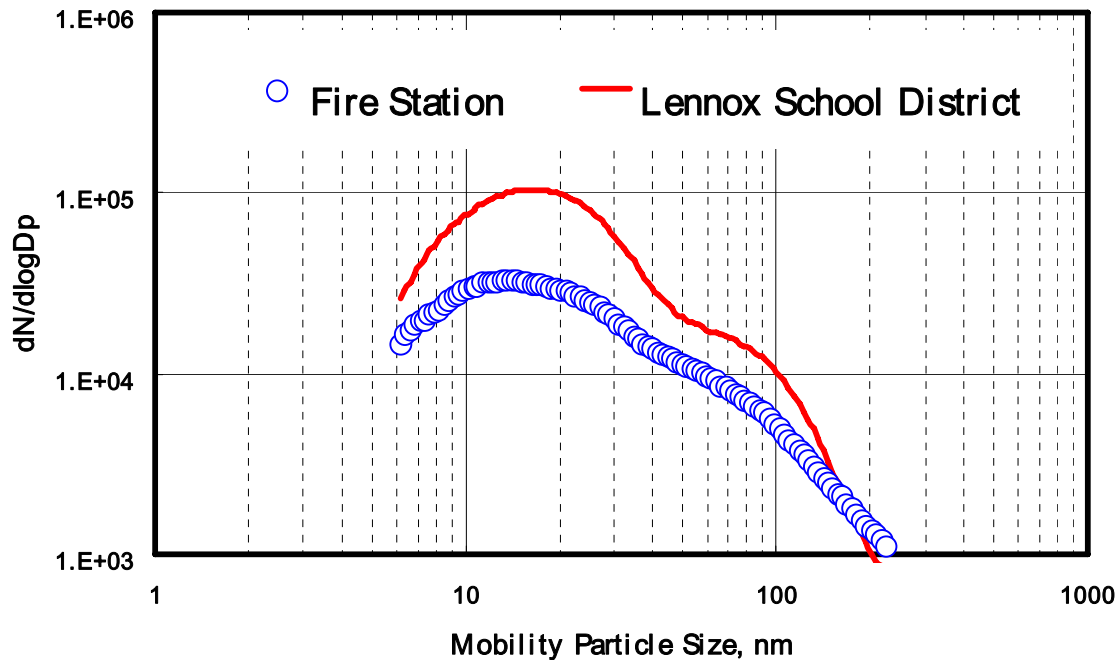


Figure 4-5: Particle size distribution of fire station and Lennox School District sites. These two locations are situated approx. 300 m S and N of the direct landing path, respectively, but could not be sampled simultaneously.

*15 nm Particles*

Table 4-2 shows concentration profiles, indicated by the 1<sup>st</sup>, 2<sup>nd</sup> (median), 3<sup>rd</sup> quartiles and 90% percentile, of 15 nm particles at 6 community sites. Within the community, there is no clear pattern associated with the distance from the airport among these six sites. Overall, the concentrations of 15 nm PM in the community are lower than those measured at the blast fence and downwind of 25R in the downwind study and approximately equal to those measured at locations downwind of 25L (compare to Table 3-3). Again, sites were not sampled simultaneously.

**Table 4-2: 15 nm Particle Concentration (dN/dlogDp in #/cm<sup>3</sup>) Profile at 6 Community Sites**

<b>Statistics Matrices for 15nm Particle Concentration Profile</b>				
<b>Location</b>	<b>1st Quartile</b>	<b>Median</b>	<b>3rd Quartile</b>	<b>90% Percentile</b>
Felton School	36	86	180	279
Local Resident	66	131	229	326
Synagogue	51	164	276	402
Whelan School	48	94	205	350
Fire Station	42	83	179	261
Lennox School District	66	123	192	229

### *PM<sub>2.5</sub>*

Table 4-3 shows concentrations of PM<sub>2.5</sub> at the 6 community sites, with reference to the overall means and standard deviations of AQMD and blast fence sites. In the community sites, PM<sub>2.5</sub> vary between 8 – 23 µg/m<sup>3</sup>. The overall average in this community is 15.6 ± 12.0 µg/m<sup>3</sup>, a level similar to that at AQMD site. The overall community PM<sub>2.5</sub> level is significantly lower than that measured at the blast fence 23.7 ± 18.5 µg/m<sup>3</sup> (p<0.001).

### *Black Carbon*

Table 4-3 lists overall black carbon mass concentrations from all six sites with reference to the levels at the blast fence and AQMD background site. The community average black carbon mass concentration is approximately equal to the background concentrations measured at the AQMD site. Both the community and AQMD have significantly lower black carbon than the blast fence.

### *PMN<sub>10-100</sub>*

Table 4-3 displays number concentrations of UFP in the size range of 10-100 nm, collected in two minute SMPS scans at six community sites. PMN<sub>10-100</sub> at the near source and background sites are provided for comparison. At the near source site, PMN<sub>10-100</sub> averaged 5.3 x 10<sup>5</sup> particles/cm<sup>3</sup>. At the background reference site, AQMD, the average concentration was 76-fold lower, 7 x 10<sup>3</sup>. Concentrations of PMN<sub>10-100</sub> at the community sites were intermediate, and ranged between 2.0 and 5.4 x 10<sup>4</sup> particles/cm<sup>3</sup>.

**Table 4-3: PM<sub>2.5</sub> mass, black carbon mass, and PMN<sub>10-100</sub><sup>a</sup> concentration at six community sites LAX blast fence and background reference site**

Location	PM <sub>2.5</sub> <sup>b</sup> Mean (N) ± SD µg/m <sup>3</sup>	Black Carbon Mean (N) ± SD µg/m <sup>3</sup>	PMN <sub>10-100</sub> Mean (N) ± SD x 1,000 particles/cm <sup>3</sup>
LAX Blast Fence	23.7 (1,497) ± 18.5	13.9 (1,416) ± 13.9	532 (70) ± 292
Community	15.6 (467) ± 12.0	1.3 (5,487) ± 1.2	38 (108) ± 25
Felton School	18.7 (63) ± 12.6	1.2 (765) ± 0.7	40 (5) ± 8
Local Resident	8.2 (62) ± 11.6	1.0 (832) ± 0.6	39 (15) ± 9
Synagogue	11.5 (85) ± 8.3	1.0 (786) ± 0.6	43 (17) ± 27
Whelan School	22.7 (71) ± 11.6	1.1 (1,100) ± 0.6	44 (22) ± 22
Fire Station	17.3 (94) ± 9.9	1.3 (987) ± 1.1	20 (31) ± 12
Lennox SD	15.1 (92) ± 13.0	1.9 (1,017) ± 2.1	54 (18) ± 35
Background Site (AQMD)	14.3 (133) ± 10.4	0.9 (1,713) ± 1.2	7 (77) ± 10

<sup>a</sup>PMN<sub>10-100</sub> is the number concentration of particles size from 10-100 nm (see methods).

<sup>b</sup>PM<sub>2.5</sub> data from Summer 2005 and 2006 were combined for BF and AQMD

### *Problems Encountered during the study*

The SMPS/CPC was found to be non-responsive in the morning of June 26, 2006. The instruments were restarted, air flow was checked and the tubing and impactor were cleaned. The

non-responsiveness or false readings due to incorrect flow (judged by flow indicator) were found periodically during the sampling time period at Lennox School District from June 26 to 30, 2006. Loss of the data due to non-responsiveness of the instruments was minimal. The invalid data was easily identified during data QA/QC procedures.

#### *4.4 Discussion*

The central finding of the community study is that the size distribution of ultrafine particle number concentrations in the community is clearly distinct from the UFP size distribution at the background reference site (Figure 4-3, with supporting data in Tables 4-2 and 3-3) and other communities in the Los Angeles area (Singh et al, 2006). The mode of the UFP number concentration was near the 10-20nm range in this community; no such mode was seen at a nearby background site located in a community that is neither downwind of LAX nor beneath aircraft flight patterns. Whether the slight differences in size distributions among the community sites are meaningful, with respect to the source of UFP is uncertain. The distributions are relatively robust given the large number of observations that were averaged to obtain them, the sites were sampled on different days and if meteorological conditions were sufficiently variable to influence the distributions then comparability among them is limited. The finding from Figure 1 that concentrations of particles <50 nm were substantially higher at all six community sites than at the background site and were intermediate between the levels observed at the LAX blast fence near source site and the background site is relatively robust. When the SMPS data were used as the basis for a metric of total UFP concentration, expressed as the number of particles between 10 and 100 nm in size, the community sites were not statistically significantly different from each other (Table 4-3) but exposure levels for the community as a whole was significantly greater than the background site.

Recent publications from the Southern California Particle Center have reported SMPS size distributions for a variety of Los Angeles area communities (Fine et al, 2004; Singh et al, 2006) This work provides an informative context for interpreting the distributions obtained here. Fine et al. report data from Rubidoux, Riverside and Claremont collected at varying times of day. At these sites, which experience greater influence of photochemically aged air masses, and were selected to avoid fresh traffic sources, the mode of the size distribution ranged from 30-100 nm with substantial diurnal variation. The UFP size distributions reported by Singh et al. (Figure 3 of their paper) varied with location and source influences and also showed substantial seasonal effects. The study included eight sites, six of which are in the Los Angeles Basin (Long Beach, Mira Loma, Upland, Riverside, Lake Arrowhead and USC); the remaining two are in nearby Southern California locations (Alpine and Lancaster). In all eight of the Singh et al. locations, the SMPS mobility diameter at which the greatest number of particles was observed (the mode of the distribution) occurred at a larger particle size than in the communities downwind of LAX studied here: distributional modes ranged between about 20 and 100nm, depending upon site and season. None of these other eight communities are known to be affected by airport derived emissions, although several of them experience heavy road traffic emissions. For example, the USC site is situated such that it receives traffic emissions from the 110 freeway. This site had the smallest size mode of the eight sites studied by Singh et al: approximately 25nm during the summer campaign and 35nm in the winter. The comparison with the study here suggests that airport or aircraft emissions may be responsible for the peak of UFP in the 10-20 nm range measured in the current study, while road traffic including I-405 is less likely to explain the

finding. While aircraft cannot be unequivocally identified as the source of the number concentration peak (between about 10 and 20 nm), it appears likely that aircraft approaching LAX contribute to the observed UFP. It is also possible that advection of emissions from the airport itself also elevate UFP concentrations in this community. This preliminary conclusion should be followed up with studies designed to carefully determine the relative source contributions of major UFP sources that could affect the community.

The size distributions at the fire station and Lennox school district sites (Figure 4-5 and Table 4-3) may be informative. Concentrations of UFP were somewhat greater at the school district site than the fire station, as indicated by the distribution height in figure 4-5 and in the average concentration of  $PMN_{10-100}$  in Table 4-3. The difference between Lennox and the fire station was especially marked for particles in the 10-20 nm range. It must be stated that the sites were not sampled simultaneously, and the differences in  $PMN_{10-100}$  are not significant, so that the interpretation of the differences may be limited. Still, it is interesting to note the relationship of the community sampling sites shown in Figure 4-1 to the average wind directions measured during the field study. The school district location was somewhat downwind from the trajectory along which approaching aircraft travel, while the fire station was somewhat upwind of approaching aircraft. Since aircraft approached LAX in slight crosswind during the study period, wind dispersion of emissions from approaching aircraft toward Lennox and away from the fire station may be proposed as a hypothesis to explain the difference in UFP exposure levels observed at the two sites. Both locations are roughly 1 km from the I-405 freeway. At this distance, the contribution of UFP from I-405 traffic, a potential confounding source, should be limited (Zhu et al, 2002). Further, any detectable effect of I-405 is expected to be equivalent at the two sites since they are situated at an equivalent distance east of the freeway. This line of reasoning suggests that I-405 has a limited effect on UFP concentration at these sites. A further analysis of data collected during non-prevailing wind directions, and detailed examination of wind trajectories during the site-specific sampling times could help distinguish between the possible sources and provide support for the hypothesis.

It is interesting to note that the difference in UFP levels between the Lennox and fire station sites were not reflected in  $PM_{2.5}$  levels, which were actually slightly higher at the fire station. Black carbon was higher at Lennox, but the difference was not as pronounced as for UFP. These findings imply that future studies designed to investigate the impact of landing aircraft on community exposure should emphasize instruments capable of capturing UFP as small as 10nm.  $PM_{2.5}$  is a poor indicator of exposure to aircraft emitted PM.

Figure 4-4 compares the shape and height of the UFP size distribution at three of the six community sites. The sites, labeled resident, synagogue, and Whelan, are located directly beneath the typical approach to runway 25L at LAX (Table 4-1). Note that the discussion of the comparison that follows is limited by the fact that sampling was not simultaneous, and meteorological and other time-varying factors may also have played a role in the observed distributional shift. The three sites are arrayed in a west to east direction over which the altitude of approaching aircraft progressively decreases. Assuming a 3 degree approach angle, aircraft are estimated to be 180m over the Whelan site, 160m over the synagogue, and 100m over the resident site. Comparing the SMPS data in Figure 4-4, resident, the most westward site, had higher concentration of UFP and a smaller particle size mode relative to the most easterly site at

Whelan School, consistent with increasing proximity to a fresh source such as aircraft. In addition, the finding suggests a possible aging effect on aircraft emissions such that the particle size distribution is shifted to slightly larger particles as distance from the source increases (sampling further to the east). Changes in chemical and physical characteristics of aircraft-emitted particles could occur between emission from the approaching aircraft and the time the plume reaches ground level monitoring equipment. A related process occurs along a horizontal scale for motor vehicle particles emitted on the 405 freeway (Zhu et al, 2002). UFP measured at increasing distances from freeways were found to increase in size and decrease in number concentration as distance increased. These changes were observed over distances within a few hundred meters from the freeway. Further studies that include simultaneous sampling should be designed that could investigate the possible explanation suggested here.

In addition to UFP, the study collected data on PM<sub>2.5</sub> and black carbon mass concentrations at the six community sites. Average concentrations of black carbon and PM<sub>2.5</sub> mass were not notably elevated in the community relative to a background reference site upwind of LAX, except at the Whelan School location at which PM<sub>2.5</sub> mass was clearly above background. This site appears to be influenced by an unidentified source of fine PM. Interpretations of comparisons to the background site are limited because this site was not sampled during the time period of the community study. The community study was performed in June 2006, and the background data derive from sampling in September 2005. Note that only PM<sub>2.5</sub> was elevated at Whelan School while the concentrations of UFP and black carbon were not notably different from the other community sites. The data in Table 4-3 show that UFP number concentrations are not correlated with mass based measures such as PM<sub>2.5</sub>, although they do show a somewhat improved correlation with black carbon in comparison to PM<sub>2.5</sub>. Future studies of the impact of aircraft on PM exposure in adjacent neighborhoods need to carefully consider relevant measures, and must focus on UFP, if the results are to be informative.

## 5. Modeling Study

### 5.1 Overview

The objective of this component of the project was to develop a model for the dispersion of LAX aircraft emissions. The model uses four two-way nested domains to simulate the LAX aircraft emission sources, dispersion to community sampling sites, as well as regional impacts in the Los Angeles air basin. The configurations of the model, detailed treatment of emissions from various aircraft, estimation of black carbon emissions, calibration of the model with near-source measured data, and calculations of black carbon dispersion to community sampling sites are reported below.

### 5.2 Model Configurations

A three-dimensional high-resolution version of the Surface Meteorology and Ozone Generation (SMOG) model coupled with the PSU/NCAR Fifth Generation Mesoscale Model (MM5) (Lu et al. 1995, 1997a) is being employed to quantify the impact of aircraft emitted black carbon in the vicinity of LAX. The SMOG/MM5 joint model is an Eulerian grid model that includes meteorological and microphysical processes and accounts for local terrain effects on winds and turbulence. Several numerical techniques have been applied in its transport code including a time splitting algorithm, a finite element method for horizontal transport, and a finite difference scheme for vertical advection and diffusion. These techniques provide efficient and accurate solutions for transport calculations with minimized computer memory demand. Aerosol processes include nucleation, coagulation, condensational growth and evaporation, sedimentation, and aqueous chemistry. The performance of the SMOG modeling system has been evaluated by comparing predictions against measurements (Lu et al., 1997b, 2003). The SMOG model has been successfully used to predict ozone concentrations throughout the South Coast Air Basin, to explain the causes of elevated pollution layers observed over Los Angeles, to calculate trace metal deposition on land and coastal waters, and to study PAH distributions and human exposure in Southern California (Lu et al. 1995, 2003 and 2005).

In order to cover the LAX area with fine resolution and include the impacts of LAX aircraft emissions on the Los Angeles basin, the model is configured to use four two-way nested domains. Table 5-1 lists the domains used for the simulation. Domain 1 covers the Los Angeles basin. Domains 2 and 3 are intermediate domains that allow the change of winds to propagate into the inner domain, as well as the dispersion of black carbon from the inner domain to the outer Los Angeles domain. Domain 4 includes the LAX aircraft emission sources and community sampling sites. Figure 5-1 shows the locations of the 4 domains in the Los Angeles basin.

**Table 5-1. Domains used for the simulation**

<b>Domains</b>	<b>Horizontal Resolution</b>	<b>Purposes</b>
Domain 1	8.1 km	The Los Angeles basin
Domain 2	2.7 km	Intermediate domain
Domain 3	0.9 km	Intermediate domain
Domain 4	0.3 km	LAX aircraft sources and community sampling sites

The model is initiated with NCEP (National Center for Environmental Prediction) ETA model analyses for specific dates. Aircraft activity data from the LAX airport for the date periods are used to calculate emissions at specific locations and time. The activity data includes aircraft engine types, departure/arrival time and status, and runways used for each aircraft (see below for detail). The black carbon (BC) emissions from each aircraft are estimated using an empirical formula from the literature, as explained in section 5.4, and then calibrated with the near-source measurements collected at the blast fence site. BC is treated as an inert tracer in the SMOG/MM5 model without chemical transformation.

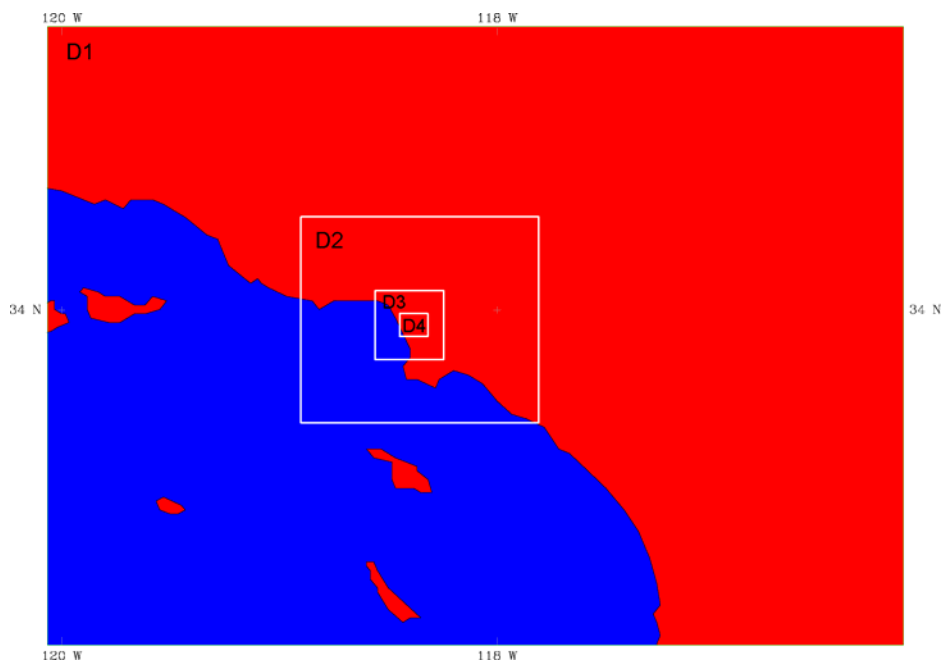


Figure 5-1. Model domains and locations used for the LAX simulation

### 5.3 Aircraft Emissions Factors

Aircraft emissions were calculated with standard LTO cycles for various aircraft and engine types. For each aircraft, the emission factors for the aircraft's specific engine at each power setting or mode of operation, as well as the time spend in each modes and the fuel flow rate at each mode, are used to compute the emission rates for various pollutants. Then the emission factors are applied to the activity of aircraft in LAX airport to calculate the emissions at a given time and location. This emission calculation procedure is consistent with EPA's Procedure for Emission Inventory Preparation (EPA, 1992), Vol. IV, Chapter 5, except that aircraft emissions at any given time and location is calculated as described instead of lump sum of an inventory period. For our study of instantaneous emissions, the time and location of aircraft emissions will be identified for dispersion calculation.

#### *Standard LTO Cycle and Time-In-Mode*

The aircraft operations of interest within the boundary layer are defined as the landing and takeoff (LTO) cycle. The cycle begins when the aircraft approaches the airport on its descent from cruising altitude, lands, and taxis to the gate. It continues as the aircraft taxis back out to the runway for subsequent takeoff and climbout as it heads back up to cruising altitude. Thus, the

five specific operating modes in an LTO are: Approach, Taxi/idle-in, Taxi/idle-out, Takeoff, Climb-out (Figure 5-2).

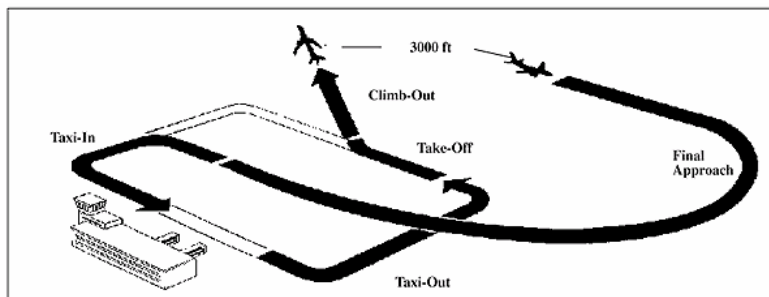


Figure 5-2. The ICAO landing and take-off cycle (LTO).

A sixth operating mode, reverse thrust, often is included in a standard LTO cycle but is not included in EPA's procedure (FAA, 2005). After aircraft land, engine thrust reversal typically is used to slow the aircraft to taxi speed (otherwise the aircraft is slowed using only the wheel brakes). Reverse thrust is now considered by EPA as an official mode and should be included in calculation procedures as a sixth operating mode when applicable. Since reverse thrust engine operating conditions are similar to takeoff, time spent in reverse thrust should be combined with takeoff mode emission indices and fuel flow as a means of accounting for reverse thrust mode emissions, under the assumption that activation of the thrust reversers does not alter the PM emission fraction in the exhaust. Aircraft reverse thrust typically is applied for 15-20 seconds on landing.

The LTO cycle provides a basis for calculating aircraft emissions. During each mode of operation, aircraft engines of a given aircraft category operate at a fairly standard power setting. Emissions for a given operation mode and aircraft can thus be calculated by knowing emission factors for specific aircraft engines at the power settings of interest.

**Table 5-2. Representative LTO cycle times for several aircraft categories (in minutes) (FAEED, 1995)**

CATEGORY	IDLE TIME	TAKEOFF TIME	CLIMBOUT TIME	APPROACH TIME
JUMBO JET	26	0.7	2.2	4
LONG RANGE JET	26	0.7	2.2	4
MEDIUM RANGE JET	26	0.7	2.2	4
AIR CARRIER TURBOPROP	26	0.5	2.2	4.5
BUSINESS JET	13	0.4	0.5	1.6
GENERAL AVIATION TURBOPROP	26	0.5	2.5	4.5
GENERAL AVIATION PISTON	16	0.3	4.98	6
PISTON TRANSPORT	13	0.6	5	4.6
HELICOPTER	7	0	6.5	6.5
MILITARY TRANSPORT	26	0.5	2.5	4.5
MILITARY JET	13	0.4	0.5	1.6
MILITARY PISTON	13	0.6	5	4.6

During the LTO cycle, aircraft operate for different periods of time in various modes depending on their particular category, the local meteorological conditions, and operational considerations at a given airport. The "Time-In-Mode," or TIM, is typically used to categorize the time of operation taking these factors into consideration. Table 5-2 shows representative LTO cycle times for several aircraft categories (FAEED, 1995).

#### *Aircraft Engine Types, Number of Engines and Emission Factors*

The emissions characteristics of aircraft vary by number and type of engine used. The engines used on each aircraft type must be determined to select the emission factors for emission calculation. The FAA Aircraft Engine Emission Database (FAEED) (FAEED, 1995) includes information on the engines mounted on specific aircraft with the operating mode-specific pollutant emission rates for those engines. Many aircraft use only a single engine model, while others have been certified to use engines from two or three different manufacturers. When a single engine is listed for an aircraft model, emissions data for that engine are used. For aircraft with engines from more than one manufacturer, defining the specific engine mix used on the fleet of aircraft operating at a specific airport may be extremely difficult. Individual airlines probably are the only source of detailed fleet data on specific engine models and they likely do not have it readily available. The market share information from the FAA Aircraft Engine Emission Database is used for selecting engine models if available. Some aircraft types are not included in the FAEED. In the majority of cases, these models were variations of aircraft that were included in FAEED. For missing models, the activity was assigned to its nearest equivalent. The number of engines mounted in an aircraft is also provided in the database. A special table was created for our modeling project to link the aircraft types in the LAX activity database to the aircraft type table with engine types.

The aircraft engine is the source of emissions of the key pollutants that result from fuel combustion. Emission rates vary depending on the fuel consumption rate and engine specific design factors. The operating parameters used in the standard for the LTO cycle can be used as default values in calculating emissions. The test data of exhaust emissions of those aircraft engines that have entered production are included in ICAO Aircraft Engine Emissions DataBank (ICAO, 2006).

The ICAO Aircraft Engine Emissions DataBank provides emission indices (i.e., emission factors) and average fuel consumption rates for aircraft engines. Generally, emission factors are listed in pounds of pollutant per 1000 pounds of fuel consumed and fuel flow is listed in pounds per minute. However, very few measurements have been made of particulate emissions from aircraft engines. Particulate emission rates were poorly correlated with smoke numbers measured in ICAO databank. An alternative method is used to estimate black carbon emissions.

#### *Aircraft Activities at LAX*

The LAX aircraft activity and fleet data, including time of activity, aircraft type, arrival or departure, runway used, and airline operators, were kindly provided by LAX sources. The activity data provides the modes of a specific aircraft's operations at any given time, which define the landing and take-off at specific runway. A sample of the aircraft activity data is shown in the Table 5-3.

**Table 5-3. Aircraft Activity Data Table from LAX.**

AIRPORT	WALL TIME	ACID	ACTYPE	DAO	RUNWAY	AIRLINE CODE
LAX	9/20/05 12:00 AM	CPA088	B744	A	25L	CPA
LAX	9/20/05 12:02 AM	UAL991	A320	D	25R	UAL
LAX	9/20/05 12:03 AM	TDX2898	B742	D	25L	TDX
LAX	9/20/05 12:06 AM	AAL30	B762	D	25R	AAL
LAX	9/20/05 12:08 AM	DAL1475	B763	D	24L	DAL
LAX	9/20/05 12:10 AM	THT101	A343	D	25R	THT
LAX	9/20/05 12:12 AM	NKS709	A321	D	25R	NKS
LAX	9/20/05 12:14 AM	VFR5227	????	O		VFR
LAX	9/20/05 12:14 AM	QFA108	B744	D	07L	QFA

The runways from South to North in LAX are 07R/25L, 07L/25R, 06R/24L and 06L/24R.

#### *Aircraft Location Calculation*

Aircraft emission locations for a specific TIM are complicated to calculate. Tables of each runway will be used for emission location calculation. Aircraft landing and takeoff speed varies from one to another. For median-sized civilian aircraft, the landing speed of 200 kph and take-off speed of 250 kph is reasonable.

*Approach:* Assuming aircraft is approaching along a straight line and landed at position X, the aircraft should be at landing speed \* approaching time when at 915m height. (~ 13 km for 200 kph approaching time and 4 min TIM<sub>appro</sub>). The location of aircraft at time t is  $V_{\text{appro}} * (t_{\text{land}} - t)$  from the airport and at altitude  $915\text{m} / \text{TIM}_{\text{appro}} * (t_{\text{land}} - t)$ , where  $t < t_{\text{land}}$ .

*Reverse thrust:* A 15-20 s reverse thrust is applied at this time to decelerate the aircraft in addition to wheel braking. Since the engine operation in reverse thrust mode is similar to take-off, the take-off engine parameters are used for reverse thrust. The deceleration distance is  $X = 0.5 * a * t^2 = 0.5 * ((V_{\text{appro}} - V_{\text{taxi}}) / \text{TIM}_{\text{reverse}}) * (t - t_{\text{land}})^2$ , where  $t_{\text{Rev}} > t > t_{\text{land}}$  and 15 s for TIM<sub>reverse</sub> is assumed.

*Taxi-In:* Distributed along the distance between runways to terminal building for TIM<sub>Idle\_in</sub> time.

*Taxi-Out:* Distributed along the distance between runways to terminal building for TIM<sub>Idle\_out</sub> time.

*Take-Off:* The aircraft accelerates to the take-off speed in Take-Off time. The location of the aircraft will be at  $X - X_0 = 0.5 * a * t^2 = 0.5 * (V_{\text{TakeOff}} / \text{TIM}_{\text{takeoff}}) * t^2$ .

*Climb-out:* Aircraft will continue to accelerate during climb-out. Assume aircraft climbs at an average angle  $\theta$  and ignore the acceleration factor, the distance of aircraft from take-off location should be  $915\text{m} / \text{TIM}_{\text{climb}} * \text{ctan}(\theta) * t$  and at height of  $915\text{m} / \text{TIM}_{\text{climb}} * t$ .

The wall time of activities is the landing and take-off time. Therefore,  $\text{TIM}_{\text{appro}}$  before landing, model start to calculate emissions for the aircraft until  $\text{TIM}_{\text{reverse}} + \text{TIM}_{\text{Idle\_in}}$  passed landing. For take-off, the emission calculation starts  $\text{TIM}_{\text{Idle\_out}}$  time before takeoff, and  $\text{TIM}_{\text{takeoff}} + \text{TIM}_{\text{climb}}$  after take off.

#### 5.4 Estimate and Calibrate Black Carbon Emissions

PM emissions result from the incomplete combustion of fuel. High power operations, such as takeoff and climbout, produce the highest PM emission rates due to the high fuel consumption under those conditions. PM emission test data for aircraft engines are sparse. For most turbine engines, EPA does limit the amount of smoke that may be emitted. This limit is specified as a smoke number. However, attempts to derive correlations between smoke number and particulates emission rates are not satisfactory.

Petzold et al. (1999) measured characteristic parameters of black carbon aerosol (BC) emitted from jet engine during ground tests and in-flight behind an aircraft. BC emitted from aircraft varies from 0.015 to 0.333 g BC/kg fuel, and depends on engine thrust levels (ETL) which range from 8% to 74% (Table 5-4). As shown in Figure 5-3, the BC emission factor (g/kg fuel) exhibits a linear relationship with ETL, as follows:  $\text{BC (g/kg fuel)} = 0.0042 * \text{ETL} (\%)$ ,  $R^2=0.97$ .

**Table 5-4. Aircraft engine thrust level and estimated BC emission factor of the operating modes in the ICAO standard LTO cycle**

Operating Mode	Engine Thrust Level (ETL)	Estimated BC Emission Factor (g/kg fuel) <sup>a</sup>
Approach	30	0.126
Taxi/idle	7	0.029
Take-off/Reverse Thrust	100	0.420
Climb	85	0.357

<sup>a</sup> Estimated by  $\text{EC} = 0.0042 * \text{ETL}$

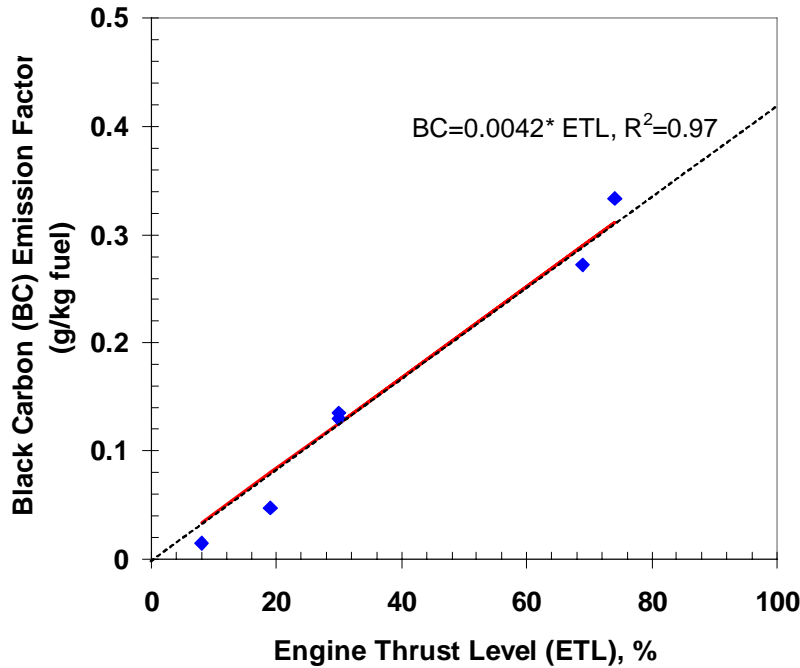


Figure 5-3. A linear relationship between black carbon emission factor and aircraft engine thrust level.

However, measurements from one aircraft cannot represent a range of aircraft with different engine types and capacities, from piston private aircraft to jumbo jets, in the LAX. In the project, near-source measurements of black-carbon have been used to calibrate BC emissions simulated in the model.

We first applied the relationship from Petzold et al. (1999) to LAX aircraft for each aircraft and each LTO cycle. Fuel consumption in each operating mode is a function of aircraft/engine types. The estimates are used to calculate aircraft emission and dispersion over the model domain. Since the model uses a time step of 0.9 seconds for domain 4, emission patterns at each location and time can be resolved in detail. The modeled values at the blast fence location are used to compare with measurements at the same location.

In the calibration step, we calculate the modeled averaged value at the blast fence location and compare it with the mean value measured at the blast fence location. The ratio of the measured mean to the modeled mean is then used to scale the emission rates in the Petzold et al.'s relationship. The final calibrated relationship is used in the LAX aircraft emissions for model prediction. An example of the calibrated predictions at the blast fence location is shown in Figure 5-4. Time-resolved, actual aircraft operations data were used to estimate BC production in the modeling runs. The take-off and landing of each individual aircraft from/to the blast fence can be identified as peaks in the figure.

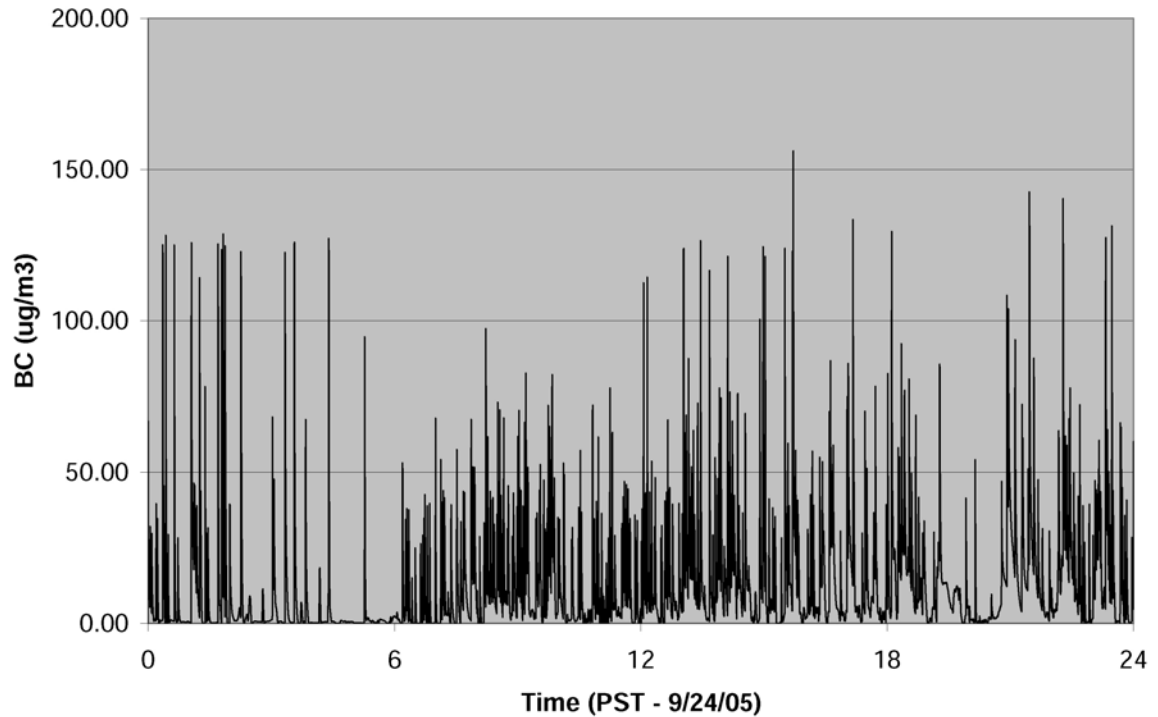


Figure 5-4. Model predicted aircraft signals at the blast fence location. The emission rates have been calibrated. The take-off and landing of aircraft near the blast fence location are shown as peaks in the figure.

Since the BC measurements at the blast fence location were averaged over every 5 minutes, a similar average has also been conducted on the model predicted values. The results are shown in Figure 5-5a and b. Since the model uses a single aircraft to account for all aircraft types and BC emission rates, the line-by-line match is imperfect. However, the main features of the measurements can be seen in the prediction, including the range of peak values.

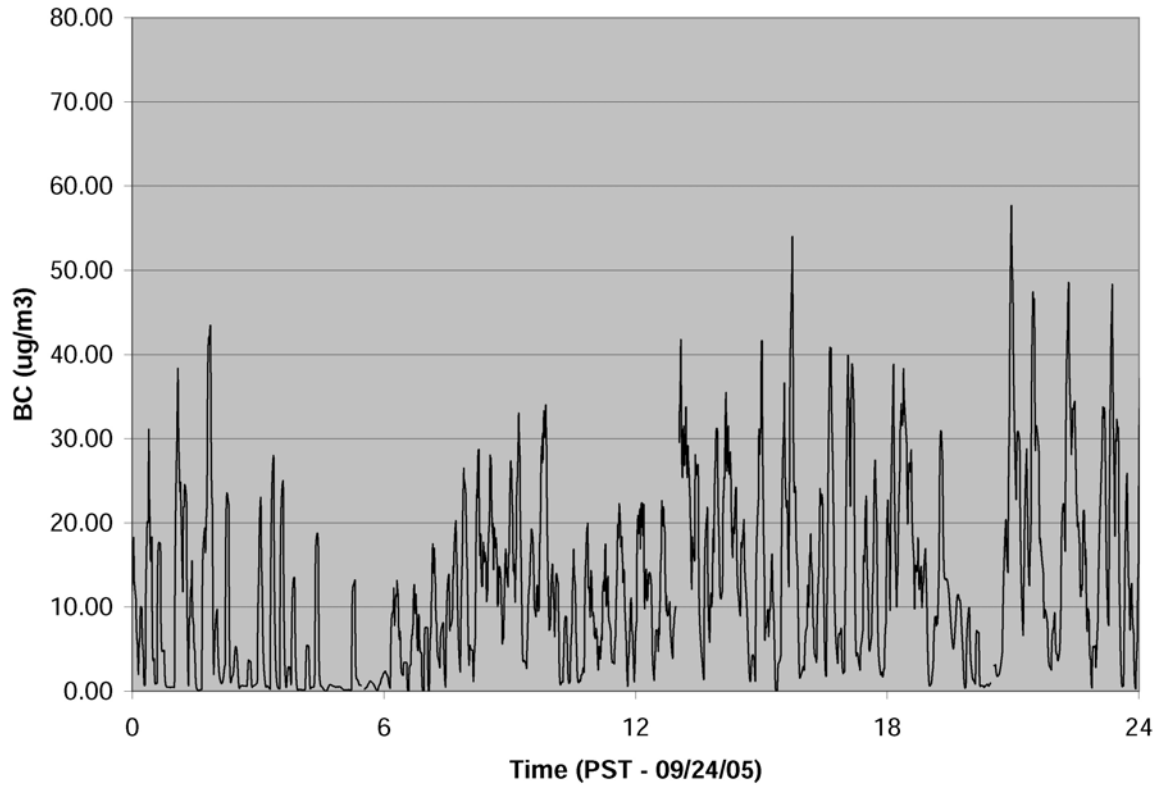


Figure 5-5a. Model predicted concentrations at blast fence with 5-minutes running average.

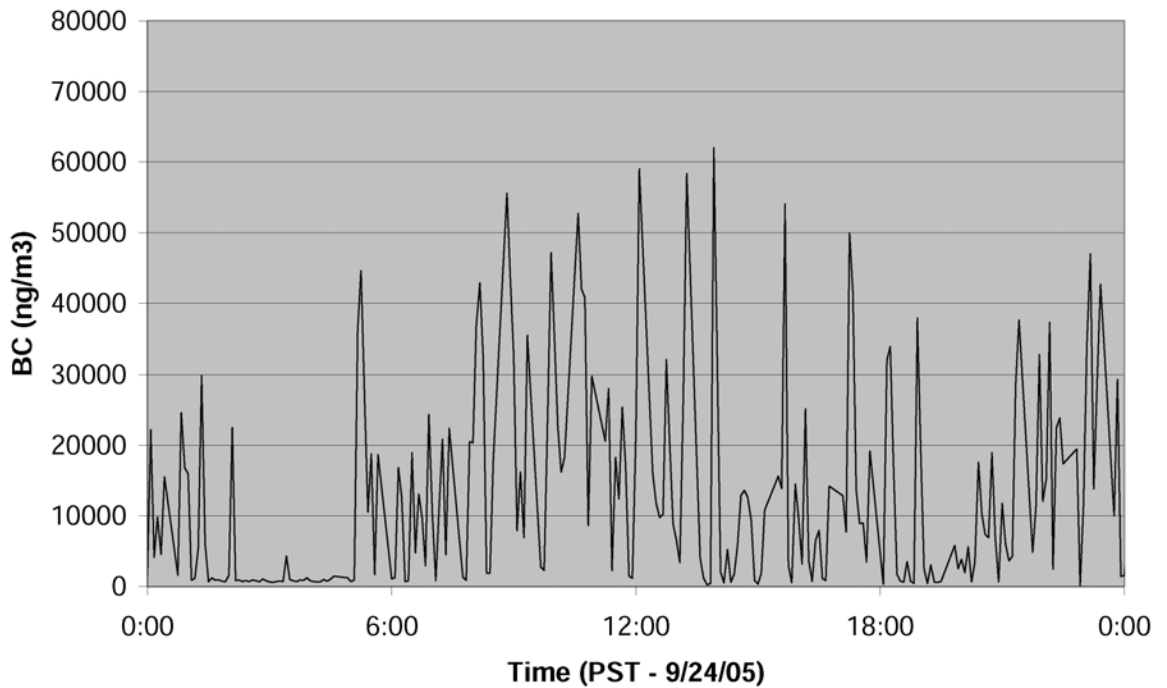


Figure 5-5b. BC measurements at the blast fence location (averaged every 5 minutes).

### 5.5 Dispersion of Aircraft Emissions to Community Locations

The black carbon emissions from aircraft activities at LAX are predicted to have significant effects on the adjacent communities through out the day. In the morning before the onset of sea-breeze winds are usually calm and disorganized, and light winds in the boundary layer confine pollutants in a local area. Black carbon is predicted to drift near the vicinity of the airport (Figure 5-6), leading to high concentrations in near the area.

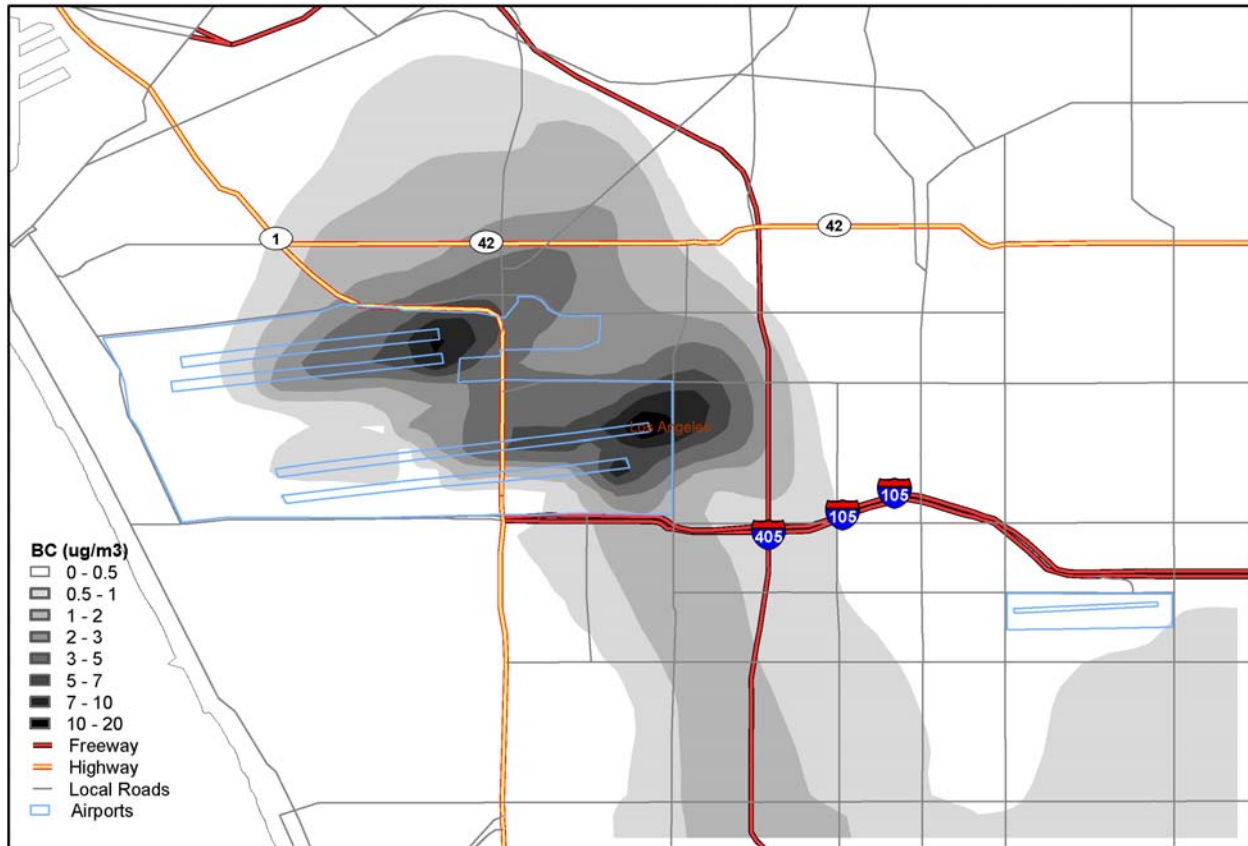


Figure 5-6. Averaged black carbon concentrations from 09/24/2005 8:00 to 9:00 PST near LAX.

By the later morning and afternoon black carbon moves to the east across the downwind communities by the onshore sea-breeze (Figure 5-7). The heavy traffic in the airport during the daytime produces significant BC that not only affects the downwind community area but also the entire Los Angeles basin (not shown).

In the evening, the winds become disorganized again. Black carbon tends to drift near the airport (Figure 5-8). Land-breeze may build-up later at night and in the early morning that could transport BC to the ocean surface.

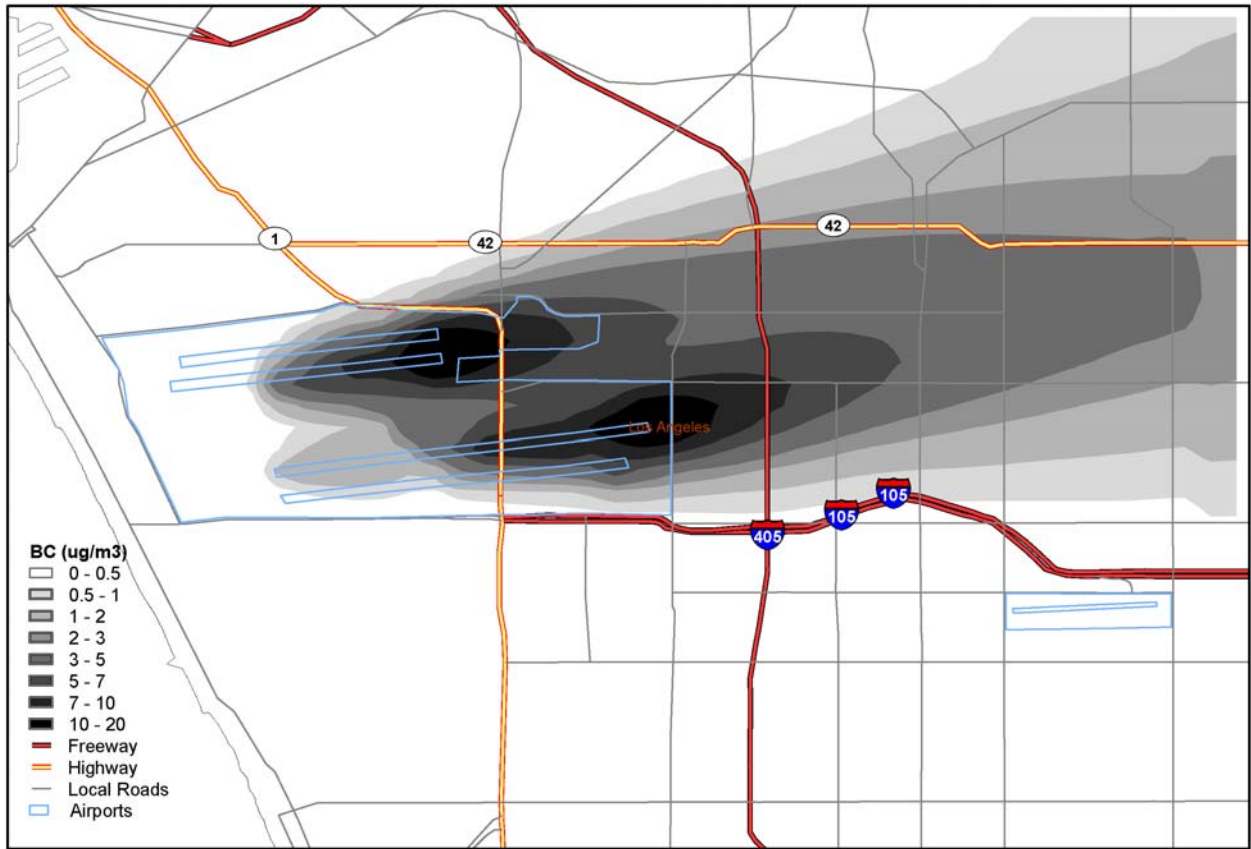


Figure 5-7. Averaged black carbon concentrations from 09/24/2005 13:00: to 14:00 PST from LAX. The sea breeze moves the black carbon to the east.

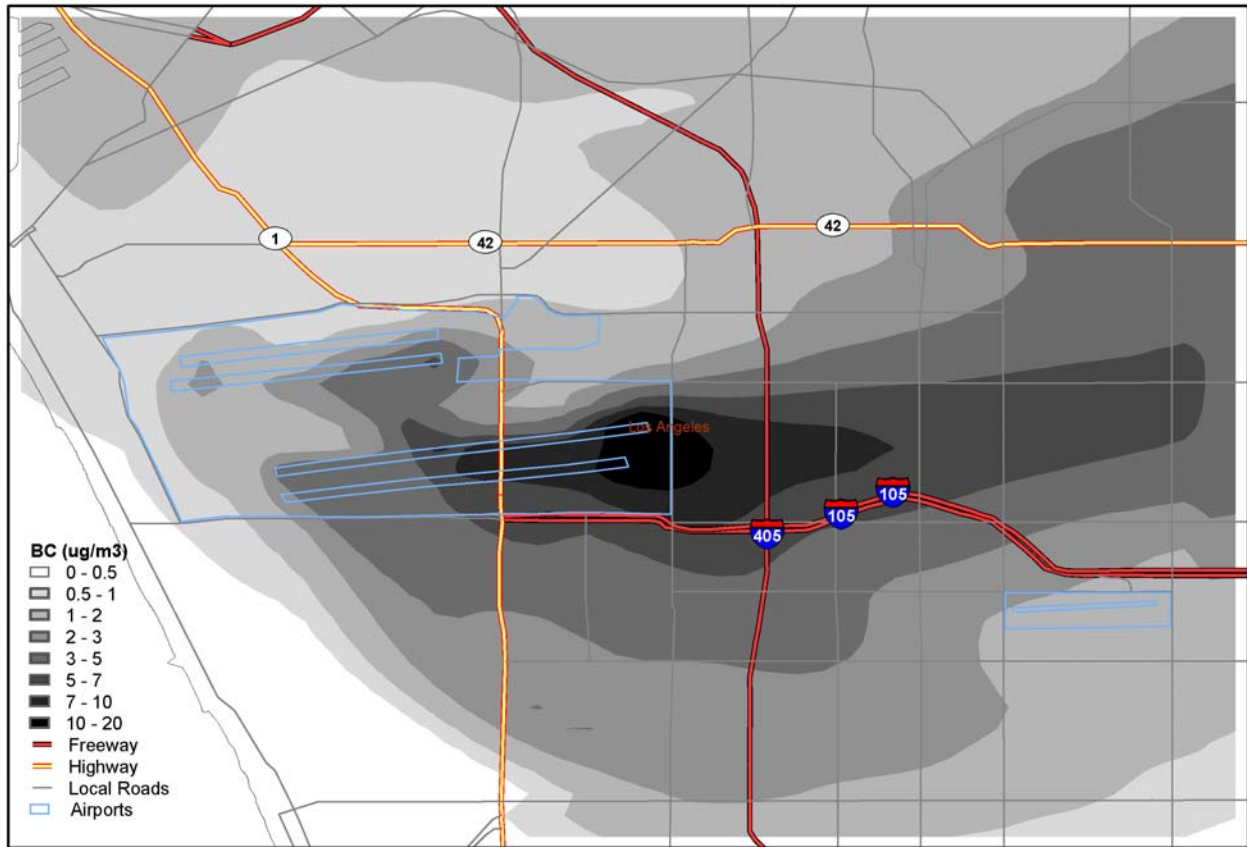


Figure 5-8. Averaged black carbon concentrations from 09/24/2005 23:00 to 24:00 PST.

### 5.6 Discussion

A three-dimensional high-resolution version of the MM5/SMOG was used to quantify the impact of aircraft-emitted black carbon in the vicinity of LAX. Four two-way nested domains are used to cover the LAX with fine resolution, as well as the impacts of LAX aircraft emissions on the Los Angeles basin. The model has demonstrated the capabilities to simulate both near source emissions and emission plumes on the regional scale.

Aircraft emissions were calculated with standard LTO cycles for various aircraft and engine types. For each aircraft, the emission factors for the aircraft's specific engine at each power setting or mode of operation, as well as the time spend in each modes and the fuel flow rate at each mode, are used to compute the emission rates for various pollutants. For our study of instantaneous emissions, the time and location of aircraft emissions are identified for dispersion calculation.

The near-source measurements of black-carbon have been used to calibrate black carbon emissions simulated in the model. We first applied the relationship from Petzold et al. (1999) to LAX aircraft for each aircraft and each LTO cycle, and then calculate the modeled averaged value at the blast fence location and compare it with the mean value measured at the blaster fence location. The ratio of the measured mean to the modeled mean is then used to scale the

emission rates in the Petzold et al.'s relationship. The calibrated relationship is used in the LAX aircraft emissions for model prediction.

The averaged concentrations near community sites predicted by the model show distinct patterns. A daytime sea-breeze moves black carbon to the east, while weak nighttime flow distributes black carbon in the vicinity of the airport. The heavy traffic in the airport produces significant BC that not only affects the downwind community area but also the entire Los Angeles basin.

It will be of future interest to compare measurements of black carbon from community sites with modeled results and to compare the impacts of airport black carbon with other sources in the Los Angeles basin.

## 6. Overall Summary and Conclusions

A study of ultrafine particles and black carbon in the vicinity of the Los Angeles International Airport was performed using near continuous monitoring methods. Particular attention was focused on characterizing the size distribution of ultrafine particles associated with near source aircraft emissions. Previous aerosol monitoring at and near airports has generally applied time-integrated methods, which are not able to capture the time varying nature of aircraft emissions. Further,  $PM_{2.5}$  and other mass based metrics do not provide complete characterization of the combustion particles from aircraft, which are predominantly in the ultrafine range and thus do not necessarily contribute extensive  $PM_{2.5}$  mass concentration on a regional scale. The project was proposed to explore monitoring methods that could provide more useful characterization of airport impacts on local and regional air quality. The study has developed groundwork for in-depth future studies that could be used for emissions inventory development, community exposure estimates, toxicological characterization, and regulatory purposes.

The project comprised three field investigations and a modeling component. Field studies were first performed to capture near source emissions, immediately downwind of a runway. The second field study was designed to assess dispersion behavior of aircraft emissions plumes 200-600 m downwind of the point at which aircraft typically initiate take-off. The third field study was an exploratory study in a residential community downwind of the airport. The community study was designed to identify which pollutants are elevated relative to background, and to use spatial and temporal patterns in the data to discern likely sources, including aircraft, of those pollutants. The modeling project was focused on developing a tool for predicting the dispersion of black carbon emitted from aircraft to sampling sites and more broadly in the regional airshed.

The major finding from the near source study is the size distribution of ultrafine particle number concentration collected at a location as near as practicable to aircraft take offs. The distribution has a single dominant mode: the highest number concentration was found at a mobility diameter of 14-16 nm, and a gradual decrease in concentration with increasing size was observed under the sampling conditions of the study. The near source site was studied in the summer and in the winter; little difference was seen in the size distribution with season. A second key finding from the near source study resulted from one second SMPS scans at set particle sizes. These scans were able to capture the very high temporal variability in ultrafine particle concentrations that occurs at the runway location. By matching the temporal profile with the concurrent time series of aircraft activity data, peaks in the concentration vs. time profiles were matched with pulses of emissions associated with aircraft take offs. This confirmed that the elevated levels of ultrafine PM observed at the near source site relative to the background site are attributable to aircraft. Black carbon and  $PM_{2.5}$  were also elevated relative to background, but the time integrated nature of the instrumentation for these pollutant metrics renders source attribution more difficult. PAH levels were not especially high at the blast fence, a perhaps unexpected finding from this study. The pattern of relative concentrations of individual PAH species appears to differ from the patterns observed in community studies conducted previously, in that semivolatile compounds were enriched relative to heavier PAH species. If confirmed in further analyses, it is possible that there is a profile of relative PAH concentrations specific to aircraft emissions that could be useful in source studies.

In the downwind study, CPC counts of 15 nm particles were collected at five downwind locations, spaced at increasing distances from the blast fence. Due to the limited scale of the study, the downwind locations had to be monitored serially, rather than concurrently. During monitoring at each location, simultaneous monitoring was conducted at the blast fence for comparison. Peaks of 15 nm particles that occurred at the blast fence associated with aircraft take offs were matched with peaks observed at distances up to 600 meters downwind, with time lags of less than one minute between the blast fence and downwind sites. Inspection of aircraft activity data from LAX provided confirmation that peaks in the particle number concentrations at the downwind sites were temporally associated with aircraft take offs and thus likely attributable to aircraft emissions. There was not a spatial gradient in the average particle number concentrations of 15nm PM as distance increases from 200-600 meters downwind of the source. However, a spatial gradient was clearly evident in the upper quartile of 15 nm particle number concentrations, such that the greatest spikes in 15 nm particle concentration were observed nearer the runway and the magnitude of spikes decreased with distance from the source. The top quartile of data includes take-off associated peaks but not background sources of UFP; thus the finding suggests dispersion of aircraft emissions with distance. The top quartile of black carbon mass concentrations also decreased with distance from the source of take-off emissions. 15nm PM and black carbon were higher downwind of the take of runway in comparison to the field sites that were located beneath a landing path, suggesting that the lower engine thrust of arriving aircraft results in lower particulate emissions than does take-off.

The community study involved sampling at six locations in one neighborhood. Three locations were directly beneath the approach to runway 25L at LAX used by arriving aircraft. As with the downwind study, sites could not be simultaneously monitored so that the spatial differences observed may be confounded by time-varying factors such as temperature, humidity or fluctuations in other UFP sources including local traffic. The major finding from the field work in the community is that the size distribution of UFP at all six sites had a dominant mode at 10-20 nm, clearly distinct from the size distribution of UFP that was observed at the background reference site. Several other community locations in the Los Angeles Basin that have been studied by others (Fine et al, 2004; Singh et al, 2006) have reported size distribution modes ranging from 25nm at a traffic source-influenced site to nearly 100nm for sites that do not receive fresh emissions from combustion sources. UFP size distributions in the community indicate that a fresh source of UFP is in close proximity. The distributions were similar in shape to that observed at the LAX near- source site, which is heavily influenced by aircraft emissions. In addition to size distribution differences, the number concentration of UFP was clearly elevated at all community sites relative to the background site. Indirect evidence suggests that the smallest UFP observed in the community study could be derived from approaching aircraft and were not likely to originate from I-405. This area is downwind of the 405 freeway (study sites range from 0.2 to 1.8 km east of the freeway), and sampling did not include a reference site that is downwind of the 405 but not LAX, so the conclusion is based on indirect evidence including comparisons with the literature on locations near the 405 and other freeways (Zhu et al, 2002, Singh et al, 2006, for example). In contrast to the findings on UFP, PM<sub>2.5</sub> and black carbon levels were not significantly elevated at the community sites studied. One exception for PM<sub>2.5</sub> was noted. The data overall suggest that residents of this community are exposed to greater levels of particles <40 nm than other community locations studied to date. Depending upon the toxicological properties of these particles, the finding could have important health implications.

Further work is needed to build upon the exploratory findings in the community study to more fully characterize community exposures, their sources, and potential risks to human health. A challenge is the logistical difficulty and great expense of performing simultaneous sampling at numerous locations.

Table 6-1 presents selected summary statistics of selected data from the three field studies, to enable comparison across the studies. The AQMD background site had the lowest concentrations of all the measures of particulate pollution studied: number concentration of UFP, black carbon mass and PM<sub>2.5</sub> mass. The blast fence near source site had the highest concentrations of UFP, BC, and PM<sub>2.5</sub>. The community sites (data averaged over the 6 sites for simplicity; site-specific data may be found in chapter 4, Table 4-3) were intermediate between blast fence and background in UFP number concentrations, while the mass-based measures were not significantly elevated over background at these community sites. There is a clear difference between the three field study locations in the highest spikes of 15 nm particles, as summarized by the 90<sup>th</sup> percentile level of the values measured in the three studies. The largest peaks in number concentration were measured at and downwind of the 25R take-off runway. The 90<sup>th</sup> percentile of 15 nm PM concentration at the community sites and downwind study locations beneath the 25L landing path were less than at sites affected directly by aircraft take off plumes. Note that the percentile levels for 15 nm particle concentration are given as ranges for the downwind and community sites because there were 5 and 6 locations, respectively, in those field studies.

**Table 6-1: Summary statistics from three field studies of 15 nm ultrafine particles (UFP), total number concentration of UFP in sizes between 10 to 100 nm (PMN<sub>10-100</sub>), black carbon (BC), and particulate matters in particles less than 2.5 µm**

Location	15nm UFP #/cm <sup>3</sup>			PMN <sub>10-100</sub> 1,000 #/cm <sup>3</sup> Mean ± Std	BC µg/m <sup>3</sup> Mean ± Std	PM <sub>2.5</sub> µg/m <sup>3</sup> Mean ± Std
	Median	75 <sup>th</sup> percentile	90 <sup>th</sup> percentile			
AQMD	-	-	-	7 ± 10	0.9 ± 1.2	14.3 ± 10.4
Blast Fence	247	2,655	6,936	532 ± 292	13.9 ± 13.9	23.7 ± 18.5
Downwind - 25R	56-115	152-390	442-1,640	--	4.6 ± 8.6	-
Downwind - 25L	61-169	128-281	229-419	--	1.0 ± 0.5	-
Community Sites	83-164	179-276	229-402	38 ± 25	1.3 ± 1.2	15.6 ± 12.0

The modeling project developed a model of dispersion of LAX aircraft emissions, represented by black carbon mass concentrations. Model development included a detailed treatment of black carbon emissions from various aircraft based upon currently available data. The model was calibrated with black carbon data measured at the near-source site. When the model was then used to calculate black carbon dispersion to community sampling sites, concentrations were predicted that were consistent with measured black carbon levels in the community.

## 7. Recommendations for Future Research

The results of this have provided important preliminary findings and fulfilled the exploratory goals of building a basis for future work to more fully characterize the contribution of aircraft and other airport activities to local and regional air quality. The studies provide the basis to conclude that aircraft emit substantial quantities of UFP and the impact of these emissions should be pursued. The study also highlights the utility of data that is highly resolved over time, and over the PM size range for describing PM source emissions. In general, more work is needed to characterize the composition, toxicological properties and contribution to local and regional pollution levels of aircraft derived PM. Specific recommendations that follow directly upon the current project findings follow:

1. A more detailed analysis of UFP concentration vs. time profiles collected in the one second SMPS scans at the blast fence should be undertaken, to determine whether we can identify aircraft characteristics such as model, engine type, wake size, or other metrics that could explain varying emissions levels observed at the blast fence. We have collected a substantial dataset that could be used for this purpose.
2. The size specific scan data should also be analyzed to determine mathematical properties of the decay behavior of aircraft take off plumes at the near source site. Such data is important for modeling the impact of emissions on surrounding air quality.
3. A complete set of CO and CO<sub>2</sub> data should be obtained along with total UFP concentrations at the blast fence to assist in development of emissions factors for in-use commercial aircraft at a field site. This would enable comparison to other field-derived PM emission factors. Because we did not observe a pronounced seasonal effect, this could be achieved with a relatively short sampling campaign.
4. A study of chemical characteristics of PM at the near source site would be valuable for several purposes, including toxicological implications and possible development of a source signature profile for use in source apportionment models. To focus on PM emitted by aircraft, chemical analysis of 15 nm particles would be of particular interest. Chemical composition of UFP collected at blast fence could also be compared to the composition of UFP collected in the community. It would be of interest to assess composition of the peak aircraft mode as well as a larger mode that may be more influenced by road traffic at the community locations. Composition data could be developed as an additional tool to the statistical analysis of temporal patterns used in this study to address the question of differential source impacts on the community.
5. Temporal analysis of particle number concentrations downwind of aircraft take-off should be extended to an analysis of study data collected beneath the approach to the LAX, to better study the emissions of landing aircraft. Some data is available from this study for a preliminary analysis.
6. To better characterize the offsite plume movement of aircraft UFP, it would be very useful to have a complete size distribution for at least one of the sites described in our downwind study. Due to limited resources, only 15 nm PM were sampled, but a more complete characterization would provide the link needed for better inference about plume movement into community sites. Size distribution data would also enhance understanding of the fate of 15 nm PM as the aerosol disperses.

7. As a general recommendation, ultrafine particle number concentration, and especially particles in the 10-20nm range should be considered a relevant metric for estimating human exposure to aircraft emissions, recognizing that other combustions sources also contribute to this size range. The results of the current study suggest that using only mass based metrics as indicators of exposure would not be adequate to characterize exposure at the community sites.
8. A detailed analysis of PM concentration vs. time profiles should be undertaken to develop more complete conclusions from the data we have collected in communities adjacent to LAX. We have tentatively concluded that the high numbers of 10-20 nm PM measured in these communities may be attributable to aircraft, but further field work is required to clarify the relative contributions of landing aircraft, offsite movement of take off plumes from LAX, and other sources. It is also important to learn whether landing aircraft passing over the community or advection of plumes from departing aircraft which, although more distant, are operating at a much higher engine thrust level, are a greater source of UFP at the community sites that were studied.
9. Total particle counts from simultaneous CPC studies would be useful to have for the community sites.
10. The community study would have benefited from concurrent monitoring at reference sites to address the question of the relative contribution of road and freeway traffic to measured UFP, black carbon and PM<sub>2.5</sub> levels. A study that performed concurrent SMPS monitoring at one of the community sites and a reference site such as Lloyd school that is affected by local traffic and the 405 but is not typically downwind of LAX would be very informative. Other control sites such as a reference upwind of both the 405 and LAX may be important to create a complete picture. Similarly, the comparisons of SMPS data between the six community sites are compromised by sampling on different days and some concurrent sampling would help clarify.
11. Data collected in the community should be used to perform calibration of the black carbon model, as was done with the near source data.
12. Development of source tracers for jet aircraft emissions would be very useful, and would obviate the need for the complex inferential approach to source attribution that relies upon analysis of temporal patterns of PM concentration.
13. There is not a literature that addresses the toxicity of or health effects of exposure to aircraft derived PM. In the short run, a high volume sample collected at LAX could be used in established toxicological experiments, in association with complete speciation of the particulate samples. In the longer run, research is needed to determine the physical, chemical and toxicological properties of the 10-20 nm particles that make up the concentration peak of take-off emissions, and to compare the toxicity of aircraft emitted PM to PM from other sources. In addition, community health studies should be a long term research goal. Because of the implications for public health, it is essential to link exposure to toxicological outcomes.

## 8. References

- Blevins, L. G., Mulholland, G. W., Benner, Jr. B. A., and Steel, E. B. (2002) Morphology and chemistry of aircraft engine soot. *Proceedings of the 2002 Spring Technical Meeting of the Western States Section of the Combustion Institute*. The Combustion Institute, Pittsburgh, PA, MS014.
- Blevins, L. G. (2003) Particulate matter emitted from aircraft engines. AIAA/ICAS International Air and Space Symposium and Exposition: The Next 100 Years. 14-17 July, Dayton, Ohio. AIAA 2003-2764.
- Eiguren-Fernandez, A., Miguel AH (2003). "Determination of Semi-Volatile and Particulate Polycyclic Aromatic Hydrocarbons in SRM 1649a and PM2.5 Samples by HPLC-Fluorescence." *Polycyclic Aromatic Compounds* 23: 193-205.
- Eiguren-Fernandez, A., Miguel AH, Froines JR, Thurairatnam S, Avol E (2004). "Seasonal and Spatial Variations of Polycyclic Aromatic Hydrocarbons in Vapor-Phase and PM2.5 in Southern California Urban and Rural Communities." *Aerosol Science & Technology* 38: 447-455.
- EPA 1992, Procedures for Emission Inventory Preparation, Volume IV: Mobile Sources, EPA420-R-92-009.
- FAA 2005, Air Quality Procedures for Civilian Airports and Air Force Bases. Air Quality Handbook, Appendix D: Aircraft Emission Methodology, [http://www.faa.gov/regulations\\_policies/policy\\_guidance/envir\\_policy/airquality\\_handbook/](http://www.faa.gov/regulations_policies/policy_guidance/envir_policy/airquality_handbook/)
- FAEED, FAA Aircraft Engine Emission User Guide and Database, U.S. Environmental Protection Agency Technology Transfer Network, Office of Mobile Sources (OMS) Bulletin Board System, 1995.
- Fine PM, Shen S, Sioutas C. (2004) Inferring the sources of fine and ultrafine particulate matter at downwind receptor sites in the Los Angeles basin using multiple continuous measurements. *Aerosol Sci Tech* 38(S1): 182-195.
- Hering S. V., Flagan, R.C., & Friedlander, S. K. (1978) Design and evaluation of new low-pressure impactor. *Environ. Sci. Technol.* **12**, 667-673.
- ICAO 2006, ICAO Aircraft Engine Emissions DataBank (<http://www.caa.co.uk>)
- Kittleson, D. B. (1998) Engines and nanoparticles: A review *J. Aerosol Sci.* **29**, 575.
- Lu R, Turco RP (1995) Air pollution transport in a coastal environment: Part II. Threedimensional simulations over the Los Angeles basin, *Atmospheric Environment*, Part A, 29, 1499-1518.
- Lu R, Turco RP, Jacobson MZ (1997a) An integrated air pollution modeling system for urban and regional scales: Part I: Structure and performance, *J Geophys Res* 102:6063-6079.
- Lu R, Turco RP, Jacobson MZ (1997b) An integrated air pollution modeling system for urban and regional scales: Part II: Simulations for SCAQS 1987, *J Geophys Res* 102:6081-6098.
- Lu R, Turco RP, Stolzenbach K, Friedlander SK, Xiong C, Schiff K, Wang G (2003) Dry deposition of airborne trace metals on the Los Angeles Basin and adjacent coastal waters. *J Geophys Res* 108(D2):4074, doi:10.1029/2001JD001446.
- Lu, R., J. Wu, R. P. Turco, A. Winer, R. Atkinson, J. Arey, S. Paulson, F. Lurmann, A. H. Miguel and A. Eiguren-Fernandez, "Naphthalene distributions and human exposure in the South Coast Air Basin," *Atmos. Environ.*, **39**, 489-507, 2005.

- Singh, M, Phuleria HC, Bowers K, Sioutas C. (2006). Seasonal and spatial trends in particle number concentrations and size distributions at the children's health study sites in Southern California. *Journal of Exposure Science and Environmental Epidemiology* **16**, 3–18.
- Xiong, C., Friedlander, S. K. (2001) Morphological properties of atmospheric aerosol aggregates. *Proc. Natl. Acad. Sci. USA*. **98**, 11851-11856.
- Zhu, Y. F., Hinds, W. C., Kim, S., and Sioutas, C. (2002) Concentration and Size Distribution of Ultrafine Particles Near a Major Highway. *Air Waste Manage Assoc.* **52**, 1032.

## Appendix A

Air toxics sampled at the LAX blast fence and the AQMD background reference site three days during the downwind study in May 2006.

### AQMD West (Site 1)

Sampling Date	5/2/2006		5/3/2006		5/4/2006	
LIMS ID	TX007314		TX007316		TX007318	
Dilution Factor	2.08		2.17		2.25	
	Concentration (ppb)	Detection Limit (ppb)	Concentration (ppb)	Detection Limit (ppb)	Concentration (ppb)	Detection Limit (ppb)
1,1,1-Trichloroethane	<.02	0.02	<.02	0.02	<.02	0.02
1,2-Dichloroethane	<.04	0.04	<.04	0.04	<.05	0.05
1,3-Butadiene	<.08	0.08	<.09	0.09	<.09	0.09
Acetone	7.9	0.6	5.4	0.7	3.4	0.7
Acetonitrile	<.6	0.6	<.7	0.7	<.7	0.7
Acrolein	<b>0.867</b>	0.6	<.7	0.7	<.7	0.7
Acrylonitrile	<.6	0.6	<.7	0.7	<.7	0.7
Benzene	<b>0.108</b>	0.1	<b>0.102</b>	0.1	<.1	0.1
Bromomethane	<.06	0.06	<.07	0.07	<.07	0.07
Carbon disulfide	<.2	0.2	<.2	0.2	<.2	0.2
Chlorobenzene	<.2	0.2	<.2	0.2	<.2	0.2
Chloroform	<.04	0.04	<.04	0.04	<.05	0.05
cis-1,3-Dichloropropene	<.2	0.2	<.2	0.2	<.2	0.2
Dibromoethane	<.04	0.04	<.04	0.04	<.05	0.05
Dichloromethane	0.22	0.2	<.2	0.2	<.2	0.2
Ethanol	2	1	1.3	1.1	<1.1	1.1
Ethylbenzene	<.4	0.4	<.4	0.4	<.5	0.5
Freon 11	0.24	0.02	0.24	0.02	0.25	0.02
Freon 113	0.062	0.04	0.059	0.04	0.059	0.05
Freon 12	0.54	0.04	0.53	0.04	0.52	0.05
m/p-Xylene	<.4	0.4	<.4	0.4	<.5	0.5
m-Dichlorobenzene	<.6	0.6	<.7	0.7	<.7	0.7
o-Dichlorobenzene	<.6	0.6	<.7	0.7	<.7	0.7
o-Xylene	<.2	0.2	<.2	0.2	<.2	0.2
p-Dichlorobenzene	<.6	0.6	<.7	0.7	<.7	0.7
Perchloroethylene	0.04	0.02	0.026	0.02	<.02	0.02
Styrene	<.2	0.2	<.2	0.2	<.2	0.2
Toluene	1.2	0.4	1.2	0.4	<.5	0.5
trans-1,3-Dichloropropene	<.2	0.2	<.2	0.2	<.2	0.2
Trichloroethylene	<.04	0.04	<.04	0.04	<.05	0.05
Vinyl chloride	<.04	0.04	<.04	0.04	<.05	0.05

### LAX Blast Fence (Site 2)

Sampling Date	5/2/2006		5/3/2006		5/4/2006	
LIMS ID	TX007317		TX007332		TX007315	
Dilution Factor	2.15		1.977		2.16	
	Concentration (ppb)	Detection Limit (ppb)	Concentration (ppb)	Detection Limit (ppb)	Concentration (ppb)	Detection Limit (ppb)
1,1,1-Trichloroethane	<.02	0.02	<.02	0.02	<.02	0.02
1,2-Dichloroethane	<.04	0.04	<.04	0.04	<.04	0.04
1,3-Butadiene	<b>0.245</b>	0.09	<.08	0.08	<b>0.199</b>	0.09
Acetone	4.1	0.6	3.5	0.6	3.5	0.6
Acetonitrile	<.6	0.6	<.6	0.6	<.6	0.6
Acrolein	<b>0.970</b>	0.6	<b>0.952</b>	0.6	<b>0.786</b>	0.6
Acrylonitrile	<.6	0.6	<.6	0.6	<.6	0.6
Benzene	<b>0.312</b>	0.1	<b>0.263</b>	0.1	<b>0.238</b>	0.1
Bromomethane	<.06	0.06	<.06	0.06	<.06	0.06
Carbon disulfide	<.2	0.2	<.2	0.2	<.2	0.2
Chlorobenzene	<.2	0.2	<.2	0.2	<.2	0.2
Chloroform	<.04	0.04	<.04	0.04	<.04	0.04
cis-1,3-Dichloropropene	<.2	0.2	<.2	0.2	<.2	0.2
Dibromoethane	<.04	0.04	<.04	0.04	<.04	0.04
Dichloromethane	<.2	0.2	<.2	0.2	<.2	0.2
Ethanol	1.6	1.1	1.1	1	<1.1	1.1
Ethylbenzene	<.4	0.4	<.4	0.4	<.4	0.4
Freon 11	0.24	0.02	0.25	0.02	0.24	0.02
Freon 113	0.062	0.04	0.071	0.04	0.06	0.04
Freon 12	0.54	0.04	0.54	0.04	0.54	0.04
m/p-Xylene	<.4	0.4	<.4	0.4	<.4	0.4
m-Dichlorobenzene	<.6	0.6	<.6	0.6	<.6	0.6
o-Dichlorobenzene	<.6	0.6	<.6	0.6	<.6	0.6
o-Xylene	<.2	0.2	<.2	0.2	<.2	0.2
p-Dichlorobenzene	<.6	0.6	<.6	0.6	<.6	0.6
Perchloroethylene	0.043	0.02	0.022	0.02	<.02	0.02
Styrene	<.2	0.2	<.2	0.2	<.2	0.2
Toluene	1.7	0.4	1	0.4	0.48	0.4
trans-1,3-Dichloropropene	<.2	0.2	<.2	0.2	<.2	0.2
Trichloroethylene	<.04	0.04	<.04	0.04	<.04	0.04
Vinyl chloride	<.04	0.04	<.04	0.04	<.04	0.04